The Role of SUMOylation in the KSHV Kaposin B-MK2 Signaling Axis

by

Sarah Veinot

Submitted in partial fulfilment of the requirements
for the degree of Master of Science

at

Dalhousie University
Halifax, Nova Scotia
November 2019

TABLE OF CONTENTS

LIST OF TABLES

LIST OF FIGURES

ABSTRACT

Kaposi's sarcoma (KS) is characterized by infection with Kaposi's sarcoma-associated herpesvirus (KSHV), aberrant inflammation and cell spindling. These phenotypes are recapitulated by expression of the viral gene product Kaposin B (KapB). KapB binds and activates the kinase MK2, which is required for both effects; how KapB activates MK2 is not known. MK2 is modified by SUMOylation and preventing SUMOylation enhanced MK2 activity. Therefore, I hypothesized that KapB disrupts MK2 SUMOylation. I confirmed MK2 SUMOylation and discovered that constitutively active MK2 is hyper-SUMOylated compared to wild type, suggesting that SUMOylation may be phosphorylation directed. However, the co-expression KapB did not alter the MK2 SUMOylation profile in this assay. I observed that overexpressed MK2 constructs stabilized ARE-mRNAs and disassembled PBs. My work uncovered a regulatory interplay between phosphorylation and SUMOylation which may provide insight into the regulation of inflammatory responses by MK2 during cellular stress, such as latent KSHV infection and tumourigenesis.

LIST OF SYMBOLS AND ABBREVIATIONS USED

Ψ	Hydrophobic amino acid
AIDS	Acquired immunodeficiency syndrome
ANOVA	Analysis of variance
ARE	AU-rich element
ATP	Adenine triphosphate
BCBL	Body cavity-based lymphoma
BECs	Blood endothelial cells
BSA	Bovine serum albumin
CDS	Coding sequence
CELO	Chicken embryo lethal orphan
CO_2	Carbon dioxide
CMV	Cytomegalovirus
DMEM	Dulbecco's Modified Eagle Medium
DNA	Deoxyribonucleic acid
Dox	Doxycycline
DR	Direct repeats
DTT	Dithiothreitol
dsDNA	Double stranded DNA
EDTA	Ethylenediaminetetraacetic acid
ERKs	Extracellular signal-regulated kinases
EV	Empty vector
FAK	Focal adhesion kinase
FBS	Fetal bovine serum
FLIP	Flice-inhibitory protein
g	Gravity
GFP	Green fluorescent protein
GM-CSF	Granulocyte-macrophage colony-stimulating factor
GPCR	G-protein-coupled receptor
HAART	Highly active antiretroviral therapy
HHV	Human herpesvirus

HI	Heat inactivated
HIV	Human immunodeficiency virus
HPV	Human papillomavirus
HRP	Horseradish peroxidase
HSP	Heat shock protein
HSV	Herpes simplex virus
HUVEC	Human umbilical vein endothelial cells
IFN	Interferon
IL	Interleukin
IP	Immunoprecipitation
JNK	c-Jun N-terminal kinase
Kap	Kaposin
KS	Kaposi's sarcoma
KSHV	Kaposi's sarcoma-associated herpesvirus
LANA	Latency-associated nuclear antigen
LECs	Lymphatic endothelial cells
LPS	Lipopolysaccharide
MCD	Multicentric Castleman disease
MEM	Minimal essential media
MKK	MAP kinase kinase
miRNA	Micro RNA
MK2	Mitogen activated protein kinase (MAPK)-activated protein kinase 2
mRNA	Messenger RNA
NEM	N-ethylmaleimide
NES	Nuclear export sequence
NLS	Nuclear localization sequence
ORF	open reading frame
PBs	Processing bodies
PBS	Phosphate-buffered saline
PDSM	Phosphorylation-dependent SUMO motif
PEI	Polyethylenimime

PEL	Primary effusion lymphoma
PIAS	Protein inhibitor of activated STAT
PML	Promyelocytic leukemia
PMSF	Phenylmethane sulfonyl fluoride
PROX1	Prospero homeobox protein 1
PSQ	Penicillin streptomycin L-glutamine
PTM	Post-translational modification
PVDF	Polyvinylidene fluoride
RLU	Relative light units
RNA	Ribonucleic acid
RNP	Ribonucleoprotein
ROCK	Rho-associated coiled-coil kinase
SAPK	Stress activated protein kinase
SENP	Sentrin protease (SUMO protease)
SF	Stress fibres
SIM	SUMO interaction motif
STAT1	Signal transducer and activator of transcription 1
STUbL	SUMO-targeted ubiquitin ligase
SUMO	Small ubiquitin-like modifier
TAE	Tris-acetate EDTA
TBS-T	Tris-buffered saline with tween-20
TNF	Tumour necrosis factor
TRE	Tetracycline response element
TTP	Tristetraprolin
UTR	Untranslated region
V	Volts
VEGF	Vascular endothelial growth factor
VZV	Varicella-zoster virus

ACKNOWLEDGMENTS

I would like to thank my supervisor, Dr. Jennifer Corcoran, for all the patience and support she has provided over the last few years, as well as my committee members Dr. John Rohde, Dr. Melanie Dobson, and Dr. Chris Richardson. This work would not have been possible without the support and guidance you have provided. I would also like to thank everyone at Dalhousie who has helped me along this journey, and of course my family, especially my husband Harley and my parents Jeff and Cindy. Your love and encouragement made all the difference.

CHAPTER 1 INTRODUCTION

1.1 Herpesviruses

Herpesviruses are large (120-260 nm), enveloped viruses, with double-stranded linear DNA (dsDNA) genomes (~120-250 kilobases [kb] in size) encased in an icosahedral-type capsid that is surrounded by a tegument layer (Grinde, 2013; Pellet and Roizman, 2013; Whitley, 1996). There are over a hundred different kinds of herpesviruses that infect a broad range of vertebrate and invertebrate species, all of which share four common biological properties (Pellet and Roizman, 2013; Whitley, 1996). Firstly, herpesviruses encode a wide array of enzymes involved in viral nucleic acid metabolism. Secondly, the transcription and synthesis of viral DNA occurs in the nucleus, as well as the assembly of the nucleocapsid. Thirdly, the release of infectious progeny virus from the cell results in host cell death, and lastly, all herpesvirus can establish lifelong infection of their hosts through the establishment latent infection. The tissues within which these viruses establish latency is specific for each virus (Pellet and Roizman, 2013; Whitley, 1996).

To establish latency, viral DNA is circularized in the nucleus into an episome that is associated with the host cell's histones, and is copied by the host DNA polymerase along with the host chromosomes during mitosis (Grinde, 2013). A defining characteristic of this latent state is the restriction of viral gene expression to a small subset of genes and the lack of progeny virion production (Grinde, 2013; Pellet and Roizman, 2013). This is in contrast to the lytic replicative cycle, in which most of the viral genome is expressed and progeny virions are released, resulting in the death of the cell (Pellet and Roizman, 2013).

Of these hundreds of herpesviruses, only eight have been shown to infect humans; they are known as the human herpesviruses, and include herpes simplex virus type 1 (HSV1), herpes simplex virus type 2 (HSV2), varicella-zoster virus (VZV), cytomegalovirus (CMV), Epstein-Barr virus (EBV), human herpesvirus 6 (HHV6), human herpesvirus 7 (HHV7) and human herpesvirus 8 (HHV8), which is also known as Kaposi's sarcoma-associated herpesvirus (KSHV) (Pellet and Roizman, 2013; Whitley, 1996). These viruses can be categorized into three groups based upon the range of cell types they infect and their method of replication. The α-herpesviruses (HSV1/2 and VZV) are characterized by short replicative cycles (hours), rapid destruction of their host cells, and the ability to infect a broad range of cell types, though latency is typically established in sensory nerve ganglia and are therefore thought of as neurotropic viruses (Grinde, 2013; Pellet and Roizman, 2013; Whitley, 1996). The β-herpesviruses (CMV and HHV6/7) have more restricted host ranges, establishing latent infection in cells of the secretory glands, kidneys and immune system. Their replicative cycles are also much longer than that of α-herpesviruses (days instead of hours). The γ-herpesviruses (EBV and KSHV) have the most restricted host range, typically establishing latency in lymphoid tissues, and are therefore known as the lymphotropic herpesviruses (Grinde, 2013; Pellet and Roizman, 2013; Whitley, 1996). EBV and KSHV are also the only known tumorigenic human herpesviruses (Grinde, 2013); for the purposes of this study, only KSHV will be discussed at length.

1.2 Kaposi's Sarcoma-Associated Herpesvirus (KSHV)

KSHV is the most recently discovered of the human herpesviruses, and was first isolated from acquired immunodeficiency syndrome (AIDS) patients (Chang et al. 1994). Structurally, it resembles other herpesviruses, encasing its genome with an icosahedral

nucleocapsid, which is surrounded by a lipid envelope that is studded with various glycoproteins involved in cell attachment and viral entry (Pellet and Roizman, 2013). The genome of KSHV is ~170 kb in size, encoding at least 90 open reading frames (ORFs), 15 of which are unique to KSHV (Pellet and Roizman, 2013; Russo et al., 1996). One of the more notable characteristics of KSHV is that it is one of two oncogenic herpesviruses. It is believed to cause the unusual neoplasm known as Kaposi's sarcoma (KS), from which it gets its name, as well as two B-cell lymphoproliferative diseases known as primary effusion lymphoma (PEL) and multicentric Castleman disease (MCD) (Ganem, 2006; Gramolelli and Schulz, 2015; Pellet and Roizman, 2013). PEL is a rare lymphoma that is usually found in HIV-infected individuals, with cells typically being monoclonal (Pellet and Roizman, 2013; Schulz, 2000). PEL results in the expansion of B-cells in body cavities such as the pericardium. Of the two forms of MCD, only the B-cell variant is associated with KSHV. In contrast to PEL, cells in MCD are polyclonal in origin. (Pellet and Roizman, 2013; Schulz, 2000). For the purposes of this study, only KS will be described in detail.

1.2.1 Pathogenesis of KS

KS is an unusual neoplasm that typically appears as flat red lesions of the skin, and was first described in the nineteenth century as a benign disease afflicting elderly men of Mediterranean decent (Ganem, 2006, 2010; Gramolelli and Schulz, 2015). However, it was discovered that there are three distinct variants of Kaposi's sarcoma besides this "classic" form of the disease based on epidemiological distribution, aggressiveness and localization, which include endemic, iatrogenic, and AIDS-associated KS (Gramolelli and Schulz, 2015). Endemic KS is a more aggressive variant than the classic form of the disease, and tends to be concentrated in eastern and central Africa,

where seroprevalence can be as high as 60% (Ganem, 2006; Schulz, 2000). Iatrogenic KS is associated with the administration of immunosuppressives following medical procedures such as organ transplants; this form of KS typically regresses following reconstitution of the immune system. The final and perhaps more well-known form of KS is the variant associated with AIDS. It is the most aggressive variant of the disease, commonly affecting visceral sites such as the lungs and gastrointestinal tract in addition to the skin, and came into prominence during the AIDS epidemic of the 1980s (Ganem, 2006, 2010; Gramolelli and Schulz, 2015). AIDS-related KS commonly resolves upon treatment of the underlying human immunodeficiency virus (HIV) infection using antiretroviral therapy (HAART) and subsequent reconstitution of the immune system (Gramolelli and Schulz, 2015). While KSHV is strongly believed to be the etiological agent behind KS, infection with the virus alone is not sufficient to lead to disease. Typically, a state of immunosuppression is needed to lead to the progression of the disease, as well as an inflammatory microenvironment, and for AIDS-related KS co-infection with HIV is another contributing factor (Ganem, 2010; Wood and Feller, 2008). Regardless of differences between variants, the histology of these lesions is similar across all forms of the disease (Ganem, 2006).

Histologically, KS is unlike most classical cancers (Ganem, 2010). Most classical cancers are monoclonal growths of a single cell type, whereas KS lesions have a complex, heterogeneous cellular morphology. Early in the development of the lesion, an inflammatory infiltrate consisting of B-cells, T-cells and monocytes is present, in addition to pronounced neovascularization (Ensoli et al., 2001; Ganem, 2010). This neovascularization is another feature that sets KS apart from traditional cancers, which

typically vascularize after the establishment of the main tumor mass (Ensoli et al., 2001; Ganem, 2010).

These early lesions contain small numbers of the major proliferative element of KS, known as spindle cells (due to their elongated morphology), which over time become the dominate cell type in these lesions (Ganem, 2006, 2010; Gramolelli and Schulz, 2015). The exact origin of these spindle cells has been debated, due largely to the heterogeneity in marker expression on the surface of spindle cells. Evidence suggests they may be endothelial in origin, due to the presence of CD31, CD34, CD36, factor XIII, En-4, and PAL-E markers on their cell surface, though the majority of cells do not stain for factor VIII, a marker for vascular endothelium (Ensoli et al., 2001; Ganem, 2006). However, the presence of lymphatic endothelium markers on spindle cells (VEGF-C, VEGF-R3, podoplanin, and LYVE-1), as well as the observation that KS does not occur in tissues lacking lymphatics, suggest a lymphatic origin for spindle cells as well (Ensoli et al., 2001; Ganem, 2006). Further complicating matters is the observation that KSHV infection reprograms blood endothelial cells (BECs) to behave more like lymphatic endothelial cells (LECs), and vice versa, by upregulating PROX1 expression (the master regulator of lymphatic differentiation) in BECs and downregulating PROX1 expression in LECs (Hong et al., 2004; Wang et al., 2004). Regardless of origin, the spindle cells of KS lesions are typically diploid and polyclonal, which is another factor that differentiates KS from classical cancers, whose cells tend to be aneuploid and monoclonal (Ganem, 2010). Based on these characteristics, KS can be thought of as involving three parallel processes: proliferation (through the spindle cells), inflammation, and angiogenesis (Ganem, 2006, 2010). Importantly, approximately 90% of the spindle cells in these lesions are latently infected with KSHV, while approximately 1-3% of cells

express markers of lytic replication (Gramolelli and Schulz, 2015; Pellet and Roizman, 2013).

1.2.2 The Dual Lifecycle of KSHV

KSHV is known to infect B-cells, T-cells, dendritic cells, mast cells, monocytes, endothelial cells, and epithelial cells (Ayers et al., 2018; Chakraborty et al., 2012; Ganem, 2010; Myoung and Ganem, 2011; Rappocciolo et al., 2006). Like all herpesviruses, KSHV can switch between a latent and lytic replicative program, though in KSHV-infected spindle cells latency is the predominate program (Ganem, 2006; Gramolelli and Schulz, 2015). During lytic replication, most of the viral genome is expressed in a tightly controlled transcriptional cascade (Pellet and Roizman, 2013). The first set of genes expressed are known as the immediate early genes, which encode transcription factors and regulatory proteins, with expression of RTA (ORF50) being key for the initiation of the lytic cycle. The delayed early genes are expressed next, which code for enzymes involved in viral DNA replication, as well as proteins involved in host immune evasion and alteration of host transcription. Once viral DNA has been replicated in the nucleus, the late genes are expressed, which code for viral structural proteins. From here, the viral genomes are incorporated into capsids and bud through host membranes to obtain their lipid envelopes (Pellet and Roizman, 2013).

While latency is the predominant replicative cycle in KS spindle cells, the lytic cycle also contributes to KS pathogenesis in a variety of ways. Since spindle cells are not immortalized by KSHV *in vivo*, infections are maintained by the lytic program replacing latently infected cells as they die, by creating progeny virus that can infect other cells (Ganem, 2006). The lytic cycle may also contribute to the inflammation and angiogenesis occurring in KS lesions through the secretion of paracrine signaling molecules, such as

viral homologs to host cytokines and chemokines (i.e. v-IL6, CC chemokines, viral G protein-coupled receptor [v-GPCR]). v-IL6 is a homolog of cellular interleukin 6 (IL6), binding directly to the cellular transmembrane protein known as gp130 to promote angiogenesis and disruption of interferon (IFN) signaling, possibly impairing innate immunity (Aoki et al., 1999; Chatterjee et al., 2002; Ganem, 2010). Viral CC chemokines have important impacts on lymphocytes, attracting Th2 class helper T cells the tumor microenvironment, aiding in immune evasion (Ganem, 2010). Additionally, viral CC chemokines can promote angiogenesis, resulting in changes in the tumor microvasculature. The lytic KSHV program also expresses transmembrane proteins that can induce the expression of host proinflammatory and proangiogenic molecules. One such protein is viral G-protein-coupled receptor (v-GPCR), which induces the expression of the proangiogenic factor vascular endothelial growth factor (VEGF) (Ganem, 2010). Transgenic mice injected with retrovirus encoding v-GPCR or murine cell lines stably expressing v-GPCR developed KS-like tumours, suggesting an integral role for v-GPCR in KS development (Montaner et al., 2003).

1.2.3 KSHV Latency Predominates in KS Lesions

During latency, viral gene expression is tightly restricted to the latency-associated region of the viral genome, which is expressed in all latently infected cells (Ganem, 2010). This region encodes proteins for the latency-associated nuclear antigen (LANA), viral cyclin (v-cyclin) viral Flice-inhibitory protein, (v-FLIP), Kaposins A, B and C as well as several microRNAs (miRNAs) (Cesarman et al., 2019; Ganem, 2006). The expression of LANA, v-FLIP and v-cyclin is controlled from a single promoter, known as the LANA promoter, generating co-terminal mRNAs through differential splicing (Ganem, 2010). LANA is the best understood of the latent gene products, facilitating

replication of the latent viral genome by binding to terminal repeat region present in the episome; the binding of LANA to the terminal repeat region facilitates semi-conservative DNA replication (Ganem, 2006; Hu et al., 2002). LANA is also responsible for the segregation of the viral genome into daughter cells during mitosis, due to its ability to bind histone proteins and tether the genome to chromosomes during mitosis (Ganem, 2010; Piolot et al., 2001). The LANA protein itself is composed of three domains: a central domain comprised of a variable number of acidic amino acid repeats, a C-terminal region involved in DNA binding, and an N-terminal region associated with chromatin attachment (Ganem, 2006; Piolot et al., 2001). Additionally, LANA promotes tumorigenesis and cell survival by binding and partially inhibiting the tumor suppressor genes p53 and Rb, as well as upregulating the expression of various proto-oncogenes (Ganem, 2010).

The transcript coding for v-cyclin also relies on the LANA promoter, but it is spliced, removing the upstream LANA ORF (Ganem, 2006). It is a viral homolog of cellular cyclin D, binding to and activating cdk6, though binding by v-cyclin confers different cdk6 substrate specificity and provides resistance to cdk inhibitors. v-cyclin deregulates the host cell cycle and causes aberrant DNA replication and damage, triggering cellular DNA damage responses, autophagy and oncogene-induced senescence, which often leads to apoptosis (Ganem, 2006; Leidal et al., 2012). However, this activity is attenuated by its antagonistic partner v-FLIP, which blocks v-cyclin-induced apoptosis and senescence (Leidal et al., 2012). v-FLIP is a homolog of cellular FLIP, and is expressed from a bicistronic mRNA with v-cyclin; v-cyclin is translated through cap-dependent initiation, whereas v-FLIP is translated from an internal ribosome entry site (IRES) present in the v-cyclin ORF (Damania and Cesarman, 2013). v-FLIP

activates NFκB, resulting in the expression of numerous anti-apoptotic and pro-inflammatory genes, as well as contributing to the spindled morphology observed in KS cells (Ganem, 2010; Matta and Chaudhary, 2004; Matta et al., 2007).

1.2.4 The Kaposin Locus

A second segment of latency genes is expressed from the Kaposin locus of the latency-associated region (Ganem, 2010). From this 1.4 kb mRNA, three proteins known as Kaposins A, B and C are translated by differential translation initiation (Figure 1.1) (Sadler et al., 1999). Translated from a canonical AUG start codon towards the 3' end of the Kaposin transcript is Kaposin A (KapA). It is a small (60 amino acid) hydrophobic protein that is found on cell membranes and the cell surface and may play a role in cell signaling (Ganem, 2006; Tomkowicz et al., 2002).

Upstream of the KapA ORF is a region containing two sets of GC-rich, 23 nucleotide direct repeats known as direct repeat (DR) 1 and 2 (Fig. 1.1). The length of these repeats can vary between different KS isolates, and the significance of the expansion and contraction of the repeats is not known, though their retention would imply that they are important for function (Sadler et al. 1999; Li et al. 2002; McCormick and Ganem 2006). Intriguingly, the amino acid sequence of the DR1 and DR2 repeats remains the same in all three reading frames (Li et al., 2002). Translated from non-canonical CUG start codons upstream of this region are Kaposin B and C (Sadler et al., 1999). Kaposin C (KapC) is translated in the same frame as KapA, and comprises both of the DR repeats as well as the K12, or KapA, ORF (Sadler et al., 1999); currently, no function has been ascribed to KapC.

Kaposin B (KapB) is translated in a different frame than KapA and KapC, and is comprised only of the residues encoded by the DR1 and DR2 repeats alone (Fig. 1.1)

(Sadler et al., 1999). Of the Kaposins, KapB is the most studied and best understood, and what we know of its function has been derived largely from ectopic expression studies. Notably, KapB has no known homology to other proteins and is predicted to have an intrinsically disordered protein structure (Corcoran, unpublished).

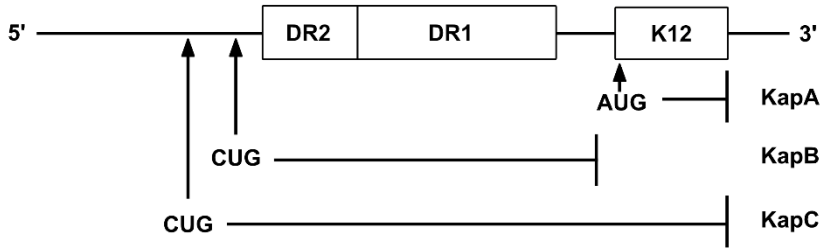

Figure 1.1 The *kaposin* locus. Kaposin A is a small protein comprised of the K12 ORF, translated from a canonical AUG start codon. The ORF encoding Kaposin C is in the same frame as K12 but translation initiates from an upstream non-canonical CUG codon and encompasses the upstream DR1 and DR2 repeats as well as the K12 ORF. Kaposin B is translated from an ORF initiating at a non-canonical CUG codon in a different frame than Kaposin A and C ORFs, and only encompasses the DR1 and DR2 repeats. Adapted from McCormick and Ganem 2005.

1.2.5 Kaposin B Recapitulates Features from KS Lesion

KS lesions are comprised of three parallel and interrelated processes: proliferation, inflammation, and angiogenesis. Also noteworthy are the cytoskeletal rearrangements observed in latently infected KS spindle cells. Ectopic KapB expression in primary endothelial cells recapitulates three of these four KS hallmarks; namely, cell spindling, angiogenesis and inflammation. KapB achieves this by modulating the p38 MAPK signaling pathway. Yeast two-hybrid screens revealed that KapB interacts with a stress-responsive kinase known as MK2 (mitogen activated protein kinase (MAPK)-activated protein kinase 2) (McCormick and Ganem 2005). This interaction was further verified using co-immunoprecipitation and GST pulldowns with purified proteins, which were used to demonstrate that the DR2 region of KapB was important for the interaction. The interaction between KapB and MK2 was further verified using immunofluorescence to examine the co-localization of KapB and MK2. Experiments with truncated MK2 mutants revealed that residues 200-270 of the C-lobe region of MK2 were critical for this interaction with the DR2 repeat region (Figure 1.2A) (McCormick and Ganem 2005). This region of MK2 encompasses the activation loop (residues 217-235), and contains threonine 222 (T222), which is phosphorylated by the upstream kinase p38. Additionally, the autoinhibitory C-terminus of MK2 binds in this region (McCormick and Ganem 2005). Importantly, binding of KapB to MK2 results in the activation of MK2, which has been demonstrated in several ways. Immunoblotting was used to show that cells expressing KapB exhibit increased levels of phosphorylated MK2, and that endogenous MK2 immunoprecipitated from KapB expressing cells displayed an increased ability to phosphorylate heat shock protein 27 (HSP27), a canonical MK2 downstream substrate, in

in vitro kinase assays. KapB is the only latently expressed gene capable of activating MK2 (McCormick and Ganem 2005).

An important consequence of increased MK2 activity is the stabilization of AU-rich element (ARE)-containing mRNAs. AREs consist of multiple copies of the sequence AUUUA, and are found in the 3' untranslated region (UTR) of many inflammatory mRNAs, and their presence results in destabilization of the mRNA transcript (McCormick and Ganem 2005; McCormick and Ganem 2006; Gaestel 2006). However, these transcripts can be stabilized by the activation of MK2 through phosphorylation of downstream substrates involved in ARE-mRNA stability (for detailed overview of p38 MAPK pathway, please see section 1.3) (McCormick and Ganem 2005; Gaestel 2006). Correspondingly, KapB-facilitated activation of MK2 results in the stabilization of ARE-mRNAs and increased expression of inflammatory cytokines, contributing to the inflammatory phenotype often seen in KS lesions (McCormick and Ganem 2005).

Activation of p38 MAPK by KapB also has consequences for the actin cytoskeleton, resulting in the activation of the cytoskeletal regulator RhoA guanosine triphosphatase (GTPase) through a non-canonical signaling axis (Corcoran et al., 2015). When HSP27 is phosphorylated by activated MK2, it recruits the Rho guanine nucleotide exchange factor (RhoGEF) p115 to RhoA, resulting in its activation (Corcoran et al., 2015; Garcia et al., 2009). Activated RhoA subsequently binds to the Rho- associated kinases ROCK1/2, resulting in changes in actin filaments and the induction of actin stress fibres (Corcoran et al., 2015; Garcia et al., 2009; Leung et al., 1996). Activation of the MK2/RhoA signaling axis by KapB results in the stabilization of inflammatory mRNAs, induction of stress fibres and angiogenesis, recapitulating features of the KS lesion (Fig. 1.2B) (Corcoran et al., 2015). More recently, increased actin contractility

caused by activation of RhoA has been shown to result in increased cytoskeletal tension, with this increased tension leading to the localization of the transcription factor YAP (yes-associated protein) in the nucleus, which through yet undefined mechanisms results in the disassembly of processing bodies (PBs; discussed in section 1.3) and increases in inflammation (Castle 2019, unpublished data).

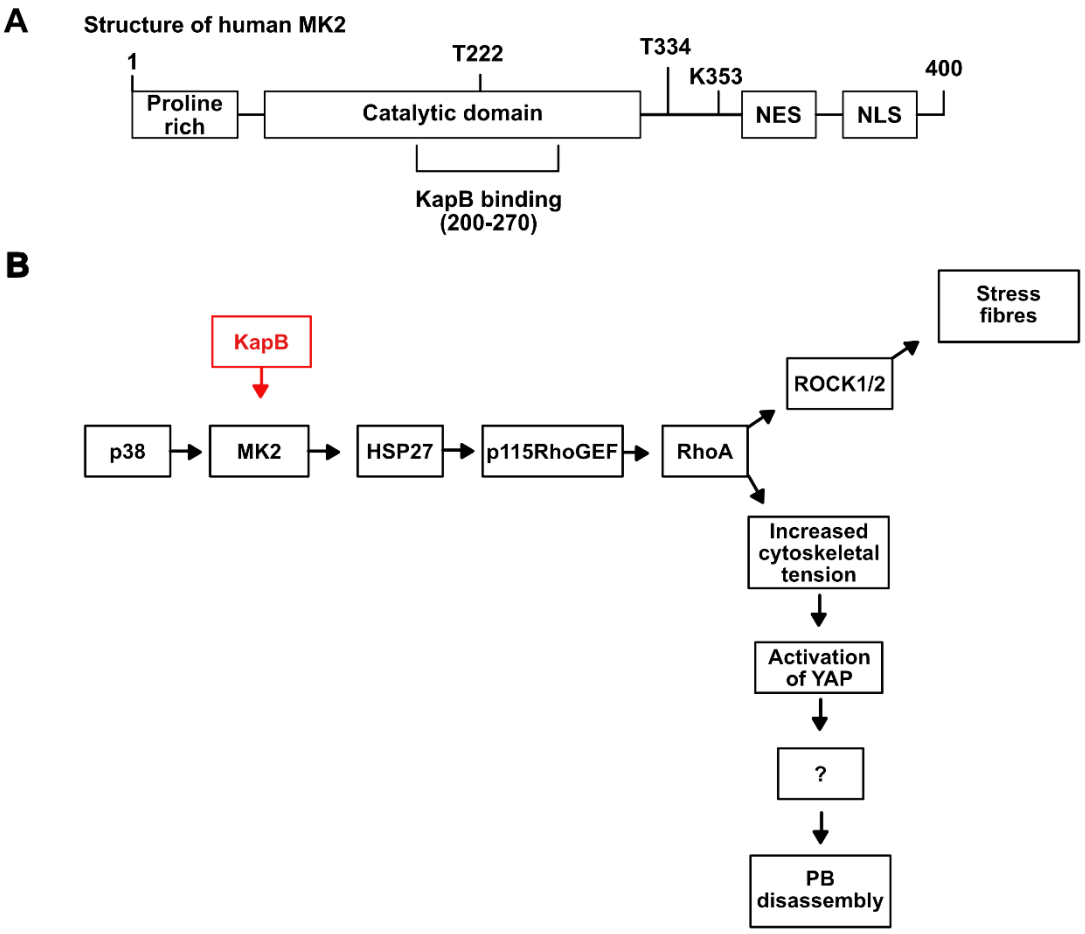

Figure 1.2 KapB binds to and activates MK2 and induces actin stress fibres and processing body disassembly. (A) The human MK2 protein consists of a proline-rich N-terminal domain, a kinase catalytic core that contains regulatory phosphorylation sites, and a C-terminal regulatory domain comprised of nuclear localization (NLS) and export sequences (NES), as well as an autoinhibitory helix that binds to the catalytic domain when the protein is inactive. KapB binds human MK2 between amino acids 200-270 of the catalytic domain. Adapted from Gaestal 2006 and McCormick and Ganem 2005. **(B)** KapB binding to MK2 results in MK2 activation. Once activated, MK2 phosphorylates HSP27, resulting in the recruitment of p115RhoGEF to RhoA and the activation of RhoA. Once activated, RhoA activates the cytoskeletal regulators ROCK1/2, resulting in the formation of actin stress fibres and cell spindling. Activation of RhoA results in increased actin contractility and increased cytoskeletal tension, resulting in the nuclear localization and activation of the transcription factor YAP. Through yet undefined mechanisms, activation of YAP leads to the disassembly of PBs. Adapted from Corcoran et al. 2015.

1.3 The Stress-Activated p38 MAPK Pathway

Living cells require ways to respond to extracellular stimuli and stressors; essential to this process is a group of kinases known as mitogen-activated protein (MAP) kinases (MAPKs) (Zarubin and Han, 2005). MAPKs are serine/threonine kinases, which include four distinct conventional classes: extracellular signal-regulated kinases (ERKs), c-jun N-terminal or stress-activated protein kinase (JNK/SAPK), ERK/ big MAP kinase 1(BMK1), and the p38 group of protein kinases (Cargnello and Roux, 2011). For the purpose of this report, only the p38 group of protein kinases will be discussed at length.

p38 kinase is involved in extracellular stress responses in mammalian cells, and is activated by various stressors such as heat shock and inflammatory cytokines (Cargnello and Roux, 2011; Raingeaud et al., 1995; Zarubin and Han, 2005). Its major role is in cellular inflammatory responses, and controls the production of cytokines by modulating transcription factors and mRNA stability (Cargnello and Roux, 2011). To date, four splice variants of p38 have been identified, ranging from p38α to δ; the expression of p38α and p38β is ubiquitous, while the expression of p38γ and p38δ is tissue specific (Zarubin and Han, 2005). Regardless of variant, all p38 kinases can be characterized by the presence of a Thr-Gly-Tyr dual phosphorylation motif, and are typically activated by dual specificity kinases termed MAP kinase kinases (MKKs), specifically MKK3/6; however, p38 can also be activated by MKK4 (Cargnello and Roux, 2011; Raingeaud et al., 1995; Zarubin and Han, 2005). Inactive p38 predominantly localizes to the nucleus of cells; upon activation, it is exported to the cytoplasm (Ben-Levy et al. 1998). Once activated, p38 can phosphorylate a variety of cytoplasmic and nuclear substrates, including the mRNA binding protein HuR and p53 (Cargnello and Roux, 2011). One of

the first p38α substrates identified was MAP kinase-activated protein kinase 2 (MAPKAPK2 or MK2) (Zarubin and Han, 2005).

1.3.1 MAPKAPK2 (MK2)

The MAPK-activated protein kinase (MAPKAPK) family encompasses 11 distinct groups of proteins, all of which belong to the calcium/calmodulin-dependent family of protein kinases (CAMKs) (Cargnello and Roux, 2011). These proteins can be classified into various subgroups, some of which include three structurally related enzymes known as MAPKAPK2 (MK2), MK3 and MK5 (Cargnello and Roux, 2011; Gaestel, 2006). While no common function has been attributed to the MKs, all seem to be involved in the regulation of gene expression and cytoskeletal dynamics, and have been implicated in inflammation and cancer (Cargnello and Roux, 2011; Gaestel, 2006). For the purposes of this study, only MK2 will be discussed at length.

MK2 is comprised of several domains. The N-terminus of MK2 is proline-rich (Fig. 1.2) and interacts with Src-homology-3 (SH3) domains, which may regulate MK2 protein interactions (Zu et al. 1994; Ben-Levy et al. 1995; Meng et al. 2002; Gaestel 2006; Cargnello and Roux 2011). Within the catalytic domain of MK2, specifically in the activation loop (217-235) is a regulatory phosphorylation site, threonine 222 (T222) in human MK2 (Ben-Levy et al. 1995; Meng et al. 2002; Gaestel 2006). This region is predicted to be intrinsically disordered and was not resolved in the MK2 crystal structure (Fig. 1.3) (Meng et al., 2002). Other regulatory phosphorylation sites, serine 272 (S272) and T334 for human MK2, are found in a hinge region between the catalytic domain and the C-terminal regulatory domains (residues 328-400) (Fig 1.2) (Ben-Levy et al. 1995; Meng et al. 2002; Gaestel 2006). Phosphorylation of any two of these three residues leads to the activation of MK2 (Ben-Levy et al. 1995).

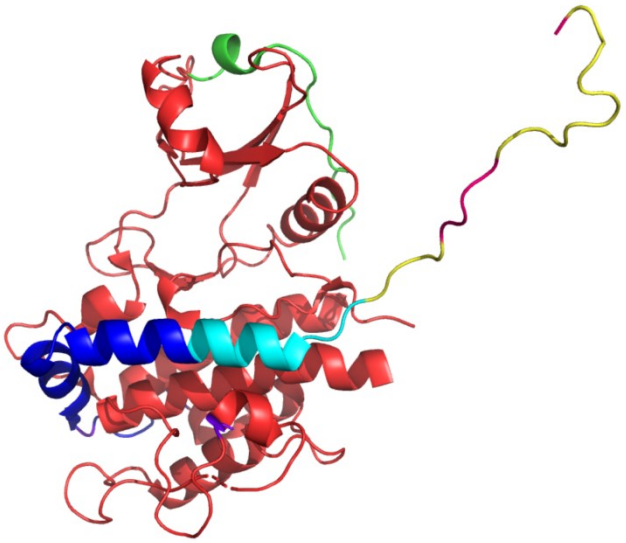

Figure 1.3 Three-dimensional structure of MK2. MK2 structure as resolved by Meng et al. 2002. Residues 1-45 (Proline-rich N-terminus) and 217-235 (activation loop) were not resolved in this structure. T272 and T334 are shown in purple. Green: residues 46-63. Red: kinase domain (64-325). Dark blue: autoinhibitory helix (328-364). Cyan: NES (356-365). Yellow: p38 docking site (366-390). Pink: bi-partite NLS (371-374, 385-389 [only residue 385 resolved]). Generated in PyMOL 2.3.3 (Schrodinger) from PBD 1KWP.

MK2 can shuttle between the nucleus and cytoplasm by virtue of a C-terminal bipartite nuclear localization sequence and export sequence (NLS and NES, respectively) (Fig. 1.2) (Ben-Levy et al. 1998; Gaestel 2006). Additionally, the C-terminus contains an autoinhibitory helix that binds tightly to the catalytic domain when MK2 is inactive, masking the NES in a hydrophobic pocket present in the catalytic domain (Cargnello and Roux, 2011; Gaestel, 2006; Meng et al., 2002). The remaining C-terminal sequence of the regulatory domain disrupts the activation loop and contains p38α and p38β binding sites and the NLS which remain accessible, allowing p38 to form a stable complex with the inactive MK2 that remains in the nucleus (Cargnello and Roux, 2011; Gaestel, 2006). Upon activation of p38 by nuclear MKK3/MKK6, p38 phosphorylates MK2 (Cargnello and Roux, 2011). Phosphorylation of T334 is the major trigger for nuclear export, since it results in a weakening of the interaction between the C-terminal autoinhibitory helix and the catalytic domain, resulting in the unmasking of the export sequence and the localization of activated MK2 to the cytoplasm, where it can phosphorylate and activate its downstream targets (Meng et al., 2002).

1.3.2 Outcomes of MK2 Activation

Owing to its ability to interact with a number of substrates, the biological function of activated MK2 is varied and complex, and the kinase is implicated in a broad range of processes such as cytoskeletal dynamics and motility, cytokine production, gene transcription and cell cycle control (Cargnello and Roux, 2011). Here, only the role of MK2 in cytoskeletal dynamics and post-transcriptional regulation of gene expression will be discussed at length.

1.3.2.1 Actin Cytoskeletal Dynamics

One of the first identified MK2 substrates was the small heat shock protein HSP27, which is a chaperone that keeps unfolded proteins from aggregating together, keeping them in a folding-competent state until they can be refolded by the chaperone HSP70 (Cargnello and Roux, 2011; Rogalla et al., 1999). MK2 phosphorylates HSP27 at S15, S78 and S82, resulting in changes in HSP27 oligomer structure. Unphosphorylated HSP27 aggregates into large oligomers and binds to the barbed (i.e. growing) end of actin filaments, preventing polymerization (Benndorf et al., 1994; Gaestel, 2006; Rogalla et al., 1999; Soni et al., 2019). Upon phosphorylation by MK2, these large oligomers decay into smaller, rod-like oligomers that lack significant chaperone activity, resulting in their release from actin filaments, and are unable to prevent actin polymerization (Benndorf et al., 1994; Cargnello and Roux, 2011; Rogalla et al., 1999; Soni et al., 2019). Additionally, phosphorylated HSP27 has been suggested to interact with the Rho guanine nucleotide exchange factor p115RhoGEF and the GTPase RhoA. The consequence of complex formation is the activation of RhoA GTPase, followed by the activation of its effector kinase, Rho-associated kinase (ROCK)1/2 and actin filament polymerization and actin stress fibre formation (Corcoran et al., 2015; Garcia et al., 2009; Shi et al., 2013). The important role of MK2 in actin cytoskeletal control was demonstrated in MK2-deficient cells; cells lacking MK2 display defects in filopodium formation and motility, suggesting a lack of actin polymerization (Kotlyarov et al. 2002). In addition to these defects, p38 levels were also decreased in MK2-deficient cells, suggesting that complex formation with MK2 stabilizes p38. Interestingly, Kotlyarov et al. (2002) noted that only full-length catalytically-active MK2 with an intact N-terminus could rescue the migratory phenotype, whereas MK2 constructs lacking the N-terminus could not, suggesting a functional role for the N-terminus of MK2 in regulating cell migration.

Furthermore, knockout of the MK2 gene in mice improved survival in response to lipopolysaccharide (LPS) treatment, and resulted in a reduction in the biosynthesis of inflammatory cytokines such as TNF, IL-6 and IFN-γ (Kotlyarov et al. 1999), providing strong evidence to support MK2 as being an important post-transcriptional regulator of gene expression. Normally, LPS treatment elicits a stress response resulting in the activation of MK2, and the outcome of this is the stabilization of a group of cellular RNA messages normally subject to rapid turnover, termed AU-rich element (ARE)-containing mRNAs (ARE-mRNAs) (Gaestel, 2006). These AREs are often found in the mRNA transcripts of inflammatory cytokines such as TNF and make these mRNAs unstable and subject to rapid degradation. MK2 activation mediates TNF biosynthesis by stabilizing ARE-mRNAs (Gaestel, 2006).

1.3.2.2 Post-Transcriptional Gene Regulation

AU-rich elements (AREs) are *cis*-regulatory elements found in the 3' UTR of numerous transiently expressed mRNAs, and consist of a core AUUUA pentamer sequence (Gaestel, 2006; Soni et al., 2019). These elements are bound by numerous RNA-binding proteins (RBPs), some of which happen to be substrates of MK2, including tristetraprolin (TTP) and human R antigen (HuR) (Cargnello and Roux, 2011). These RBPs bind to ARE sequences and either stabilize (HuR), destabilize (TTP), or affect the translation of ARE-mRNAs (Gaestel, 2006). HuR binding stabilizes transcripts by competing with destabilizing RBPs, such as TTP, for ARE-mRNA binding (Soni et al., 2019). In contrast, TTP facilitates transcript deadenylation by presenting ARE-containing transcripts to mRNA decay machinery to facilitate their degradation (Soni et al., 2019). Phosphorylation of S52 and S178 (14-3-3 binding sites) of TTP by MK2 results in TTP being bound by 14-3-3 proteins, interfering with TTP-mediated degradation of ARE-

mRNA transcripts, leading to increased production of cytokines such as TNF (Cargnello and Roux, 2011; Soni et al., 2019). Additionally, the formation of TTP/ARE-mRNA /14-3-3 protein complexes results in their exclusion from cytoplasmic ribonucleoprotein (RNP) granules known as processing bodies (PBs) (Gaestel, 2006).

Processing bodies (PBs) are cytoplasmic granules that are comprised of non-translating mRNAs in complex with proteins associated with translational repression and mRNA decay (Luo et al., 2018). Examples of proteins found in PBs include the deadenylation complex Ccr4-Not, Lsm1-7, and the decapping coactivator and enzyme Dcp1/2, and the decapping activator EDC4 (Hedls) (Parker and Sheth, 2007). Additionally, several mRNA-binding proteins have been found in PBs, including TTP and BRF-1, and evidence suggests that TTP may deliver ARE-mRNAs to PBs for translational repression (Franks and Lykke-Andersen, 2007; Parker and Sheth, 2007). PBs have also been observed to associate with both actin and microtubule cytoskeletal elements, suggesting a link between PBs and the cytoskeleton (Aizer et al., 2008).

The precise function of PBs in cells is a matter of controversy; it was initially believed that PBs were sites of mRNA decay, but the observation that macroscopically visible PBs are not required for mRNA decay to occur has brought this claim into question (Eulalio et al., 2007; Luo et al., 2018). Additionally, mRNAs contained within PBs can recycle back into the cytoplasm to be translated (Brengues et al., 2005). Lastly, while the poly(A) tails of mRNAs found in PBs are more variable in length compared to their cytoplasmic counterparts, truncated mRNA transcripts could not be isolated from PBs (Hubstenberger et al., 2017). Due to these observations, an alternative, though not mutually exclusive, hypothesis has been proposed: that PBs are storage sites for translationally-repressed mRNAs and inactive mRNA decay enzymes (Luo et al., 2018).

1.3.3 Post-Translational Modification of p38 and MK2

While the p38-MAPK pathway regulates a wide array of cellular events, the pathway itself is subject to regulation by various post-translational modifications (PTMs). p38 alone is regulated by three different PTMs, one of which being acetylation. Lysine 53 (K53) and K152 of p38 are acetylated; acetylation of K53 increased p38 ATP binding and kinase activity, whereas the function of K152 acetylation is unclear (Zou and Blank, 2017). Proteomics studies identified at least five lysines within p38 that can undergo ubiquitination, though there is little information regarding the role of ubiquitination in p38 regulation. Lastly, p38 is regulated by phosphorylation, which can both activate and reduce kinase activity depending on the phosphorylation event. MKK3/6 dually phosphorylates p38 on threonine 180 (T180) and tyrosine 182 (Y182), resulting in its activation. Phosphorylation on Y323 results in the autophosphorylation of T180, while phosphorylation of T241reduces the autophosphorylation activity of p38β. Lastly, phosphorylation of S261 of p38β reduces the activity of T180 phosphorylated p38β (Zou and Blank, 2017).

Numerous MK2 protein modifications have been identified in high-throughput proteomic screening studies analyzing protein modifications using methods such as mass spectrometry, and are summarized in the MAPKAPK2 entry in the PhosphoSitePlus database (Cell Signaling Technology). To date, the functional significance of many of these additional modifications is unknown. The known major regulatory protein modifications are phosphorylation at T222, S272, and T334; the phosphorylation of any two of these three residues results in the activation of MK2 (Ben-Levy et al. 1995; Soni, Anand, and Padwad 2019). However, it has also been suggested that MK2 activity is regulated by SUMOylation (Chang et al. 2011).

1.4 SUMOylation

SUMOylation is a highly dynamic PTM involving the attachment of small ubiquitin-like modifiers (SUMOs) to target lysine residues within proteins (Flotho and Melchior, 2013; Pichler et al., 2017).

1.4.1 SUMO Conjugation

Similar to ubiquitin, all SUMO proteins are expressed as premature precursors that must first be maturated and activated by SUMO proteases, resulting in the exposure of the C-terminal di-glycine motif (Flotho and Melchior, 2013). The process of SUMO conjugation begins with a singular E1 enzyme, which is in contrast to ubiquitination which utilizes two E1 enzymes (Zhao, 2007). The E1 enzyme of SUMOylation consists of two subunits termed SAE1/2 (or Aos1/Uba2), which implement a two-step process involving ATP hydrolysis, ultimately resulting in the formation of a thioester bond between the C-terminal di-glycines of SUMO and the SAE2 portion of E1 (Fig. 1.4) (Flotho and Melchior, 2013).

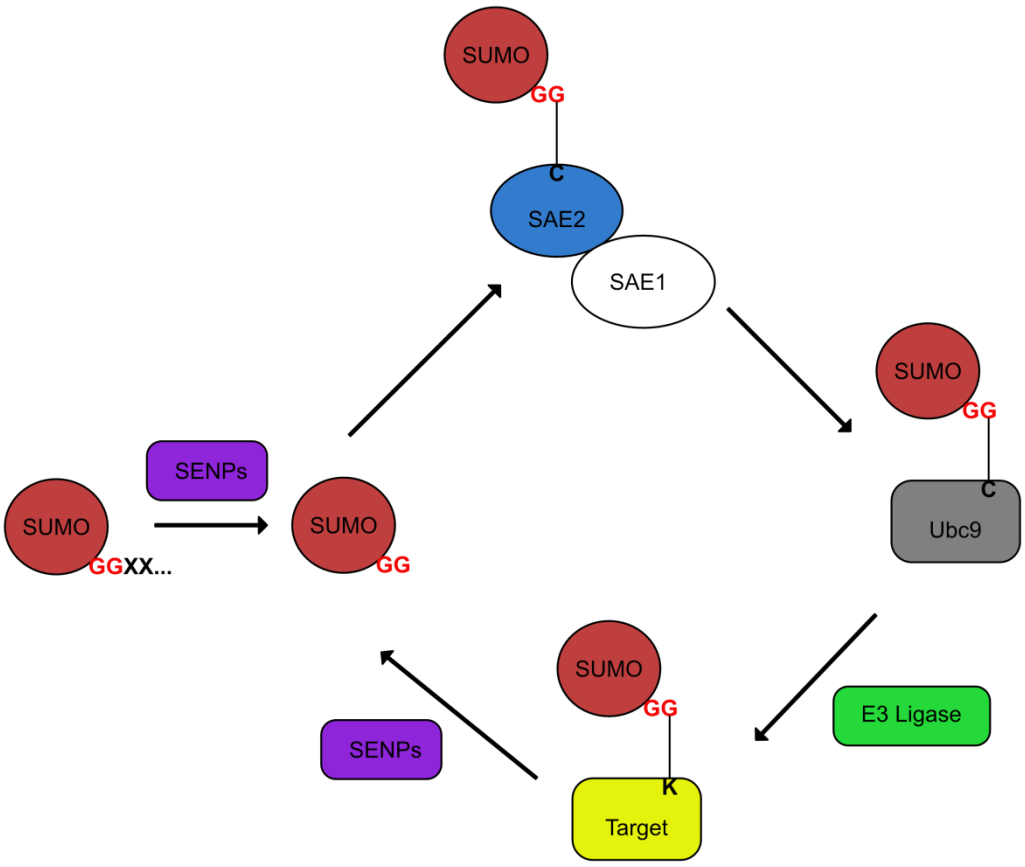

Figure 1.4 The reversible SUMOylation cycle. SUMO proteins are initially expressed as precursors, which must be matured by SUMO proteases (SENPs) to reveal the C-terminal di-glycine (GG) motif. Matured SUMO is activated by the E1 SAE1/2 complex in an ATP consuming reaction, resulting in the formation of a thioester bond between SAE2 and the SUMO protein. SUMO is then transferred to the catalytic cysteine residue of the E2 Ubc9 protein, which facilitates transfer of the SUMO protein to a lysine residue within the target protein with the help of an E3 ligase resulting in the formation of an isopeptide bond. The process is reversible with the help of SENPs, which cleave the isopeptide bond between SUMO and the target to release free SUMO back into the cellular environment.

The SUMO protein is then transferred to the sole E2 enzyme, known as Ubc9, through the interaction of Ubc9 with SAE2; this is also in contrast to ubiquitination, which utilizes a number of E2 enzymes (Flotho and Melchior, 2013; Zhao, 2007). The role of Ubc9 in SUMOylation is to both deliver activated SUMO proteins to the substrate and also select the substrates through the direct recognition of SUMO motifs (ΨKXE, where Ψ is a hydrophobic amino acid) (Flotho and Melchior, 2013). This is in contrast to ubiquitination, which does not have a consensus modification motif (Huang et al., 2016). An additional level of regulation of the SUMOylation cycle is imposed at the E2 level; interaction of Ubc9 with Rhes protein has been shown to enhance the transfer of SUMO from SAE1/2 to Ubc9 and promote the SUMOylation of Ubc9 at K14, K49 and K153, altering Ubc9 substrate preferences (Knipscheer et al., 2008; Subramaniam et al., 2010). Phosphorylation of Ubc9 at S71by CDK1/cyclin B may enhance Ubc9 activity, though this modification has yet to be confirmed *in vivo* (Su et al., 2012).

While substrates have the potential to be SUMOylated by Ubc9 alone, the affinity of Ubc9 for substrates is usually low; therefore, unless Ubc9 is overexpressed, E3 ligase enzymes are required for efficient SUMOylation to occur *in vivo* (Flotho and Melchior, 2013). Two major classes of SUMO E3 ligases have been identified: the PIAS group of proteins, as well as the nucleoporin RanBP2. E3 ligases facilitate the transfer of SUMO from Ubc9 to the substrate in two ways: they stabilize the interaction between the Ubc9-SUMO intermediate and the substrate while holding the Ubc9-SUMO bond in a favorable conformation for attack by the substrate lysine residue (Flotho and Melchior, 2013). There are six different PIAS proteins (PIAS1 and its isoforms PIASxα and PIASxβ, PIAS3, PIASy and Nse2/Mms21), each of which contain an SP-RING domain which is required for interaction with Ubc9 (Flotho and Melchior, 2013). The unrelated

RanBP2 protein forms a complex with Ubc9 and SUMOylated RanGAP1 to form the functional E3 ligase (Werner et al., 2012).

The process of SUMOylation is itself regulated by various PTMs, namely phosphorylation, ubiquitination and acetylation. The interplay between ubiquitination and SUMOylation is large and complex and will not be covered in detail. The acetylation of SUMO1 at K37, or SUMO2 at K33, interferes with SUMO's ability to interact with SUMO interaction motifs (SIMs), impacting the formation of SUMO-mediated protein complexes, and possibly interactions between the Ubc9-SUMO intermediate and the substrate (Flotho and Melchior, 2013; Pichler et al., 2017; Ullmann et al., 2012). SIMs typically consist of regions of hydrophobic residues that are flanked by acidic residues, and facilitate non-covalent interactions with SUMO proteins (Flotho and Melchior, 2013). Alternatively, the phosphorylation of serine residues within SIMs can enhance affinity between SUMO proteins and SIMs (Flotho and Melchior, 2013).

1.4.2 SUMO Deconjugation

The deconjugation of SUMO from substrates is an important aspect of the SUMOylation cycle. The deconjugation of SUMO from substrates in mammals depends on six SUMO proteases (SENP1-3, 5-7), a C98 protease known as USPL1, and two deSUMOylating isopeptidases (DeSI-1/2), which are permuted papain-fold peptidases of ds-RNA viruses and eukaryotes (PPPDEs) that tend to localize to the cytoplasm (Nayak and Müller, 2014). The SENPs differ from each other in respect to localization and SUMO paralog preference. SENP1 and SENP2 are primarily associated with nuclear pore complexes, whereas SENP3 and SENP5 tend to localize to the nucleolus. SENP6 and SENP7 tend to be found in the nucleoplasm. In terms of isoform preference, SENP1 and SENP2 can cleave SUMO1, SUMO2 and SUMO3 linkages, whereas SENP3,

SENP5, SENP6 and SENP7 preferentially cleave SUMO2/3; additionally, SENP6 and SENP7 are involved in the removal of SUMO proteins from SUMO chains (Nayak and Müller, 2014; Zhao, 2007).

1.4.3 SUMO Isoforms

To date, four SUMO isoforms have been identified (SUMO1-4) which share a common structure consisting of a single α-helix surrounded by β-sheets, and a C-terminal di-glycine motif that is exposed by removal of C-terminal residues of the initial SUMO protein by SUMO specific proteases, as is seen for ubiquitin (Bayer et al., 1998; Flotho and Melchior, 2013). However, unlike ubiquitin, the ~20 amino acid N-terminus of SUMO proteins is flexible (Bayer et al., 1998). SUMO1-3 is expressed ubiquitously in most tissues, whereas SUMO4 is thought to mostly be expressed in immune cells (Guo et al., 2004; Pichler et al., 2017). Furthermore, while SUMO4 is very similar to SUMO2/3 (based on sequence), it is not known to be processed by currently identified SUMO proteases; therefore, the function of SUMO4 is currently unknown (Flotho and Melchior, 2013). In one report, SUMO4 interacted with the protein IκBα to downregulate the NFκB response (Flotho and Melchior, 2013; Guo et al., 2004). SUMO2/3 proteins are almost identical to each other (~97% sequence identity), whereas SUMO1 shares 47% sequence identity with SUMO2 (Flotho and Melchior, 2013; Saitoh and Hinchey, 2000). Under normal physiological conditions, SUMO1 is constitutively conjugated to substrates, whereas SUMO2/3 is preferentially conjugated under stress conditions (Saitoh and Hinchey, 2000). The SUMO machinery is predominantly concentrated in the nucleus, and plays an important role in regulating processes such as gene expression, DNA damage responses, and cell cycle progression (Eifler and Vertegaal, 2015). Typically, ten times more SUMO2/3 is expressed in cells compared to SUMO1, and it is

more rapidly deconjugated from substrates compared to SUMO1 (Flotho and Melchior, 2013; Saitoh and Hinchey, 2000). Another factor differentiating SUMO1 from SUMO2/3 is the ability to form chains; due to the presence of a SUMOylatable lysine (K11), SUMO2/3 can form chains, whereas SUMO1 lacks this SUMOylation site and as a PTM is restricted to the mono-SUMOylation of a target lysine, or as a SUMO2/3 chain terminator. Little is known about the functional significance of SUMO chain formation, though they appear to be important for substrate targeting by SUMO-targeted ubiquitin ligases (STUbLs) (Flotho and Melchior, 2013; Sriramachandran and Dohmen, 2014). STUbLs interact with SUMO chains and ubiquitinate them, resulting in outcomes such as the degradation of the substrate or altered localization and function (Sriramachandran and Dohmen, 2014). STUbLs are important coordinators of DNA damage responses; depletion of the human STUbL RNF4 from cells using siRNA resulted in hypersensitivity to certain types of DNA damage, as well as a reduction in the percentage of cells with K63-linked ubiquitin chains at sites of DNA damage (Sriramachandran and Dohmen, 2014; Yin et al., 2012). In contrast, the percentage of cells with K48-linked ubiquitin chains at sites of DNA damage was unaffected by RNF4 depletion, suggesting that these RNF4-mediated ubiquitination events may not be solely degradative (Sriramachandran and Dohmen, 2014; Yin et al., 2012).

SUMOylation is conserved in most eukaryotic cells and appears to be essential for survival in most cases, though the importance of one SUMO paralog over another often depends on the organism in question. Mice lacking SUMO3 are viable and do not show major developmental defects, and while the loss of SUMO1 in mice is not lethal, it is associated with developmental deficits and a loss of promyelocytic leukemia protein (PML) nuclear bodies, suggesting that SUMO2/3 can compensate for a loss of SUMO1,

at least partially (Eifler and Vertegaal, 2015; Evdokimov et al., 2008). SUMO2 appears to be the only essential paralog, since SUMO2-deficient mice showed severe developmental defects and died during embryonic development; this is because SUMO2 is critical for cell cycle control (Eifler and Vertegaal, 2015). In zebrafish and other organisms such as *Arabidopsis thaliana* SUMO paralogs appear to serve redundant functions (Saracco et al., 2007; Yuan et al., 2010).

1.4.4 SUMOylation and Protein Function

Many of the first proteins to be confirmed to be modified by SUMOylation were nuclear proteins, and because of this, this PTM has been implicated in coordinating a broad range of activities including cell cycle progression, cell division and proliferation, as well as the regulation of cell survival or apoptosis pathways (Zhao, 2007). However, while the SUMO machinery is concentrated in the nucleus, it has also been detected in the cytoplasm, and as experience in the field grows, more non-nuclear SUMOylated proteins are being identified, potentially implicating this modification in all aspects of cell biology (Flotho and Melchior, 2013). Precisely how SUMOylation impacts protein function is substrate specific, though it appears that SUMOylation affects substrates in three major non-exclusive ways. The first is that SUMO modification can interfere and/or compete with other PTMs and protein interactions by blocking interaction sites (Flotho and Melchior, 2013). Such a process has been shown to inactivate enzymes and prevent the aggregation of unfolded proteins (Flotho and Melchior, 2013; Krumova et al., 2011). Secondly, the conjugation of SUMO to a protein can result in conformational changes that can influence protein activity, as is seen for several DNA repair enzymes (Flotho and Melchior, 2013). More commonly, modification of a protein by SUMO

provides a necessary interaction site for downstream effectors in certain pathways (Flotho and Melchior, 2013).

An interesting observation is that the propensity of a given target to be modified by SUMOylation is often modulated by the phosphorylation state of the substrate. Many variations of the traditional SUMO motif have been identified, with one such variation being known as a phosphorylation-dependent SUMO motif (PDSM), an N-terminally extended SUMO motif containing a phosphorylated serine (ΨKXEXX[pS]P)(Flotho and Melchior, 2013; Yao et al., 2011). The SUMOylation of a number of transcription factors has been shown to be dependent on phosphorylation of the substrate, while for other proteins, phosphorylation negatively regulates SUMOylation through mechanisms such as the phosphorylation-dependent recruitment of SENPs to substrates (Flotho and Melchior, 2013). In particular, when SUMOylation is inhibited in cells by treatment with ginkgolic acid (which prevents formation of the SUMO-E1 intermediate), tyrosine phosphorylation is decreased; conversely, overexpression of SUMO proteins, and the resultant increase in global SUMOylation, was tied to increases in tyrosine phosphorylation, suggesting a link between the two modifications (Lowrey et al., 2017; Yao et al., 2011). In the case of the tyrosine kinase focal adhesion kinase (FAK), ginkgolic acid-mediated decreases in SUMOylation were correlated with decreased FAK activity (Yao et al., 2011). Another example of phosphorylation-regulated SUMOylation comes from the signal transducer STAT1. STAT1 is phosphorylated by p38 MAPK at S727, and this phosphorylation event is associated with increases in SUMO1 modification of STAT1 at K703 (Vanhatupa et al., 2008).

1.4.5 Regulation of MK2 by SUMOylation

In 2011, murine MK2 was found to be SUMOylated at K339 (equivalent to K353 in human MK2) (Chang et al. 2011). When K339 in murine MK2 was mutated to arginine to prevent SUMOylation at this site, the MK2 SUMOylation profile was diminished but not completely abolished, suggesting that this site is a major target for SUMOylation, but there are likely other SUMOylation sites within MK2. Importantly, this loss of SUMOylation was associated with increased and prolonged HSP27 phosphorylation compared to WT MK2. Additionally, loss of MK2 SUMOylation at K339 exacerbated actin stress fibre formation in response to TNF treatment. These results suggest that MK2 SUMOylation may act as a dampener for MK2 kinase activity (Chang et al. 2011).

1.5 Viruses and SUMOylation

Given that SUMOylation regulates a wide variety of processes, particularly those involved in immunity and anti-viral responses, it is not surprising that viruses have developed ways to hijack this process for their own benefit (Lowrey et al., 2017). Disruption of global SUMOylation is a common feature of herpesvirus infection; repression of SUMOylation promotes viral propagation during lytic infection, while increased SUMOylation appears to promote herpesvirus latency. A similar observation can be made during influenza infection, which upregulates global cellular SUMOylation (Lowrey et al., 2017). Specific examples of viral reprogramming of cellular SUMOylation have been observed during most steps of the process; some specific examples are discussed in detail below.

1.5.1 Viruses That Antagonize SUMOylation

The SUMO-activating machinery is a common target for the inhibition of SUMOylation, not just for viruses, but also for pharmacological compounds such as ginkgolic acid and Davidiin, which interfere with the formation of the E1-SUMO intermediate (Lowrey et al., 2017). The avian adenovirus CELO (chicken embryo lethal orphan) interferes with the formation of the E1-SUMO intermediate, through the degradation of the SAE1/2 complex. The viral ubiquitin ligase Gam1 forms a complex with SAE1/2, resulting in the ubiquitination and subsequent degradation of the SAE1 subunit (Boggio et al., 2007). The increasing levels of unpaired SAE2 triggers its subsequent degradation by the proteasome (Boggio et al., 2007). This leads to an accumulation of unmodified SUMO substrates, the accumulation of SUMO1 in the cytoplasm, and the loss of PML nuclear bodies, leading to enhanced viral propagation (Lowrey et al., 2017). In addition to mediating the degradation of SAE1/2, the chicken adenovirus Gam1 protein also mediates the degradation of Ubc9 by the proteasome (Boggio et al., 2004). The most common aspects of SUMOylation targeted by viruses are the E3 ligases, which includes the RanBP2 and the PIAS group proteins (Lowrey et al., 2017). Viruses can down regulate E3 ligases to repress SUMOylation, as is observed by the HPV E6 protein, which targets PIASy, decreasing its ligase activity to suppress the SUMOylation of p53, preventing cellular senescence (Bischof et al., 2006). Another mechanism utilized by viruses to antagonize SUMOylation is SUMO-targeted ubiquitin ligases (STUbLs). STUbLs recognize SUMOylated proteins and ubiquitinate them, which commonly results in their degradation (Sriramachandran and Dohmen, 2014). An example of a virally expressed STUbL is the ICP0 protein of HSV1, which in addition to

its STUbL activity also disrupts the recruitment of PIAS1 to sites of viral replication, promoting lytic replication (Lowrey et al., 2017).

1.5.2 Viruses That Co-Opt or Refocus SUMOylation

Viruses have been demonstrated to manipulate SUMOylation by co-opting or hijacking the SUMOylation machinery, and many do so through direct interactions with Ubc9 (Lowrey et al., 2017). During EBV latency, the viral LMP1 protein can bind to and hijack Ubc9 to promote the SUMOylation of cellular targets involved in innate immunity, resulting in the maintenance of viral latency (Bentz, Whitehurst, and Pagano 2011; Bentz et al. 2015). Human papillomavirus (HPV) also hijacks Ubc9 using its E2 protein, which is itself SUMOylated through the interaction, resulting in the repression of viral promoters and the activation of cellular promoters (Wu et al., 2008). Many viruses increase the expression of various PIAS proteins to promote viral replication, including HSV1, which increases the expression of PIASy and recruits it to viral genomes in the nucleus, resulting in the regulation of anti-viral immune responses and the promotion of viral replication (Conn et al., 2016; Lowrey et al., 2017).

1.5.3 KSHV and SUMOylation

Some viruses express so-called “E3 ligase mimics”, which can be best thought of as viral E3 ligases; one is the K-bZIP protein of KSHV (Lowrey et al., 2017). Many functions have been ascribed to K-bZIP, including hijacking Ubc9 to promote the SUMOylation of transcription factors and histones, ultimately resulting in the repression of certain viral promoters, similar to how the LMP1 protein of EBV functions (Izumiya et al., 2005). However, unlike LMP1, K-bZIP also functions as a SUMO E3 ligase, showing specificity for SUMO2/3, and promotes the SUMOylation of p53 and Rb, ultimately regulating lytic reactivation (Chang et al. 2010; Lowrey, Cramblet, and Bentz

2017). In addition, K-bZIP is SUMOylated at K158, a modification required for its activity as a transcriptional repressor (Chang and Kung 2014). Another KSHV protein, LANA, is SUMOylated at K1140 and has both N- and C-terminal SIM domains, which are important for the maintenance of the latent viral genome (Cai et al., 2013). In addition, preliminary evidence suggests that LANA may function as an E3 ligase, recruiting the Ubc9-SUMO intermediate to cellular histones to promote their SUMOylation (Campbell and Izumiya, 2012). RTA, the KSHV protein associated with lytic reactivation, also functions as a STUbL; without this function, RTA cannot induce KSHV replication (Campbell and Izumiya 2012; Chang and Kung 2014). This function allows RTA to decrease the amounts of SUMO-modified proteins, and preferentially degrades its antagonist K-bZIP (Chang and Kung 2014). Another example of KSHV antagonizing SUMOylation is observed through its viral protein kinase (vPK). vPK is a serine/threonine kinase that localizes to the nucleus, and phosphorylates K-bZIP at T111, resulting in decreased K-bZIP SUMOylation and a loss of its activity as a transcriptional repressor (Chang and Kung 2014).

1.5.4 KapB and SUMOylation

Currently, the mechanism behind the KapB-mediated activation of MK2 is unknown (McCormick and Ganem, 2005). KapB activates the MK2/RhoA signaling axis to induce the formation of stress fibres, the stabilization of inflammatory ARE-mRNAs, and the disassembly of PBs, all of which may be linked to increased MK2 activity mediated by KapB (Corcoran et al., 2015; McCormick and Ganem, 2005). Others have observed similar phenotypes when MK2 SUMOylation at K353 is disrupted. This disruption of SUMOylation leads to increased and prolonged HSP27 phosphorylation compared to WT MK2, and exacerbates stress fibre induction in response to TNF (Chang

et al. 2011). Due to these similarities in phenotype, it was logical to hypothesize that KapB might regulate MK2 through its SUMOylation.

1.6 Rationale and Goals

Given the propensity for herpesviruses to disrupt SUMOylation (Lowrey et al., 2017), and the similarity between the MK2 phenotypes induced by KapB expression and a loss of SUMOylation, *I hypothesize that KapB disrupts MK2 SUMOylation*. To address this hypothesis, my research goals were : 1) To use immunoprecipitation to characterize the SUMOylation status of MK2 in both the presence and absence of KapB expression, and 2) to determine if a non-SUMOylatable version of MK2 phenocopies KapB, specifically KapB-induced stabilization of ARE-mRNAs and PB disassembly.

CHAPTER 2 MATERIALS AND METHODS

2.1 Cell Culture

Human embryonic kidney 293T cells (HEK293T) (ATCC), human cervical epithelial carcinoma (HeLa) cells expressing a tetracycline-regulated trans-activator (HeLa Tet-Off) (Clontech), and HeLa Flp-In T-REx cells stably expressing GFP-Dcp1a or GFP-3x FLAG (a generous gift from Dr. Anne-Claude Gingras, Lunenfeld Ist.) were maintained at 37°C in a 5% CO_2 humidified atmosphere in Dulbecco's Modified Eagle Medium (DMEM) (Gibco) with 100 U/mL penicillin, 100 µg/mL streptomycin, 2mM L-glutamine (1% PSQ) (Gibco) and 10% heat-inactivated fetal bovine serum (HI-FBS) (Gibco). To induce the expression of either GFP-Dcp1a or GFP-3x FLAG, cells were treated with 1 µg/mL doxycycline (dox, Sigma Aldrich Canada). Cells were sub-cultured at 90% confluency, washing with phosphate-buffered saline (PBS, Gibco) then treated with 0.25% trypsin-ethylenediaminetetraacetic acid (EDTA) (Gibco). Media was refreshed as needed.

2.2 Plasmids and Subcloning

The plasmids used and/or generated in this study are listed in Table 2.1. Plasmids generated in this study were verified by Sanger DNA sequencing (GENEWIZ). All DNA stocks were prepared using the Qiagen Plasmid Plus Midi Kit (Qiagen) according to manufacturer’s directions.

Table 2.1 Plasmids used in this study.

Plasmid	Source
pcDNA3.1-FLAG-MK2	This study
pcDNA3.1-FLAG-MK2-KR	This study
pcDNA3.1-FLAG-MK2-EE	This study
pcDNA3.1-FLAG-MK2-KR-EE	This study
pcDNA 3.1(+)	Invitrogen
pcDNA-KapB (BCBL)	Dr. Craig McCormick (Dalhousie University
pEGFP-KapB	Dr. Crag McCormick (Dalhousie University)
pLJM1-HA-SUMO3	Dr. Craig McCormick (Dalhousie University)
pLJM1-Ubc9-HA	Dr. Craig McCormick (Dalhousie University)
pLJM1-LANA	Dr. Craig McCormick (Dalhousie University)
pCMV-myc-SUMO2	Dr. Jayme Salsman (Dalhousie University)
pEGFP	Clontech
pLJM1-BSD	Dr. Craig McCormick (Dalhousie University)
pTRE2-FLUC-ARE	Dr. Craig McCormick (Dalhousie University)
pTRE2-RLUC	Dr. Craig McCormick (Dalhousie University)

2.2.1 Design of Constructs Purchased from Biobasic

The coding sequence (CDS) for human MK2 was referenced from NCBI GenBank (reference sequence NM_032960.4). MK2-K353R was designed by altering the CDS, changing lysine codon 353 (AAG) to arginine (CGT). A FLAG epitope tag was incorporated upstream of the MK2 CDS and fused in frame to MK2 through a six-glycine linker sequence. BamHI and NheI restriction sites flanking the FLAG-MK2 sequence were included to permit subcloning into the mammalian expression vector pcDNA 3.1. Gene blocks based on these sequences were purchased from Biobasic Canada Inc. in the bacterial expression plasmid pUC57.

2.2.2 Designing Mutagenesis Performed by Biobasic

To create pcDNA3.1-FLAG-MK2-T222E-T334E (FLAG-MK2-EE) and pcDNA3.1-FLAG-MK2-K353R-T22E-T334E (FLAG-MK2-KR-EE), previously subcloned and sequence-verified pcDNA3.1-FLAG-MK2 was sent to Biobasic Canada Inc. to perform the site-directed mutagenesis. Two threonine codons at positions 222 (ACT) and 334 (ACC) were altered to encode glutamic acid (GAG) and the lysine codon at position 353 (AAG) was substituted to an arginine codon (AGG). Sequences were verified using CMV-Forward primer from GENEWIZ [5'-CGCAAATGGGCGGTAGGCGTG-3'] and pcDNA Rev primer [5'-AACAACAGATGGCTGGCAAC-3']. Since constructs remained in pcDNA3.1 throughout mutagenesis, subcloning was not required.

2.2.3 Subcloning

pUC57-FLAG-MK2, pUC57-FLAG-MK2-K353R (FLAG-MK2-KR) and pcDNA 3.1 (+) were digested with the enzymes NheI and BamHI. Digested products

were subjected to 1% agarose gel-electrophoresis using 1X TAE buffer (40 mM Tris, 20 mM acetic acid, 1 mM EDTA) and 100 V. The digested products were visualized using the ChemiDoc Touch Imaging system (BioRad) and the MK2 DNA fragment of interest excised and extracted from the gel using the QIAQuick Gel Extraction kit (Qiagen) following manufacturer's instructions. Digested and purified FLAG-MK2 and FLAG-MK2-KR DNA fragments were ligated into linearized pcDNA 3.1 (+). Sequences were verified using CMV-Forward primer from GENEWIZ [5'-CGCAAATGGGCGGTAGGCGTG-3'] and pcDNA Rev primer [5'-AACAACAGATGGCTGGCAAC-3'].

2.3 Transfection

For immunoprecipitation experiments designed to detect SUMOylation, HEK293T cells were seeded in 10-cm dishes so that they would be ~80% confluent by the next day. Cells were transfected the next day with 10 µg total DNA (500 ng EGFP, 2 µg LANA [or pLJM1] or FLAG-MK2 [various constructs] [or pcDNA3.1], 2 µg Ubc9-HA [or pLJM1], and 5.5 µg myc-SUMO2 [or pcDNA3.1] or HA-SUMO3 [or pLJM1]). DNA was diluted in 500 µL OPTI-Mem (Gibco). A solution consisting of 30 µL 1 mg/mL polyethyenimine (PEI, 40 kDa, Polysciences, pH 7.0) and 500 µL OPTI-Mem was added. The DNA/PEI mix was incubated for 15 minutes at room temperature. Cells were washed once with PBS, supplied with 4 mL serum-free DMEM and the DNA/PEI solution added to plates dropwise. After 4-6 hours, media was replaced with DMEM supplied with 1% PSQ and 10% HI-FBS. After 48 hours of incubation, cells were lysed for immunoprecipitation. Alternately, if the experiment included KapB expression, cells were transfected with 12 µg total DNA (500 ng EGFP, 2 µg FLAG-MK2 [various

constructs] [or pcDNA3.1], 2 µg Ubc9-HA [or pLJM1], 2 µg KapB [BCBL] [or pcDNA3.1], and 5.5 µg HA-SUMO3[or pLJM1]), and the remainder of the procedure was as above. For co-immunoprecipitation experiments for KapB and MK2, cells were transfected with 4.5 µg total DNA (500 ng EGFP, 2 µg FLAG-MK2, 2 µg KapB [BCBL] [or pcDNA3.1]) or 4.0 µg total DNA (2 µg FLAG-MK2 [or pcDNA3.1], 2 µg GFP-KapB [or pEGFP]) and 13.5 or 12 ul 1mg/ml PEI, respectively. The remainder of the procedure was as above.

2.4 Immunoprecipitation

For immunoprecipitation experiments to detect SUMOylation, transfected HEK293T cells were collected using a cell scraper and cold PBS supplemented with 10 mM N-ethylmaleimide (NEM, Sigma Aldrich) and protease inhibitor cocktail (cOmplete™, Mini, EDTA-free Protease Inhibitor Cocktail, Roche) and pelleted by centrifugation at 500x g for 5 minutes at 4°C. Cells were lysed in 200 µL cold denaturing lysis buffer (2% SDS, 10% glycerol, 62.5 mM Tris pH 6.8) supplied with 20 mM NEM and protease inhibitor cocktail, boiled for 5 minutes then sonicated for 90 seconds total at 30% amplitude, in 30-second bursts of sonication then cooling. Lysates were cleared by centrifugation at 13,000xg for 15 minutes at 4°C, and ~40 µL of concentrated lysate was reserved for immunoblotting to verify construct expression. Lysates were diluted with 800 µL cold IP buffer (50 mM Tris pH 8.0, 150 mM NaCl, 1% NP-40) supplied with 20 mM NEM and protease inhibitor cocktail. LANA or MK2 antibody (see Table 2.2 for details) was added to diluted lysates at 1:100 dilution and incubated with rotation overnight at 4°C. Equilibrated protein G magnetic beads (SureBeads™ Protein G Magnetic Beads, Bio-Rad) (50 µL) were added to each lysate and the mixture incubated for 1 hour at 4°C with rotation. Beads were washed 3 times for 5 minutes with cold IP

buffer, and protein released in 35 µL 2X Laemmli sample buffer (4% SDS, 20% glycerol, 120 mM Tris pH 6.8) by boiling at 95°C for 5 minutes.

For co-IP experiments, cells were resuspended in 500 µL modified radio-immunoprecipitation (RIPA) buffer (50 mM Tris pH 7.4, 150 mM NaCL, 1 mM EDTA, 1% Nonidet P-40 [NP-40], 0.1% SDS) supplemented with 1 mM dithiothreitol (DTT), 1 mM phenylmethane sulfonyl fluoride (PMSF), 20 mM NEM, 0.1 mM iodacetamide, and protease inhibitor cocktail. Cells were lysed with rotation for 30 minutes at 4°C. Cellular debris was then pelleted by centrifugation at 10,000xg for 5 minutes, and the supernatant aspirated into a fresh tube. After overnight antibody incubation, 25 µL equilibrated protein G magnetic beads was added to each lysate. The rest of the procedure was as above, releasing protein in either 35 or 60 µL 2X Laemmli buffer, depending on the intended downstream analysis.

Table 2.2 Antibodies used in this study for immunoprecipitation.

Antibody	Source	Dilution
α-MAPKAPK2 (rabbit)	Cell Signaling Technology (#12155)	1:100
α-LANA (rat)	Santa Cruz Biotechnology (sc-57808)	1:100
α-KapB (rabbit)	Dr. Craig McCormick (Dalhousie Univ.)	1:100
α-GFP (mouse)	Cell Signaling Technology (#2955)	1:100
IgG1 (mouse)	Cell Signaling Technology (#5415)	1:100

2.5 Protein Electrophoresis and Immunoblotting

HEK293T cells in 12-well plates were washed with PBS and lysed in 200 µL 2X Laemmli buffer. For immunoprecipitation experiments, 40 µL lysate was reserved prior to antibody incubation and mixed with 13.3 µL 4X Laemmli buffer (30 mM Tris pH 6.8, 50% glycerol, 1% SDS) to a final concentration of 1X. Total protein concentration was quantified using the DC™ protein assay kit (BioRad) according to manufacturer's instructions. A standard curve was generated using serial dilutions (0 to 2.8 µg/mL) of bovine serum albumin (BSA, Bioshop) in matched buffer. Absorbance at 750 nm was measured using the BioTek Eon microplate reader and Gen5 software (version 2.03.1). Following quantification, DTT was added to lysates to a final concentration of 15 mM, and bromophenol blue (Sigma) added to a final concentration of .0006% (w/v). Lysates were boiled for 5 minutes at 95°C prior to electrophoresis.

Unless otherwise indicated, total cellular protein (10 µg) was resolved using 10%-SDS-polyacrylamide gel electrophoresis (SDS-PAGE) at a constant current of 17 A until the dye front ran off the bottom of the gel. Alternately, for the large LANA protein, electrophoresis conditions were modified, resolving proteins on a 7.5% polyacrylamide gel at a constant voltage of 100 V. For actin immunodetection, samples were run in duplicate gels; signal overlap between actin and other proteins of interest precluded cutting of membranes to probe for both from a single membrane. Proteins were transferred onto PVDF membrane (Trans-Blot® Turbo™ Midi PVDF, BioRad), modifying the preset mixed molecular weight transfer conditions (25V, 7 minutes) to 10 minutes for most transfers, and for LANA, 15 minutes. Membranes were blocked in either 2.5% BSA or 2.5% skim milk in 1X TBS-T (150 nM NaCl, 10 mM Tris, pH 7.8, 0.01% Tween-20 [Sigma]) for 45 minutes at room temperature with rocking. Antibodies

were diluted as indicated (Table 2.3) and incubated with the membranes overnight at 4°C with rocking. Membranes were washed twice for 10 minutes at room temperature using 1X TBS-T. Secondary IgG antibodies conjugated to horseradish peroxidase (HRP) were diluted in 2.5% BSA or skim milk and incubated with membranes for 45 minutes at room temperature with rocking. Membranes were washed 4 times for 5 minutes at room temperature using 1X TBS-T, before being incubated with Clarity Western ECL Substrate (BioRad) according to manufacturer's instructions. The ChemiDoc Touch Imaging system was used to visualize chemiluminescence signal. Images were processed using Image Lab 6.0 (BioRad).

Table 2.3 Antibodies used in this study for immunoblotting.

Antibody	Source	Dilution
α-MAPKAPK2 (rabbit)	Cell Signaling Technology (#12155)	1:1000 in 2.5% BSA
α-LANA (rabbit)	Dr. Craig McCormick (Dalhousie Univ.)	1:1000 in 2.5% milk
α-myc (mouse)	Cell Signaling Technology (#2276)	1:500 in 2.5% milk
α-HA (mouse)	Cell Signaling Technology (#2367)	1:500 in 2.5% milk
α-FLAG (mouse)	Cell Signaling Technology (#8146)	1:1000 in 2.5% BSA
α-FLAG (rabbit)	Cell Signaling Technology (#14793)	1:1000 in 2.5% milk
α-KapB (rabbit)	Dr. Craig McCormick (Dalhousie Univ.)	1:1000 in 2.5% milk
α-IgG (HRP conjugated) (rabbit)	Cell signaling Technology (#7074)	1:2000 in same solution as primary
α-IgG (HRP conjugated) (mouse)	Cell signaling Technology (#7076)	1:2000 in same solution as primary
β-actin (HRP conjugated) (rabbit)	Cell Signaling Technology (#5125)	1:4000 in 2.5% BSA

2.6 Immunofluorescence

HeLa Flp-In T-REx GFP-Dcp1a or GFP-3x FLAG cells were seeded at 30,000 cells/mL in 12-well plates onto glass coverslips (1.5 mm thickness, 12 mm diameter, Electron Microscopy Sciences). After 24 hours of incubation, the expression of either GFP-Dcp1a or GFP-3x FLAG was induced by treating cells with 1 µg/mL dox. The next day, cells were transfected with 1 µg DNA (various MK2 constructs, BCBL KapB, empty vector). DNA was diluted in 50 µL OPTI-Mem, mixed with 3 µL 1 mg/mL PEI in 50 µL OPTI-Mem, and incubated for 15 minutes at room temperature. Cells were washed once with PBS and supplied with 4 mL serum-free DMEM and the DNA/PEI solution added to plates drop-wise. After 4-6 hours, media was replaced with DMEM supplied with 1% PSQ and 10% HI-FBS. After 48 hours, cells were washed with PBS and fixed at room temperature for 10 minutes in 4% paraformaldehyde (v/v) (Electron Microscopy Sciences) in 1X PBS (137 mM NaCl, 2.7 nM KCl, 10 mM Na2HPO4, 1 mM KH2PO4). Cells were washed 3 times with PBS, then permeabilized with 0.1% Triton-X100 (v/v) (Sigma) in 1X PBS for 5 minutes at room temperature. Cells were subsequently washed 3 times with PBS, then blocked in 1% human AB serum (Sigma) in 1X PBS (blocking buffer) for 30 minutes at room temperature. Coverslips were then incubated with primary antibodies according to the antibody dilutions and incubation times found in Table 2.4. Primary antibody was removed with three quick washes of PBS at room temperature. Coverslips were then incubated with fluorescent secondary antibody in a dark environment, then removed with three quick washes of PBS at room temperature. Alexa Fluor™ 647 phalloidin dye (#A22287, Molecular Probes) was diluted 1:100 in 1X PBS, then incubated with coverslips for one hour at room temperature in the dark. Cells were washed once with PBS, then mounted onto microscope slides (FisherBrand) using with

ProLong Gold antifade mounting medium (Invitrogen). Slides were allowed to cure overnight.

Table 2.4 Antibodies used for immunofluorescence.

Antibody	Source	Staining Procedure
α-Hedls (mouse IgG1)	Santa Cruz Biotechnology (sc-8418)	1:1000 in blocking buffer O/N at 4°C
α-FLAG (mouse IgG1)	Cell Signaling Technology (#8146)	1:1600 in blocking buffer O/N at 4°C
α-KapB (rabbit)	Dr. Craig McCormick (Dalhousie Univ.)	1:1000 in blocking buffer for 30 minutes at R/T
Alexa Fluor® 555-conjugated donkey anti-mouse IgG H+L	Molecular Probes (#A31570)	1:1000 in blocking buffer for 1 hour at R/T
Alexa Fluor 555-conjugated donkey anti-rabbit IgG H+L	Molecular Probes (#A31572)	1:1000 in blocking buffer for 1 hour at R/T

2.7 Quantification of Dcp1a Puncta

Transfected HeLa Flp-In T-REx GFP-Dcp1a cells were analyzed using a Zeiss LSM 510 Upright Laser Scanning Confocal Microscope and 63x oil immersion objective. The number of Dcp1a puncta per cell was counted manually, and the mean number of Dcp1a puncta per cell per condition calculated. At least 60 cells per condition were counted.

2.8 Luciferase Assay

The luciferase reporter assay used to detect changes in ARE-mRNA stability has previously been described (Corcoran et al., 2011). Briefly, HeLa Tet-off cells were seeded in 12-well plates so that they would be 80% confluent within 24 hours (using 100,000 cells/mL seeding density). Media was replaced with antibiotic-free DMEM containing 10% HI-FBS. Cells were co-transfected with 100 ng of reporter plasmid master mix (pTRE2-FLUC-ARE and pTRE2-RLUC, 9:1 ratio) and 900 ng of expression/empty plasmid, using 3 µl of Fugene HD (Roche) according to manufacturer directions. Twenty-four hours after transfection, dox was added (1 µg/ml) to stop *de novo* transcription from the pTRE reporter plasmids. Cells were incubated for 12 hours and then lysed with 250 µL 1X passive lysis buffer and processed using the dual-luciferase assay kit (Promega). Cell lysate (5 µL) was manually added to 25 µL Luciferase Assay Reagent II to obtain firefly luciferase activity. Stop & Glo® Reagent (25 µL) (with appropriately diluted substrate) was added to the same tube to obtain Renilla luciferase activity. Firefly and Renilla luminescence was determined using the GloMax 20/20 luminometer (Promega) and is expressed as relative light units (RLU). Firefly RLUs were normalized to Renilla RLUs to account for differences in transfection efficiency, and data is represented as relative luciferase activity. The mean-fold change in relative

luciferase activity was obtained by normalizing the relative luciferase activity of the various constructs to empty vector and represents changes in ARE-mRNA stability caused by each construct compared to empty vector.

2.9 Statistical Analysis

Graphing and statistical analyses were performed using GraphPad Prism 8.2.0 software. The 'n' value represents the number of biologically independent experiments performed and is noted in figure legends. A one-way analysis of variance (ANOVA) with a Tukey multiple comparisons test was used to analyze sample means between multiple conditions. Results were considered statistically significant when $p \leq 0.05$. Statistical significance is also noted in figure legends.

CHAPTER 3 RESULTS

3.1 MK2 SUMOylation is Enhanced by Phospho-mimicking Residues

In order to determine if KapB activates MK2 by disrupting its SUMOylation, the previously reported SUMOylation of MK2 had to first be recapitulated as a positive control (Chang et al. 2011). This had to be reaffirmed because, despite SUMOylation being a covalent protein modification, it is difficult to detect (Xiao et al., 2015). This is due in large part to two factors: only a small pool of the target protein (5-10%) will be modified by SUMO at a time, and the SUMO modification is rapidly lost from target proteins during cell lysis due to the presence of SUMO proteases (SENPs), which rapidly deconjugate SUMO from the targets (Xiao et al., 2015). To overcome these factors, several steps can be taken to increase the odds of detection.

Overexpression of the SUMO-conjugating enzyme Ubc9, in addition to the activated form of the SUMO protein and the target protein, has been found to increase SUMO modification (Flotho and Melchior, 2013; Karhausen et al., 2018). This is because Ubc9 typically has low affinity for substrates in the absence of E3 ligases, though the overexpression of Ubc9 will nonetheless drive the system (Flotho and Melchior, 2013).

Due to the low rates of SUMO modification at any given time, cells transfected with the target and SUMOylation machinery should be grown in large numbers, and lysed in a small volume of denaturing lysis buffer that contains a high percentage of sodium dodecyl sulfate (SDS), to obtain a highly concentrated cellular lysate (Xiao et al., 2015). This form of lysis has several benefits over traditional non-denaturing approaches, the first being that SENPs are immediately denatured and inactivated. Additionally, denaturing lysis will remove any non-covalent SUMO interactions, leaving behind only

covalent SUMO modifications (Horita et al., 2018; Xiao et al., 2015). However, antibodies are unable to detect their targets under these conditions, so the SDS must be significantly diluted out using low-SDS immunoprecipitation (IP) buffer and a five to ten-fold dilution. Due to the possibility of protein renaturation and subsequent reactivation of SENPs following this dilution, N-ethylmaleimide (NEM), a potent inhibitor of isopeptidases such as SENPs, should be added to both the denaturing and non-denaturing buffers prior to lysis and immunoprecipitation, in addition to standard protease inhibitor cocktails. Isopeptidase inhibitors are not typically included in standard inhibitor cocktails, so they must be supplemented (Xiao et al., 2015). The denaturing immunoprecipitation protocol utilized here was adapted from Salsman et al. (2008).

To demonstrate that this approach could be used to detect protein SUMOylation, the KSHV protein LANA was used as a positive control. LANA is a latently-expressed protein that is critical for the establishment and maintenance of latency (Ganem, 2006). Cai et al. (2013) demonstrated that LANA is SUMOylated at lysine 1140, preferentially by SUMO2. This suggests LANA is SUMOylated in responses to stress, since under normal physiological conditions, substrates are SUMOylated by SUMO1, whereas SUMO2/3 are conjugated under stress conditions (Saitoh and Hinchey, 2000; Zhang et al., 2017).

Cells were co-transfected with plasmids that would constitutively overexpress LANA, HA epitope-tagged Ubc9, and myc epitope-tagged SUMO2, or just with LANA expression plasmid to verify the specificity of the SUMOylation signal. Cells were also co-transfected just with plasmids expressing Ubc9 and SUMO2 in order to verify the specificity of any SUMOylated species; LANA should only be SUMOylated by myc-SUMO2 when all three proteins are co-expressed together. LANA was

immunoprecipitated and the whole cell lysates (WCLs) and immunoprecipitants analyzed by western blot (Fig. 3.1). Immunoblotting of WCLs (Fig. 3.1A-C) shows that all constructs expressed the expected proteins prior to the IP. The multiple species detected for the anti-myc SUMO2 WCL blot were expected, since overexpression of Ubc9 and SUMO2 increases global SUMOylation, leading to the SUMOylation of many cellular proteins as indicated by species of different molecular weights detected (Fig. 3.1B). The 130-250 kDa banding pattern observed in the anti-LANA WCL blot may be due to protein degradation or different PTMs that may affect the LANA protein (Ganem, 2006). As expected, LANA was precipitated when expressed by itself, but no signal was detected by probing with the anti-myc antibody (Figure 3.1D). When Ubc9 and SUMO2 were expressed without LANA, LANA was not precipitated. Additionally, there was no signal detected in this lane by the anti-myc antibody, affirming signal specificity. Only when LANA, Ubc9 and SUMO2 were expressed together was a signal detected on both the anti-LANA and anti-myc immunoblots (Fig. 3.1D). The smeared appearance of the anti-myc signal may be due to protein degradation or other PTMs that may be modifying LANA and affecting its size. These results reaffirm that the latent KSHV protein LANA is SUMOylated and that denaturing IP can be used to detect SUMOylation.

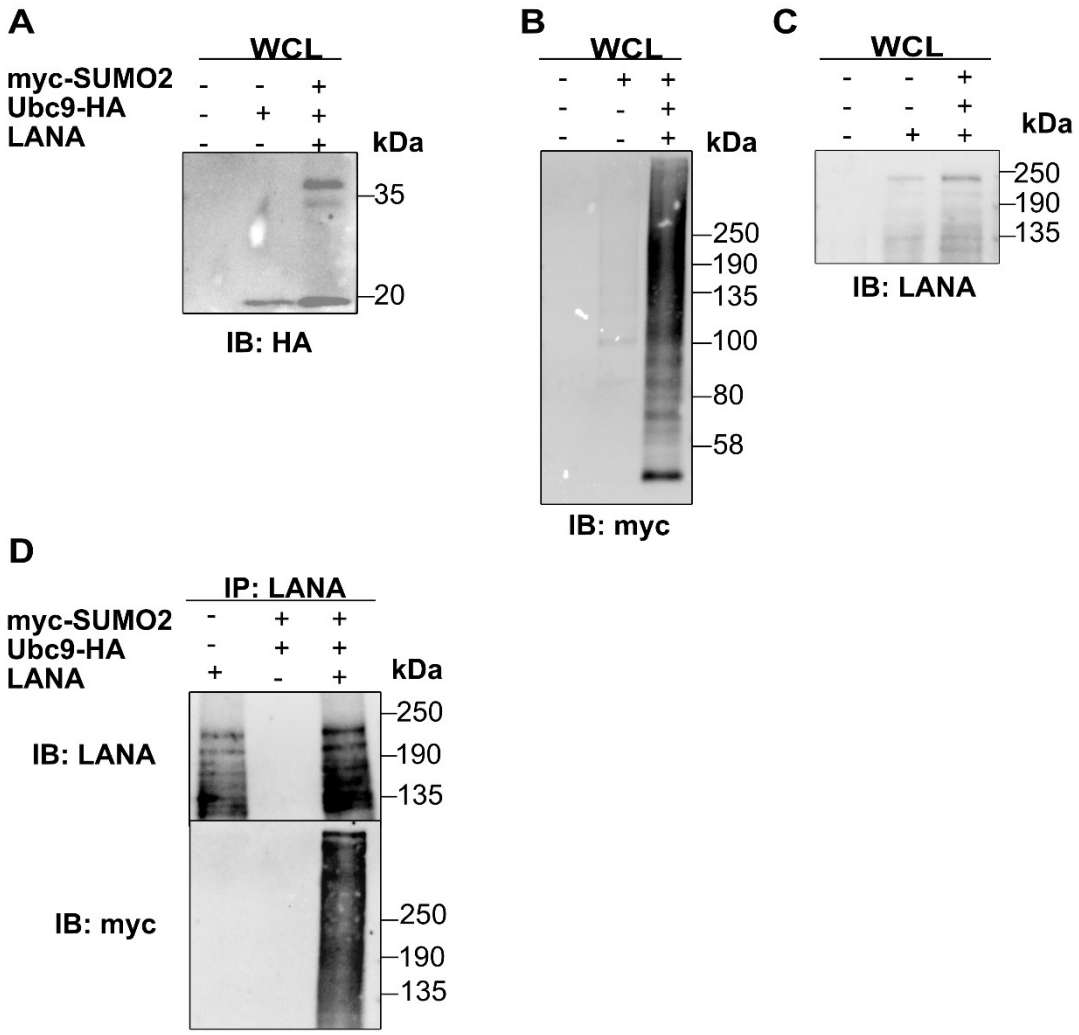

Figure 3.1 LANA is SUMOylated. 293T cells were co-transfected with plasmids expressing the indicated proteins (myc-SUMO2, Ubc9-HA or LANA) or empty vectors. Cells were lysed 48 hours later in denaturing buffer. Concentrated lysates were diluted and LANA immunoprecipitated. Whole cell lysates (WCL; ~1% total input) reserved prior to immunoprecipitation **(A-C)** and LANA immunoprecipitants **(D)** were analyzed by immunoblotting for LANA (135-250 kDa; >250 kDa when SUMOylated), myc (unconjugated SUMO at 13 kDa or SUMO-conjugated proteins), or HA (Ubc9; 19 kDa) epitope tags. One representative of three independent experiments is shown.

In order to determine if KapB disrupts MK2 SUMOylation, MK2 SUMOylation first had to be reaffirmed. Using the above denaturing IP approach, cells were co-transfected with plasmids expressing HA epitope-tagged Ubc9 and SUMO3, as well as a plasmid encoding one of four FLAG-tagged MK2 constructs, one encoding wild type MK2 and the other three being different mutants. The first is "SUMOylation-deficient" MK2 (FLAG-MK2-KR), in which the SUMO-targeted lysine 353 (K353) was mutated to arginine (R) to block SUMOylation at that site (Chang et al. 2011). The second mutant had two threonines (T222 and T334) mutated to glutamic acid (E) to give a constitutively-active MK2 (FLAG-MK2-EE). Phosphorylation of these two regulatory threonines by the upstream kinase p38 results in MK2 activation under normal conditions (Gaestel, 2006). Mutating these threonines to glutamic acid mimics this phosphorylation event, leading to its constitutive activity. The final mutant encoded a constitutively-active and "SUMOylation-deficient" version MK2 (FLAG-MK2-KR-EE), with both the KR and EE mutations incorporated. Constitutively-active constructs were used to assess the effects of constitutive activity on MK2 SUMOylation, since SUMOylation and phosphorylation appear to have co-regulatory functions (Flotho and Melchior, 2013; Yao et al., 2011).

Lysates from cells expressing these constructs was analyzed by western blot (Fig. 3.2). Signal is detected on immunoblots of WCL fractions reserved prior to IP when probed with anti-FLAG and anti-HA antibodies, indicating that the constructs expressed the expected proteins prior to IP (Fig. 3.2A-B). The detection of multiple species when probing with anti-HA antibody indicates that cellular proteins were also SUMOylated when Ubc9 and SUMO3 were expressed (Fig. 3.2B). As expected, FLAG-MK2 precipitated when expressed without Ubc9 and SUMO3, but signal was not detected

when blots were probed with an anti-HA antibody (Fig. 3.2C). Since MK2 antibody was used for immunoprecipitation, endogenous MK2 as well as FLAG-tagged MK2 would be precipitated, but the former would not be detected by anti-FLAG immunoblotting; however, untagged, endogenous MK2 could still be SUMOylated by Ubc9-HA and HA-SUMO3, and contribute to the SUMOylation (HA) signal. As indicated by the faint signal on the anti-HA immunoblot when only Ubc9 and SUMO3 are expressed (Fig. 3.2C, lane 5), endogenous MK2 may have been SUMOylated and precipitated, though these contributions are likely minimal. Since there is also a faint signal detected in the same lane of the anti-FLAG immunoblot (Fig. 3.2C, lane 5) it is possible that this faint signal is due to spillover from the adjacent well. The slight changes in mobility observed between the different MK2 constructs on all anti-FLAG immunoblots may be due to the presence of the phospho-mimicking glutamic acid residues. Signal was detected in both anti-FLAG and anti-HA immunoblots when MK2, Ubc9 and SUMO3 were expressed together, as indicated by the higher molecular weight species detected by the anti-HA antibody when MK2 species were immunoprecipitated (Fig. 3.2C, lanes 6-9).

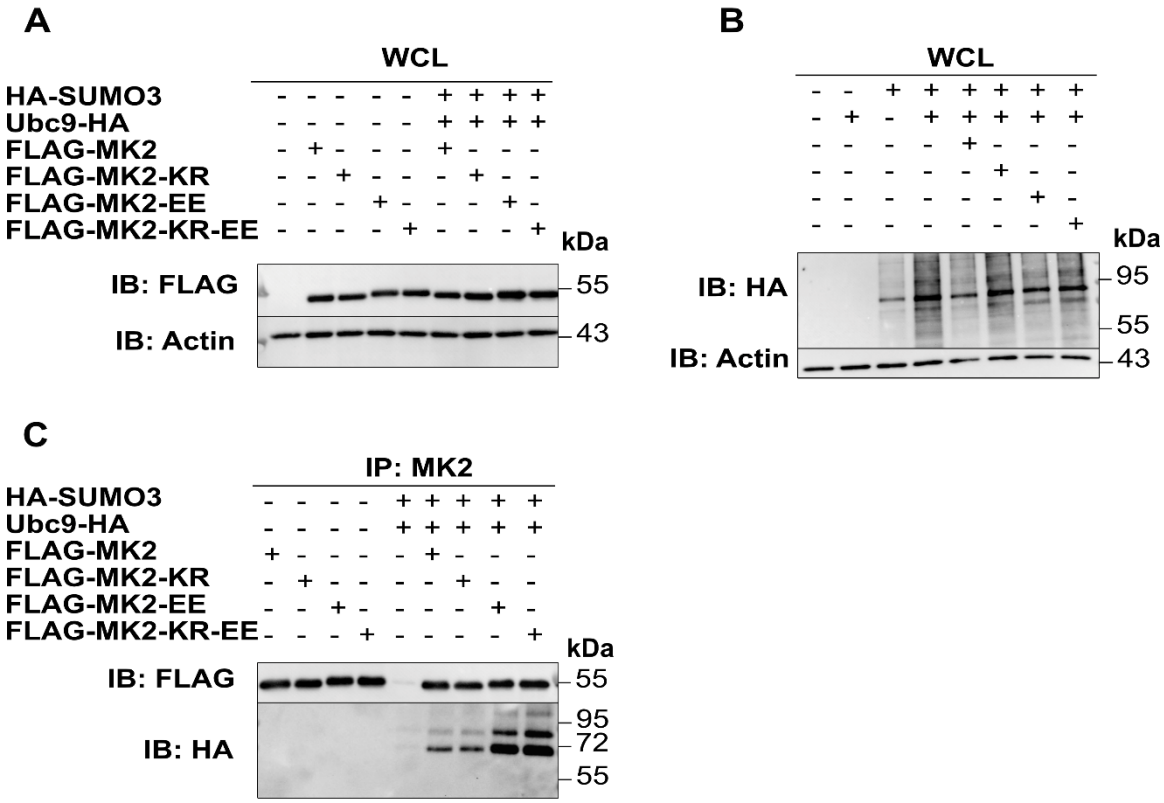

Figure 3.2 Constitutively active MK2 is hyper-SUMOylated. 293T cells were co-transfected with plasmids expressing HA-SUMO3, Ubc9-HA and a plasmid encoding the indicated FLAG-tagged version of MK2 (FLAG-MK2, FLAG-MK2-KR, FLAG-MK2-EE, or FLAG-MK2-KR-EE) or empty vectors. Cells were lysed 48 hours later in denaturing buffer. Concentrated lysates were diluted and MK2 immunoprecipitated. Whole cell lysates (WCL; ~1% total input) reserved prior to immunoprecipitation **(A-B)** and MK2 immunoprecipitants **(C)** were analyzed by immunoblotting with anti-FLAG antibody (MK2; 46.5 kDa), anti-HA antibody (unconjugated SUMO at 13 kDa or SUMO-conjugated proteins. Ubc9 at 19 kDa; not shown), or anti-β-actin antibody (42 kDa). One representative of three independent experiments is shown.

Proteins modified by HA-SUMO3 are expected to be 13 kDa larger. Unmodified FLAG-MK2 migrates at 46.5 kDa; when modified by one HA-SUMO3 protein, it would be predicted to migrate at ~59.5 kDa, then 72.5 kDa, 85.5 kDa and 98.5 kDa as more SUMO3 proteins are conjugated. These results indicate that MK2 is modified by at least two SUMO3 proteins, and that the glutamic acid mutations present in the constitutively active mutants increase the levels of 2xSUMO3 modified MK2, while promoting conjugation of more SUMO3 proteins to MK2 (Fig. 3.2C, lanes 6-9). Significant signal was detected in the anti-HA immunoblot when the so-called "SUMO-deficient" MK2-KR mutants (MK2-KR, MK2-KR-EE) were expressed together with Ubc9 and SUMO3 (Fig. 3.2C, lanes 7 and 9). The SUMO-targeted lysine in these mutants [previously identified by Chang et al. (2011)] has been mutated to arginine to block SUMOylation at this site. The observation that these KR mutants exhibit little difference in anti-HA signal intensity compared to their non-KR counterparts (MK2, MK2-EE) (Fig. 3.2C, lanes 6 and 8) indicates that other SUMO sites are present in MK2, and that K353 may not be the major SUMOylation site. Chang et al. (2011) also observed that their MK2-KR construct was SUMOylated, though the signal was diminished compared to wild type MK2. Additionally, Chang et al. (2011) performed their experiments with murine MK2, which may behave differently from human MK2, which is the form used here.

3.2 MK2 SUMOylation is not Affected by the Co-Expression of KapB

The mechanism that KapB uses to activate MK2 is currently unknown; since SUMOylation appears to have a dampening effect on MK2 activity (Chang et al. 2011), it was hypothesized that KapB might be activating MK2 by disrupting its SUMOylation. In order to determine if MK2 SUMOylation was affected by KapB expression, Ubc9-HA, HA-SUMO3 and either FLAG-MK2 or FLAG-MK2-EE were expressed in the presence and absence of KapB (BCBL-1; 48 kDa). Immunoblots of reserved inputs (WCL) indicate that all constructs expressed the expected proteins prior to IP (Fig. 3.3A-C). Similar to previous immunoblots, laddering was apparent on the anti-HA immunoblot, indicating that cellular proteins were SUMOylated due to Ubc9 and SUMO3 overexpression (Fig. 3.3B) The multiple species detected around 48 kDa on the anti-KapB immunoblot (Fig. 3.3C) are likely due to its variable number of DR1 and DR2 repeats, leading to different KapB isoforms (Sadler et al. 1999; McCormick and Ganem 2005). When MK2 was precipitated from cell extracts that expressed MK2 and MK2-EE without Ubc9, SUMO3, or KapB, they were precipitated by the MK2 antibody as indicated by the signal on the anti-FLAG immunoblot, but signal was not detected on the anti-HA blot (Fig. 3.3D). When Ubc9 and SUMO3 were expressed without either MK2 or KapB, a signal could not be detected on either the anti-FLAG or anti-HA immunoblot. The SUMOylation profile of MK2 in the absence of KapB was like that observed in Fig. 3.2C and appeared to be unchanged by the expression of KapB (Fig. 3.3D, lanes 6 and 7), suggesting that KapB may not be disrupting MK2 SUMOylation in an overexpression system. Interestingly, KapB appears to have a different banding pattern when co-expressed with FLAG-MK2 and FLAG-MK2-EE (Fig. 3.3C).

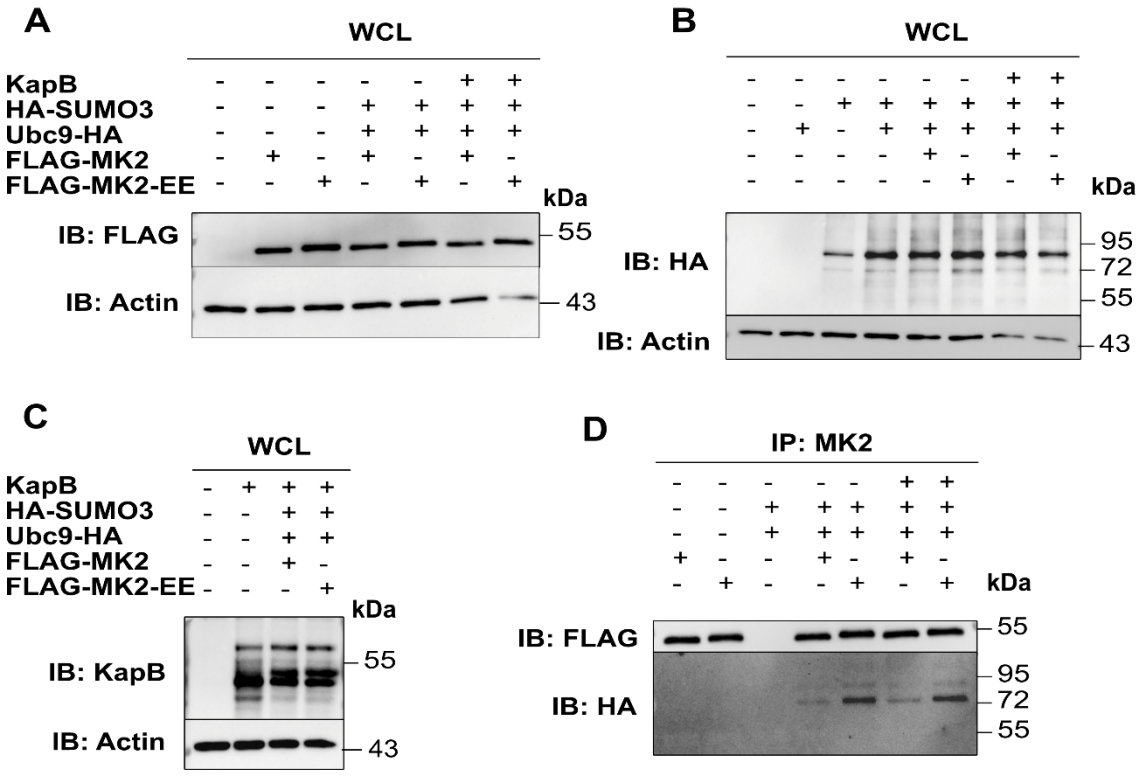

Figure 3.3 MK2 SUMOylation is not impacted by KapB expression. 293T cells were co-transfected with plasmids expressing HA-SUMO3, Ubc9-HA, KapB (BCBL-1) and a plasmid encoding either FLAG-MK2 or FLAG-MK2-EE or empty vectors. Cells were lysed 48 hours later in denaturing buffer. Concentrated lysates were diluted and MK2 immunoprecipitated. Whole cell lysates (WCL; ~1% total input) reserved prior to immunoprecipitation **(A-C)** and MK2 immunoprecipitants **(D)** were analyzed by immunoblotting with anti-FLAG antibody (MK2; 46.5 kDa), anti-HA antibody (unconjugated SUMO at 13 kDa or SUMO-conjugated proteins. Ubc9 at 19 kDa; not shown), anti-KapB antibody (BCBL-1; 48 kDa) or anti-β-actin antibody (42 kDa). One representative of three independent experiments is shown.

One reason why KapB did not appear to alter MK2 SUMOylation could be because KapB may be activating MK2 by a different mechanism unrelated to SUMOylation, such as through shielding activated MK2 from phosphatases or by displacing the autoinhibitory helix of MK2 (McCormick and Ganem 2005). Another possibility is that KapB may preferentially bind a subset of the total MK2 pool, which includes phosphorylated and/or SUMOylated MK2, and unmodified MK2. If KapB preferentially binds a certain form of MK2 and alters its SUMOylation, it may not be detectable using this immunoprecipitation experimental design.

3.3. Co-IP Experiments to Interrogate the Fraction of MK2 That Binds KapB

One possible explanation for why KapB co-expression with MK2 did not impact the SUMOylated population of MK2 (Fig. 3.3D) is that KapB is only binding a specific fraction of MK2 that is unSUMOylated and/or phosphorylated. Therefore, I wanted to understand what "version" of MK2 co-precipitates with KapB. As a first step, a pilot co-immunoprecipitation experiment was performed in order to verify that FLAG-MK2 and KapB co-immunoprecipitate, as previously demonstrated (McCormick and Ganem 2005). For the first pilot experiment, cells were co-transfected with either empty vector or plasmids that would express FLAG-MK2 and wild type KapB (BCBL-1). Since the interaction between KapB and MK2 is non-covalent (McCormick and Ganem 2005) proteins were extracted under non-denaturing conditions to preserve non-covalent interactions. KapB was immunoprecipitated from cell lysates using a rabbit polyclonal KapB antibody. Immunoblots of the reserved input fractions that were probed using anti-FLAG and anti-KapB antibodies indicated that FLAG-MK2 and KapB constructs were strongly expressed (Figure 3.4A-B). As with Fig 3.3 the species detected for KapB in the WCL was altered by the expression of FLAG-MK2 (Fig. 3.4B). Because rabbit KapB

antibody was used for both the immunoprecipitation and the immunoblot, a species of approximately 50 kDa was detected in each lane of the anti-KapB immunoblot (Fig. 3.4C). Given that the size of BCBL-1 KapB (48 kDa) is like that of the antibody heavy chain (~50 kDa), it is difficult to determine conclusively if KapB was immunoprecipitated in this experiment. A non-specific species detected by the anti-FLAG antibody were neither KapB nor MK2 were expressed (Fig. 3.4C, lane 1) indicate that the polyclonal KapB antibody is not specific enough to be used for co-IP. These species are likely due to the large amounts of antibody heavy chain present in the immunoprecipitant which were then detected by the anti-FLAG antibody.

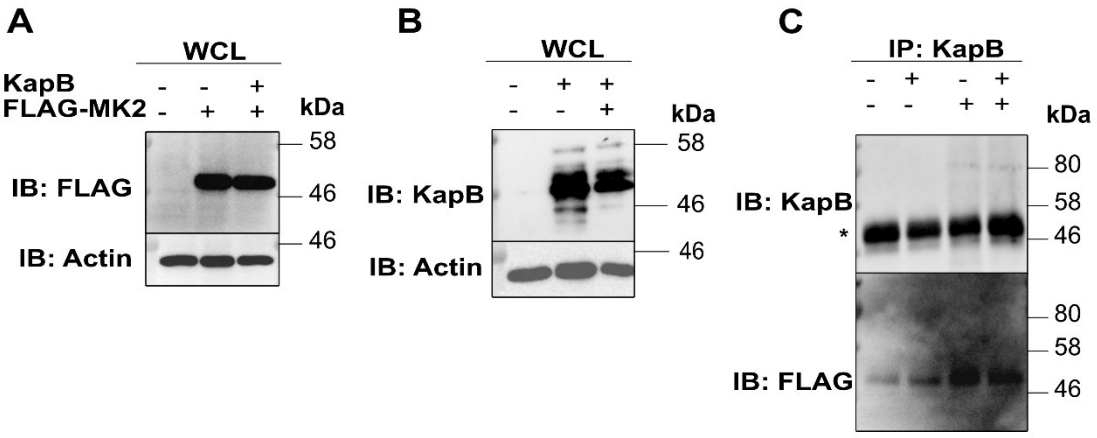

Figure 3.4 MK2 was not co-immunoprecipitated with anti-KapB antibody. 293T cells were co-transfected with plasmids expressing KapB (BCBL-1) and FLAG-MK2 or empty vectors. Cells were lysed 48 hours later in non-denaturing lysis buffer and MK2 immunoprecipitated. Whole cell lysates (WCL; ~1% total input) reserved prior to immunoprecipitation **(A-B)** and KapB immunoprecipitants **(C)** were analyzed by immunoblotting with anti-FLAG antibody (MK2; 46.5 kDa), anti-KapB antibody (BCBL-1; 48 kDa) or anti-β-actin antibody (42 kDa). N = one independent experiment.

In an attempt to eliminate background, a second pilot experiment was set up to reaffirm that KapB co-precipitates with MK2 (McCormick and Ganem 2005) using GFP-tagged KapB (BCBL-1; 75 kDa [BCBL KapB: 48 kDa. GFP: 27 kDa]), so that a monoclonal mouse anti-GFP antibody could be used to precipitate KapB. Adding the GFP-tag to KapB (BCBL-1) does not affect its functionality; the Corcoran lab has previously demonstrated that GFP-KapB still disassembles processing bodies and stabilizes ARE-mRNAs, thus retaining functionality (MacNeil and Corcoran, unpublished observations). The second pilot experiment was set up much like the first, though additional controls were incorporated. Cells were either transfected only with empty vector or co-transfected with vector and pEGFP, in order to determine if the EGFO moiety would result in interactions. FLAG-MK2 was expressed alone or with EGFP, so that potential interactions between GFP protein and FLAG-MK2 could be analyzed. The rest of the conditions were as before, expressing GFP-KapB with empty pcDNA3.1 and with FLAG-MK2, to determine if FLAG-MK2 would co-precipitate with GFP-KapB. Additionally, a mirrored immunoprecipitation experiment using normal mouse IgG1 isotype control instead of GFP antibody was performed to determine non-specific background signals caused by the primary immunoblot antibodies.

As with previous immunoprecipitation experiments, total lysate input fractions were reserved and immunoblotted to confirm construct expression prior to the IP. As expected, GFP-KapB was detected by anti-KapB antibody in all cell extracts where it was expressed (Fig. 3.5B), and the intensity of the species increased when FLAG-MK2 was co-expressed. However, in the mirrored IgG1 control immunoprecipitation, a band of similar size was detected in lane 2 (indicated by **) (Fig. 3.5D), indicating that it may be non-specific binding. Unexpectedly, MK2 appeared to be precipitated by anti-GFP

antibody from cell lysates where it was expressed with or without GFP protein. This indicates that MK2 may be binding to both GFP protein and the immunoprecipitation beads or may be binding another cellular protein that could be binding to the beads. These samples do not produce the expected signal in the FLAG blot (Fig 3.5C), indicating that these species are likely not FLAG-tagged MK2. Furthermore, species of approximately the same size were detected on the immunoblots from the IgG1 control immunoprecipitation. For both the KapB and MK2 blots (Fig. 3.5D) a ~50 kDa band of about the same intensity was detected in each lane (indicated by *), which remains at fairly constant intensity in the KapB blot; this is likely caused by the heavy chain of the antibody present in the immunoprecipitant, which would be expected to migrate at ~50 kDa. The intensity of this band is more variable in the anti-MK2 immunoblot, increasing in intensity when GFP was expressed with MK2, as was observed with the GFP IP (Fig. 3.5C, lane 4). Interestingly, no signal was detected on the FLAG blot, indicating that these bands are likely not FLAG-MK2 and likely caused by the antibody heavy chain in the immunoprecipitant, or perhaps non-specific proteins which may have been precipitated by GFP and IgG1 antibodies and recognized by MK2 antibody. These results demonstrate that GFP-KapB was precipitated by anti-GFP antibody, but it cannot be determined if FLAG-MK2 was co-precipitated with GFP-KapB due to uncertainty about the identity of the ~50 kDa band detected by the anti-MK2 antibody for both the GFP and IgG1 immunoprecipitations (Fig. 3.5 C-D). Consequently, I was unable to use these resources to determine if KapB is preferentially binding a certain fraction of MK2.

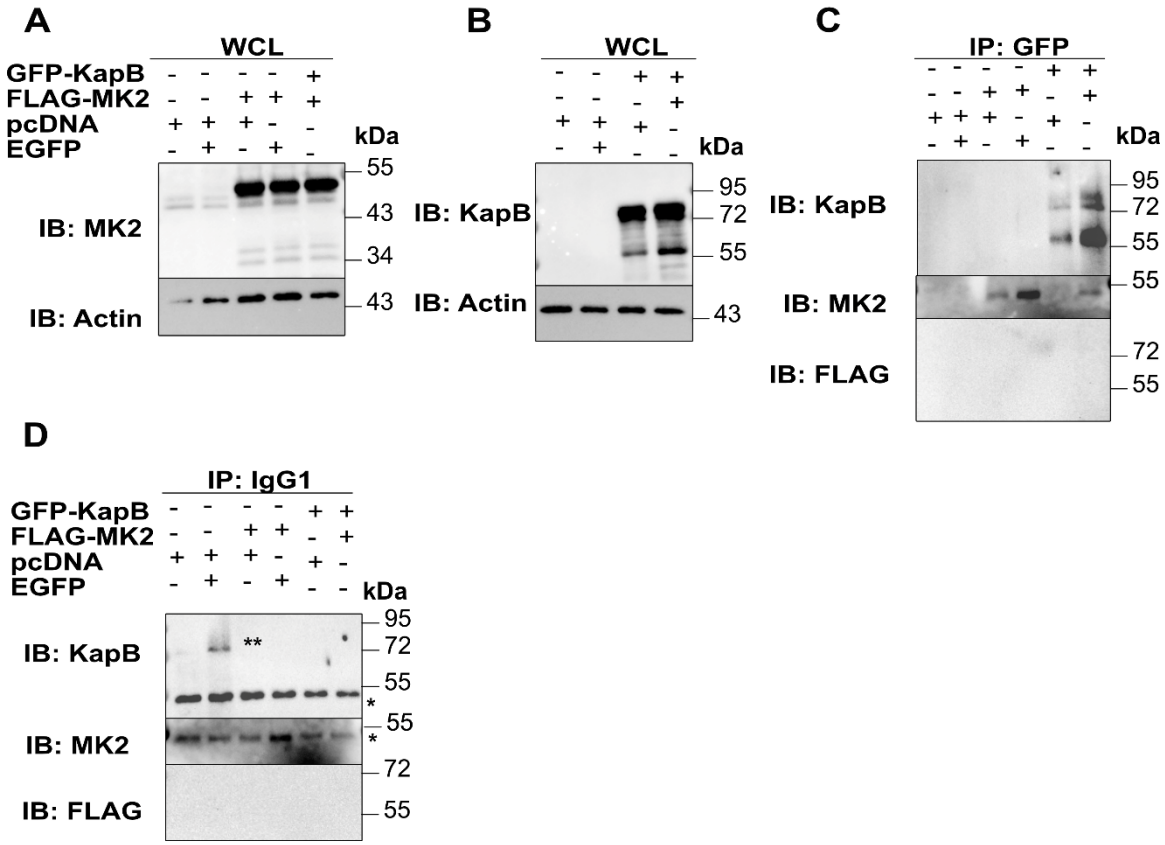

Figure 3.5 MK2 was not specifically co-immunoprecipitated with GFP-KapB. 293T cells were co-transfected with plasmids expressing KapB (BCBL-1), FLAG-MK2, EGFP or empty vector. Cells were lysed 48 hours later in non-denaturing lysis buffer and GFP immunoprecipitated. Whole cell lysates (WCL; ~1% total input) reserved prior to immunoprecipitation **(A-B)** and GFP or IgG1 immunoprecipitants **(C-D)** were analyzed by immunoblotting with anti-FLAG antibody (MK2; 46.5 kDa), anti-KapB antibody (BCBL-1; 48 kDa), anti-MK2 antibody (MK2; 46.5 kDa) or anti-β-actin antibody (42 kDa). * = unknown species observed at ~50 kDa. ** = unknown species observed at ~72 kDa. N = one independent experiment.

3.4 Overexpression of MK2 Stabilizes an ARE-mRNA Reporter

Since Chang et al. (2011) proposed that SUMOylation was a dampener for MK2 activity, I wanted to understand if SUMO-deficient MK2 was more active and phenocopied KapB in several established assays in our lab. First, a luciferase assay for ARE-mRNA degradation was performed to determine how SUMO deficiency of MK2 impacted a reporter ARE-mRNA compared to KapB. This assay utilizes a firefly luciferase (FLuc) construct that harbours an AU-rich element (ARE) derived from the one identified in the 3' UTR of the mRNA encoding granulocyte macrophage colony-stimulating factor (GM-CSF), making the RNA transcript subject to decay unless stabilized by the protein of interest (Corcoran et al., 2011). This FLuc construct was co-transfected with a Renilla luciferase (RLuc) construct, which lacked an ARE element in its 3' UTR and therefore served as a control for transfection efficiency. Expression of FLuc and RLuc was driven from a pTRE promoter, which has a tetracycline response element (TRE) placed upstream of the promoter. The system works with HeLa tet-off cells, which constitutively express a tetracycline-controlled transactivator (tTA), which binds to the tetracycline operator sequences present in the TRE promoter of the luciferase constructs (Gossen and Bujard, 1992). In the absence of the tetracycline analog, doxycycline (dox), expression from the TRE promoters is facilitated by constitutively expressed tTA; however, when cells are treated with doxycycline, it binds to tTA and halts transcription from TRE-controlled promoters (Gossen and Bujard, 1992). HeLa tet-off cells were transfected with these FLuc and RLuc expression constructs alongside the gene of interest, and then 24 hours later dox was added to halt *de novo* transcription from the TRE promoters. After 12 hours, cell lysates were collected and the level of FLuc and RLuc protein activity measured. FLuc activity was normalized to RLuc and relative

luciferase activity of each construct was again normalized to empty vector to represent data as fold change over empty vector.

Compared to empty vector, constitutive expression of KapB (BCBL-1) caused a ~45-fold increase in relative luciferase activity, indicating that FLuc-ARE mRNA was stabilized (Fig. 3.6). The fold increase in relative luciferase was less pronounced with FLAG-MK2 and the FLAG-MK2-KR construct, 28 and 25-fold (Fig. 3.6). Transfection of the constitutively-active FLAG-MK2-EE construct resulted in a 35-fold change in relative luciferase activity compared to vector, a statistically significant result if compared to vector, but not relative to FLAG-MK2. FLAG-MK2-KR-EE and KapB both resulted in a statistically significant ~45-fold increase over empty vector and FLAG-MK2 (Fig. 3.6). Based on this data, all transfected constructs caused >25-fold increase in relative luciferase activity, indicating that all constructs stabilized FLuc-ARE to varying extents.

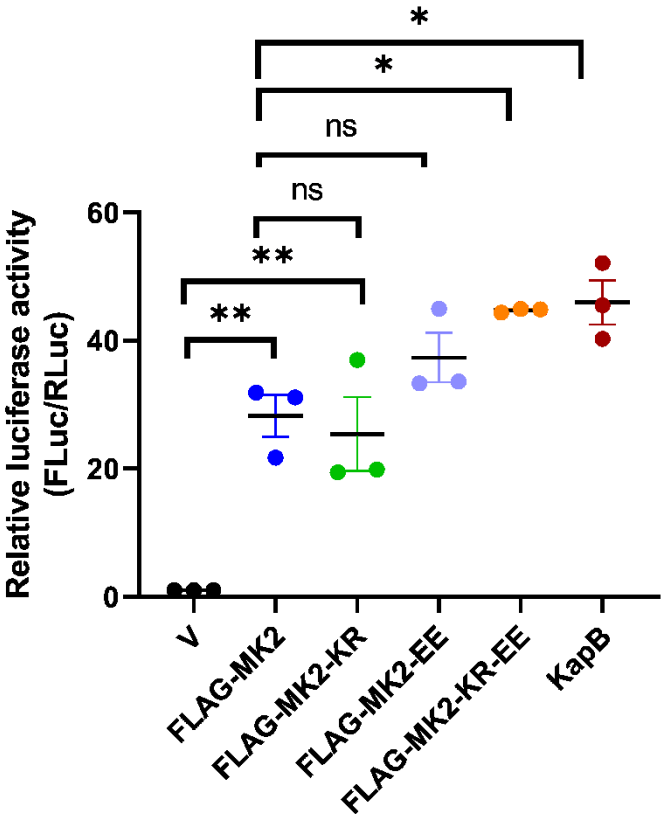

Figure 3.6 MK2-KR-EE enhances ARE-mRNA stabilization. HeLa tet-off cells were transfected with empty vector (V) or a plasmid that expressed FLAG-MK2, FLAG-MK2-KR, FLAG-MK2-EE, FLAG-MK2-KR-EE or KapB, as well as firefly (pTRE-FLUC-ARE) and renilla (pTRE-RLUC) luciferase expression constructs. After 24 hours of incubation, cells were treated with dox (1 µg/mL) to stop de novo transcription from pTRE promoters, and 12 hours later cells were lysed and processed using the dual-luciferase assay kit (Promega). Firefly/renilla luciferase activity was measured using a GloMax 20/20 luminometer (Promega). Firefly luciferase activity was normalized to renilla luciferase activity to account for differences in transfection efficiency. Results are expressed as fold change in relative luciferase activity compared to vector, which was normalized to 1. Results displayed on graph represent the mean ± standard error of mean (SEM) from three biologically independent experiments. A one-way ANOVA with a Tukey's multiple comparisons test was used to determine statistical significance. * = $p \leq 0.05$, ** = $p \leq 0.01$, ns = not statistically significant.

3.5 Overexpression of MK2 Causes PB Disassembly

Processing bodies (PBs) are cytoplasmic ribonucleoprotein (RNP) granules mainly comprised of translationally repressed mRNAs in complex with proteins involved in mRNA repression and 5'-3' decay (Luo et al., 2018). Their specific function in cells is a matter of controversy; due to the presence of mRNA decay intermediates in PBs, many have suggested that they are sites of mRNA decay. However, recent studies have demonstrated that while mRNAs in PBs have more variable poly (A) tail lengths than cytoplasmic mRNAs, 5'-end degraded transcripts could not be detected in PBs, suggesting that mRNAs which accumulate in PBs are mostly intact (Hubstenberger et al., 2017). These findings have led to the formulation of an alternative, though not mutually exclusive hypothesis: that PBs are storage sites for inactive mRNA decay machinery and translationally-repressed mRNAs (Luo et al., 2018).

Despite the controversy, evidence suggests that ARE-binding proteins (ARE-BPs) such as tristetraprolin (TTP) and BRF-1 target ARE-mRNAs to PBs (Franks and Lykke-Andersen, 2007). However, upon activation of MK2, ARE-BPs such as TTP are phosphorylated by MK2, preventing ARE-mRNAs from associating with mRNA decay machinery, resulting in their stabilization (Cargnello and Roux, 2011). KapB is also associated with the disassembly of PBs, which correlates with a stabilization of ARE-mRNAs. Having demonstrated that each MK2 construct causes at least a 20-fold increase in normalized FLuc-ARE activity over vector (reflecting increased ARE-mRNA stability) (Fig. 3.6), PB dynamics in cells expressing these MK2 constructs was analyzed.

In order to determine if any of the MK2 constructs could disassemble PBs to the same extent as KapB, HeLa cells overexpressing a dox-inducible GFP-tagged Dcp1a (mRNA decapping enzyme subunit; PB-resident protein) were utilized. HeLa Flp-In

TREx GFP-Dcp1a (or GFP-3xFLAG) cells express either GFP-Dcp1a or GFP-3xFLAG from a tetracycline-inducible promoter, and stably express a tetracycline repressor protein (Boudreau, 2018). Treatment of GFP-Dcp1a cells with dox (a tetracycline analog) results in the formation of green cytoplasmic foci that co-stain with Hedls/EDC4 (decapping activator, a PB-resident protein required for maintenance of pre-existing PBs) (Luo et al., 2018), and a diffuse green cytoplasmic signal for GFP-3xFLAG cells. Since PBs are complexes of RNPs and multiple proteins that are involved in mRNA decay, the co-staining of overexpressed GFP-Dcp1a with endogenous Hedls, a key protein for PB structure and maintenance, indicates that GFP-positive foci behave like *bona fide* PBs.

Previous work from the Corcoran lab has demonstrated that expression of KapB after the induction of GFP-Dcp1a resulted in the disassembly of GFP-Dcp1a foci in a time- and dose-dependent manner (Boudreau 2018, unpublished data). To reaffirm this finding, a pilot experiment transfecting GFP-Dcp1a (or GFP-3xFLAG) cells with either vector or the KapB (BCBL-1) expression plasmid was performed. GFP-3xFLAG cells were used to verify that GFP-Dcp1a foci were not an artifact of GFP expression. In dox treated GFP-3xFLAG cells transfected with vector, endogenous PBs were present as indicated by red Hedls staining, but no yellow foci were present, indicating that GFP-positive foci in GFP-Dcp1a cells are not an artifact of GFP expression (Fig. 3.7A). When both GFP-3xFLAG and GFP-Dcp1a cells transfected with vector were not treated with dox, GFP expression was not detected, indicating that overexpression of GFP-Dcp1a was dox inducible (Fig. 3.7A, B). Co-localization of Dcp1a-GFP (green) with Hedls (red) produces a yellow signal; in dox-treated GFP-Dcp1a cells stained for Hedls, GFP-Dcp1a foci co-stained with Hedls foci 84.9% of the time, producing yellow foci (Fig. 3.7B). This indicated that these GFP foci often co-localize with other PB resident proteins. In

GFP-Dcp1a cells transfected with vector, an average of 3.98 GFP-positive foci were observed in cells (Fig 3.7C, D); this number dropped to an average of 0.41 GFP-positive foci in KapB-expressing cells, an almost 10-fold decrease in GFP foci upon KapB expression. This result recapitulates the finding that KapB causes the disassembly of PB-like foci in GFP-Dcp1a cells.

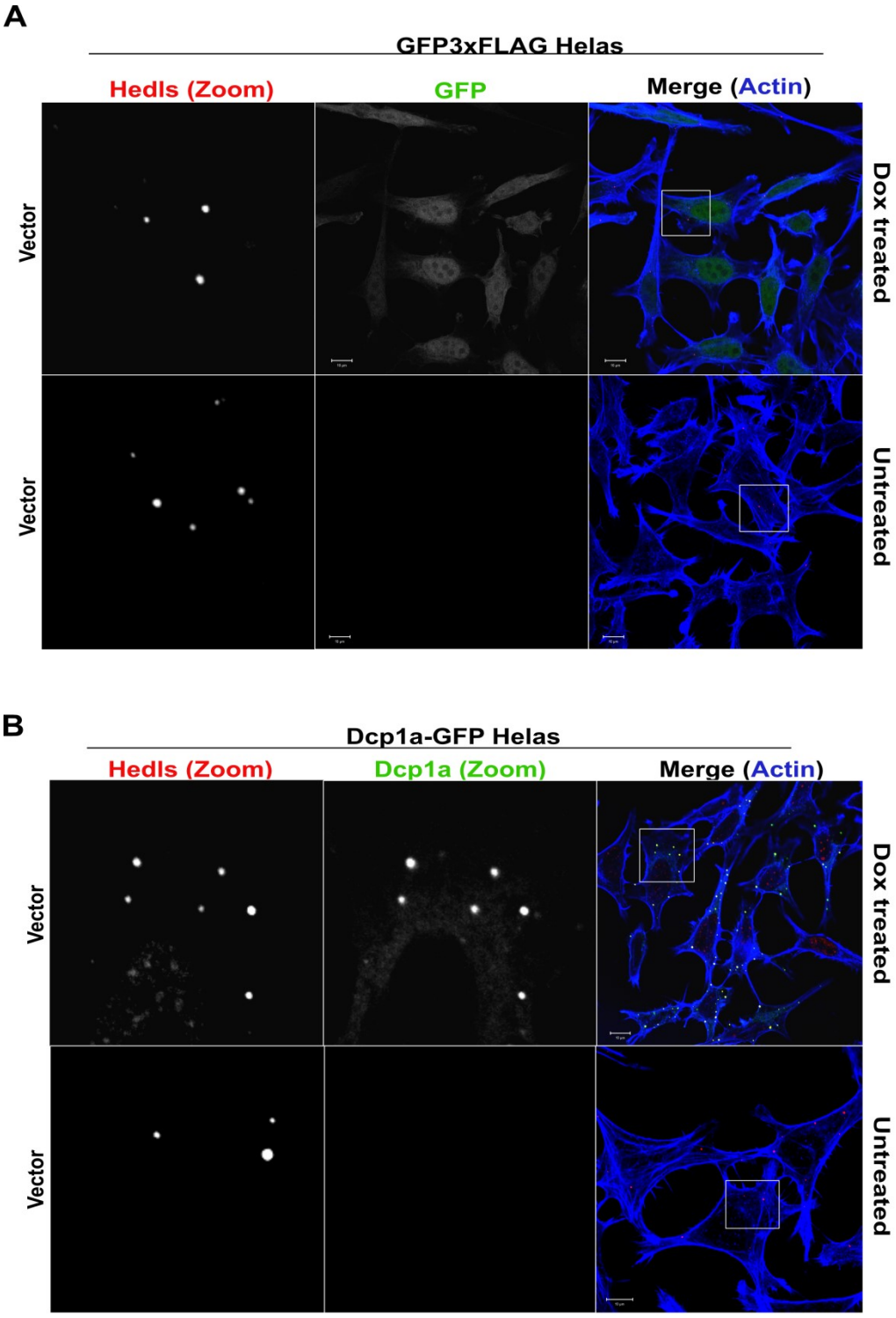
A
GFP3xFLAG Helas
Hedls (Zoom)
GFP
Merge (Actin)
Vector
Vector
Dox treated
Untreated
B
Dcp1a-GFP Helas
Hedls (Zoom)
Dcp1a (Zoom)
Merge (Actin)
Vector
Vector
Dox treated
Untreated

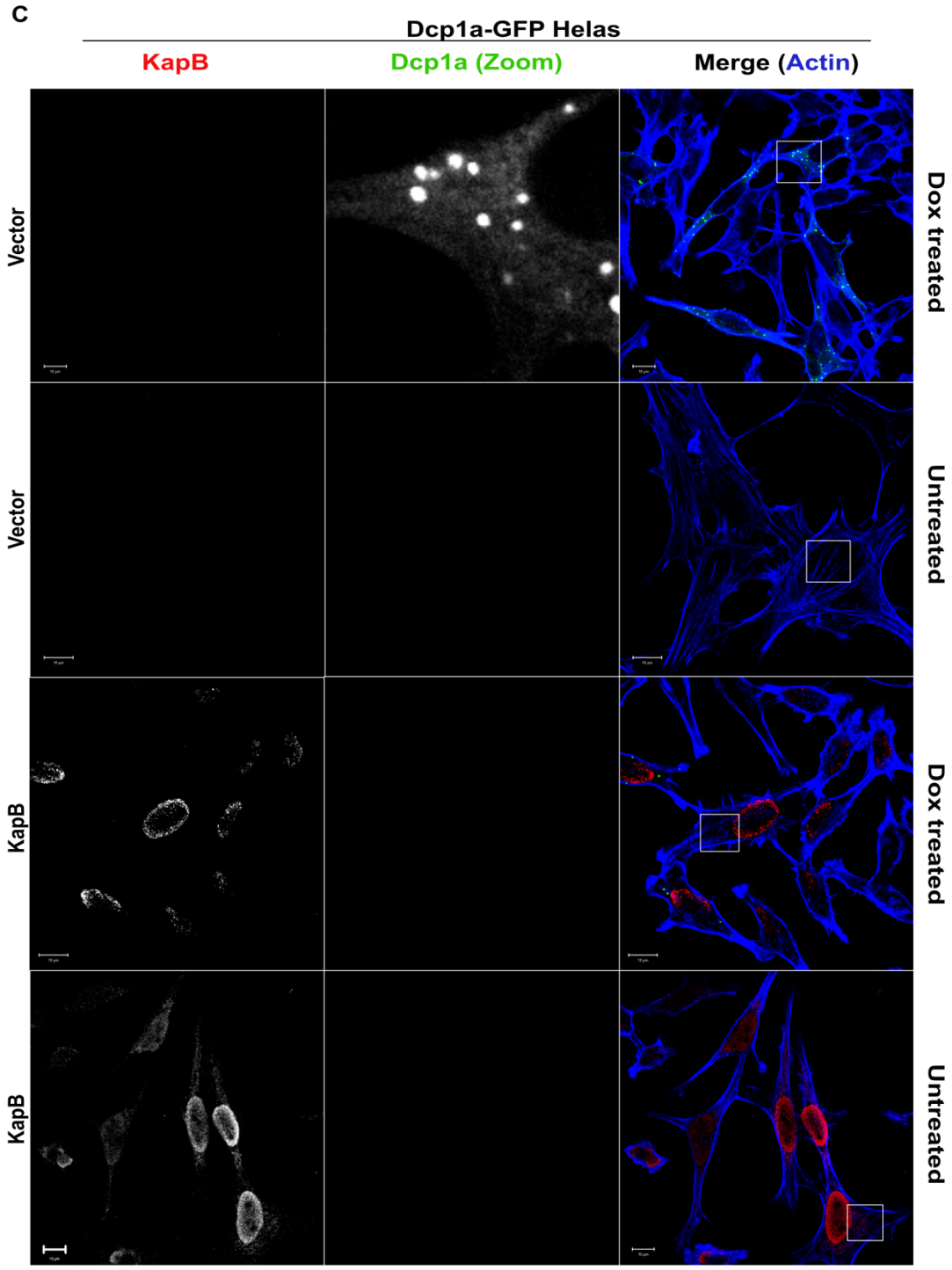
C
Dcp1a-GFP Helas
KapB
Dcp1a (Zoom)
Merge (Actin)
Vector
Vector
KapB
KapB
Dox treated
Untreated
Dox treated
Untreated

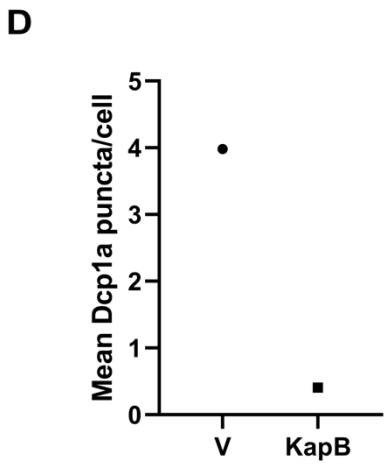

Figure 3.7 KapB disassembles GFP-Dcp1a puncta in pilot experiment. **(A-B)** HeLa Flp-In TREx cells expressing dox-inducible GFP-3xFLAG **(A)** or Dcp1a-GFP **(B)** were treated with dox (1 μg/mL) or not treated. Cells were stained for Hedls, which was visualized using Alexa Fluor® 555-conjugated secondary antibody (red). Actin was visualized using Alexa Fluor™ 647 phalloidin dye (false-coloured blue). GFP channels are shown as black and white in the panels at left and centre and as green in the merge image at right. **(C)** After 24 hours of GFP-Dcp1a expression, GFP-Dcp1a cells were transfected with empty vector (V) or KapB. After 48 hours, cells were fixed with paraformaldehyde and permeabilized for immunofluoresence. Cells were stained for KapB which was visualized using Alexa Fluor® 555-conjugated secondary antibody (red), while actin was visualized as in (A-B). GFP-Dcp1a is shown as black and white and zoomed in when alone, and green in the merge image. **(D**) The mean GFP-Dcp1a foci for at least 60 cells/condition for (C) was calculated and graphed. Scale bar = 10 μM. N = 1 biologically independent experiment.

To determine if any of the FLAG-MK2 constructs could disperse these PB-like foci to the same extent as KapB, the above assay was repeated, though in the absence of GFP-3xFLAG cells; the presence of FLAG in these cells would confound the FLAG staining required to visualize overexpressed FLAG-tagged MK2 constructs. On average, 3.77 GFP foci were observed in vector-transfected cells (Fig. 3.8A, D). The expression of FLAG-MK2 resulted in an almost 3-fold reduction in GFP foci, with on average 1.39 GFP foci observed per cell. The reduction in GFP foci was slightly less in cells expressing FLAG-MK2-KR, which had an average of 1.74 GFP foci per cell, though was not significantly different from wild type FLAG-MK2 (Fig.3.8A, D). The reduction in GFP foci in cells expressing constitutively-active FLAG-MK2-EE and FLAG-MK2-KR-EE was not significantly different from the reduction caused by FLAG-MK2, with on average 1.33 and 1.32 GFP foci being observed per cell, respectively (Fig. 3.8A, D). In GFP-Dcp1a-expressing cells stained for Hedls, GFP-Dcp1a foci co-stained with Hedls foci 96.9% of the time, as indicated by a yellow signal, providing support that these GFP foci are PBs (Fig. 3.8C, D). While all MK2 constructs caused a statistically significant reduction in GFP foci compared to vector, none of the constructs were significantly different from each other. The predominantly cytoplasmic localization of these constructs suggests that MK2 may have been activated in each condition, since inactive MK2 is retained in the nucleus, and could explain the lack of phenotypic difference. MK2 activation could be due to cellular stress. Like the pilot experiment (Fig. 3.7C), KapB-expressing cells had on average 0.52 GFP foci per cell, a more then 7-fold reduction in foci compared to vector transfected cells (Fig. 3.8B). However, this decrease was not much greater than the reductions caused by expression of the FLAG-MK2 constructs.

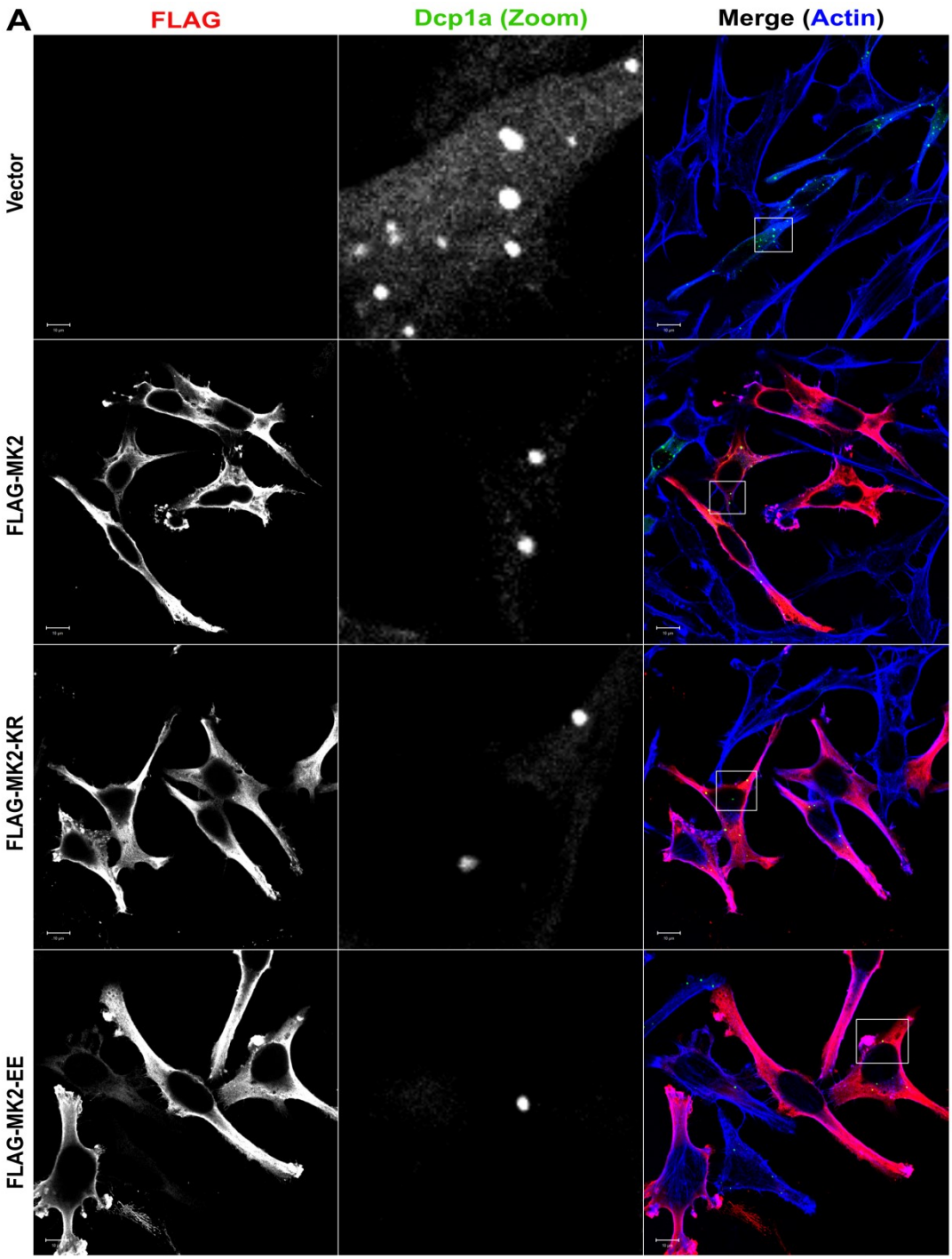
A
FLAG
Dcp1a (Zoom)
Merge (Actin)
Vector
FLAG-MK2
FLAG-MK2-KR
FLAG-MK2-EE

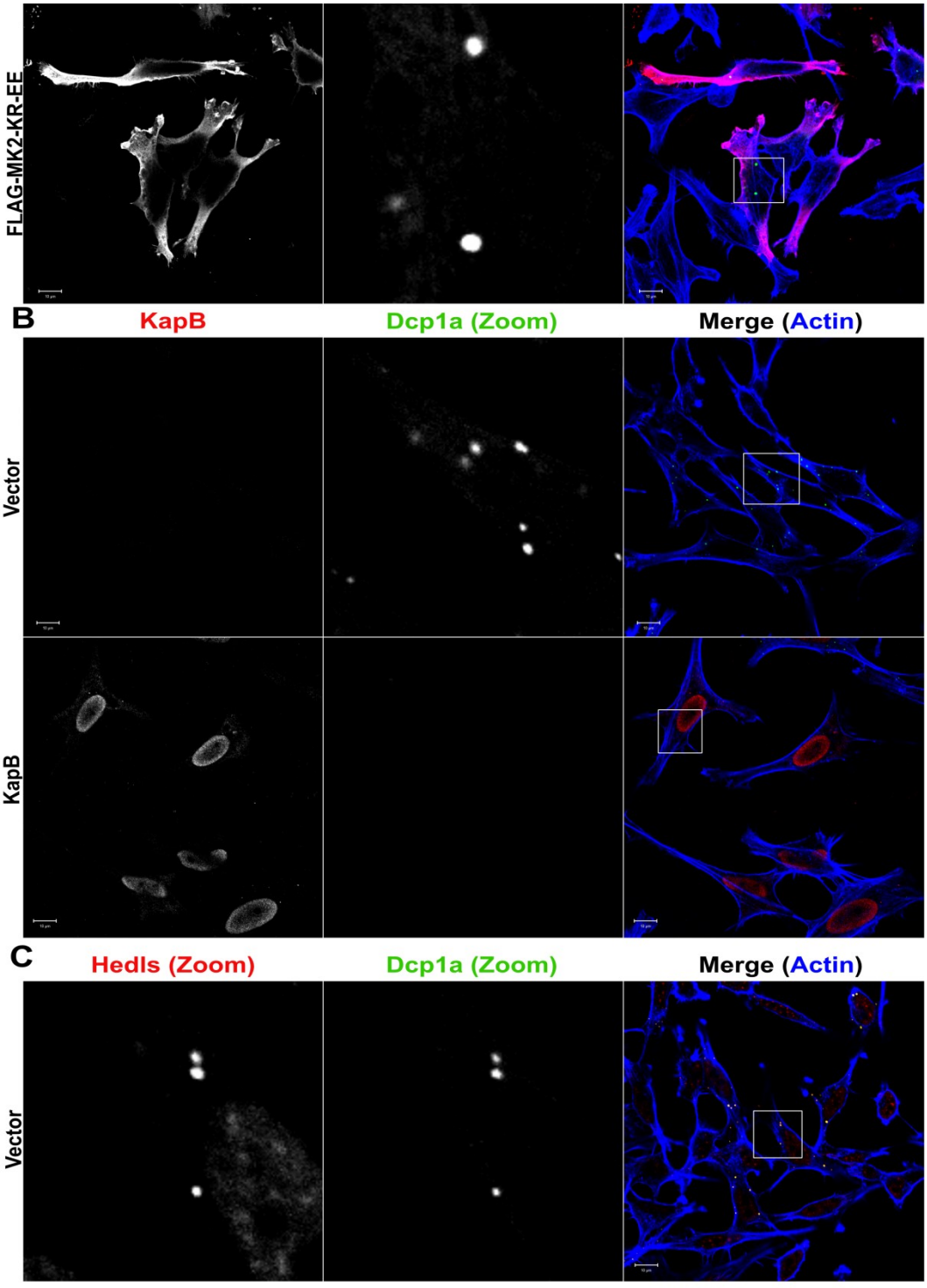
FLAG-MK2-KR-EE
B
KapB
Dcp1a (Zoom)
Merge (Actin)
Vector
KapB
C
Hedls (Zoom)
Dcp1a (Zoom)
Merge (Actin)
Vector

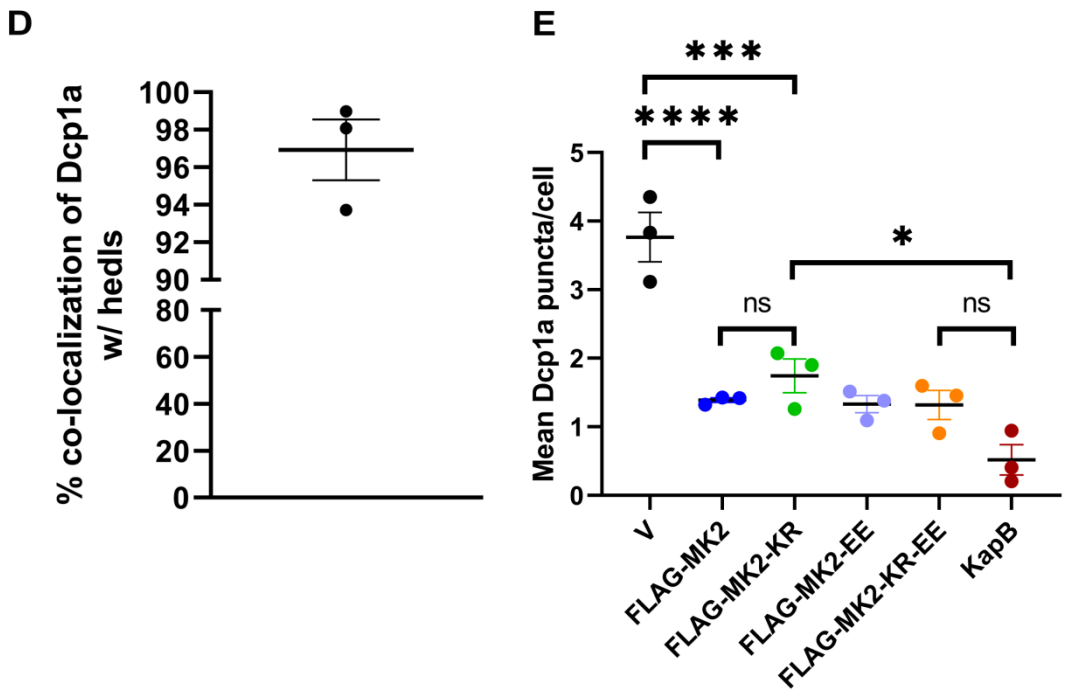

Figure 3.8 All MK2 constructs disassemble Dcp1a puncta. HeLa Flp-In TREx cells expressing Dcp1a-GFP were treated with dox (1 µg/mL). After 24 hours, cells were transfected with either an empty vector (V) or plasmids expressing FLAG-MK2, FLAG-MK2-KR, FLAG-MK2-EE, FLAG-MK2-KR-EE or KapB. **(A-C)** Dcp1a-GFP cells processed in parallel were stained with one of the following antibodies: anti- FLAG (A, to detect FLAG-MK2 constructs), anti-KapB (B) or anti-hedls (C, to visualize endogenous PBs). All were visualized using Alexa Fluor® 555-conjugated secondary antibodies (red). Actin and GFP were visualized as described in Fig 3.7. **D)** GFP puncta were counted for at least 60 cells to obtain total amount of GFP-Dcp1a puncta. Number of GFP puncta co-staining with Hedls (indicated by yellow signal) was divided by total number of GFP-Dcp1a puncta to obtain percent co-localization. Results displayed on graph represent the mean ± standard error of mean (SEM) for three biologically independent experiments. **E)** GFP puncta were manually counted for at least 60 cells per condition. Mean puncta/cell per condition was calculated. Results displayed on graph represent mean Dcp1a-GFP puncta/cell per condition and the mean ± standard error of mean (SEM) for three biologically independent experiments. A one-way analysis of variance (ANOVA) with a Tukey multiple comparisons test was used to determine statistical significance. * = ≤ $p<0.05$.*** = ≤ $p<0.001$. **** = ≤ $p<0.0001$, ns = not statistically significant. Scale bar = 10 µM. One representative of three independent experiments is shown.

3.6 Summary of Results

Using immunoprecipitation, the SUMOylation of MK2 was reaffirmed, and it was discovered that substitution of T222 and T334 with phospho-mimicking glutamic acid results in increased levels of 2x SUMO3-conjugated MK2 (Fig. 3.2C). While the expression of KapB did not appear to impact MK2 SUMOylation (Fig. 3.3D), FLAG-MK2-KR-EE caused a ~40-fold increase in ARE-mRNA stability compared to vector, an increase like that seen with KapB expression (Fig. 3.6). Expression of all MK2 constructs resulted in the disassembly of Dcp1a puncta, with little phenotypic difference observed between the different MK2 constructs (Fig. 3.8A, E). None of the MK2 constructs, when expressed, resulted in the same degree of Dcp1a puncta loss as when KapB was expressed, though there was not much difference between the various MK2 constructs and KapB (Fig. 3.8B). More experiments would have to be conducted to determine whether there is significant difference between the MK2 constructs regarding the disassembly of PBs.

CHAPTER 4 DISCUSSION

4.1 Overview

The ectopic expression of KapB in primary endothelial cells recapitulates the cell spindling, inflammation and angiogenic phenotypes that are commonly associated with KS lesions (McCormick and Ganem 2005; Corcoran, Johnston, and McCormick 2015). The expression of KapB is also associated with the disassembly of PBs, which is correlated with increased expression of inflammatory cytokines (Corcoran et al., 2015). KapB elicits these cellular effects by binding to and activating a stress-responsive kinase known as MK2, thus setting off a complex signaling cascade that ultimately results in the induction of stress fibres, the stabilization of inflammatory ARE-mRNAs, and the dispersal of PBs (Fig. 1.2B) (McCormick and Ganem 2005; Corcoran, Johnston, and McCormick 2015). However, the mechanism by which KapB activates MK2 is unknown.

Chang et al. (2011) demonstrated that MK2 is SUMOylated, and when SUMOylation at K353 was prevented (K353R), MK2-K353R caused increased and prolonged HSP27 phosphorylation compared to WT-MK2, as well exacerbated stress fibre induction upon TNF treatment compared to WT-MK2. These phenotypes are like those seen when KapB activates MK2; therefore, I hypothesized that KapB was activating MK2 by disrupting its SUMOylation.

To address this hypothesis, I asked two major questions: 1) Does KapB disrupt the MK2 SUMOylation profile? and 2) Does a SUMO-deficient MK2 mutant phenotypically behave like KapB? I observed that constitutively-active MK2 is hyper-SUMOylated compared to non-constitutively active MK2, and that the MK2 SUMOylation pattern is not altered by the co-expression of KapB. This suggests that

phosphorylation may play a role in regulating MK2 SUMOylation and that KapB is not disrupting MK2 SUMOylation. Furthermore, I discovered that the MK2-KR-EE mutant could stabilize inflammatory ARE-mRNAs to a similar level as KapB. All MK2 constructs appeared to induce PB disassembly; however, none performed as well as KapB, including MK2-KR-EE. In the discussion that follows, I will propose possible mechanisms by which KapB may interfere with MK2 SUMOylation that reconcile with these data. Regardless of whether KapB is activating MK2 by disrupting its SUMOylation or another distinct mechanism, my experiments have uncovered a complex regulatory interplay between phosphorylation and SUMOylation in regulating MK2 activity.

4.2 Analyzing MK2 SUMOylation and KapB Interactions Using IP

To determine if KapB was disrupting MK2 SUMOylation, the MK2 SUMOylation profile was first established in the absence of KapB, using denaturing IPs. Following this, I performed the same experiment while also co-expressing KapB; these data demonstrated no difference in the MK2 SUMOylation profile in the presence of KapB (Fig. 3.3D). For the study of transient post-translational modifications such as SUMOylation, denaturing IP has a number of advantages over native IP (i.e. RIPA buffer-based) approaches, such as the immediate inactivation of SUMO proteases, which can rapidly deSUMOylate target proteins upon cell lysis if not inactivated (Horita et al., 2018; Xiao et al., 2015). Denaturing IP also has the advantage of disassociating non-covalent protein interactions, which can give false-positive SUMOylation results through SUMO-SIM interactions, as well as isolating proteins from all cellular compartments (Horita et al., 2018). However, there are several limitations to the use of denaturing IP, which has largely hampered their popularity as an IP approach.

4.2.1 Limitations of Denaturing IP

One of the biggest drawbacks associated with denaturing immunoprecipitation is the use of denaturing lysis buffers, which are often incompatible with many immunoprecipitation reagents such as antibodies (Horita et al., 2018). However, this problem is resolved by diluting the SDS in the concentrated cell lysate with a low SDS IP buffer, as was done here. The bigger drawback of denaturing lysis is that it leads to significant DNA contamination of the lysates, which must be addressed through shearing of the genomic DNA (Horita et al., 2018). This is typically achieved through syringe homogenization or sonication, both of which can result in damage to the proteins being studied, as well as add considerable time to the preparation of lysates. To reduce protein damage during sonication, lysates in this study remained on ice for the duration of sonication. Furthermore, sonication can require a significant amount of optimization, which can interfere with experimental reproducibility (Horita et al., 2018). This issue was occasionally encountered in this study; even after the sonication protocol was optimized (described in section 2.4), occasionally some samples would require an additional 30 seconds of sonication to fully shear DNA and reduce sample viscosity. It is possible this could have resulted in additional protein damage and variation between samples in an experiment. However, crisp bands are observed on most of the immunoblots (Fig. 3.2, 3.3) indicating that protein degradation was likely minimal. Another way to deal with DNA in the lysates is through DNase treatment; however, this also requires optimization and alterations to the lysate buffer before and after DNase treatment. The development of specialized DNA filters may help remove genomic DNA, which could both improve sample processing time and minimize protein damage and signal loss (Horita et al., 2018).

A step that should have been taken while performing these IPs was quantifying protein concentration in lysates prior to IP, then diluting samples to the same concentration so that the same concentration of protein was present in each condition (Horita et al., 2018). Without this step, it cannot be known for sure how much differences in lysate concentration contributed to the different intensities of immunoblotting signals after IP; however, to this end quantification of reserved input fractions revealed only small variations in protein concentration between lysates from different experimental conditions within an experiment. This means any differences between the protein concentration in different experimental IP conditions was likely minimal and is supported by the rather similar intensities of the bands detected with the anti-FLAG antibody in the IP immunoblots (Fig. 3.2C, 3.3D). However, it is possible different protein concentrations between the lysates may have contributed to some variation in the SUMO signals between conditions (Fig. 3.2C, 3.3D)

4.2.2 Limitations of Native KapB Co-IP

After observing that KapB did not alter MK2 SUMOylation (Fig. 3.3D), it was suspected that KapB may be preferentially binding a small subset of the MK2 population and altering its SUMOylation, and that the denaturing IPs may not sensitive enough to detect changes in this small subset. However, attempts to determine what subset this may be were inconclusive (Fig. 3.4, 3.5), due to the limitations of native co-IP. While denaturing immunoprecipitation was used to determine the MK2 SUMOylation profile, the same approach could not be used to determine what fraction of the MK2 pool KapB may be interacting with. This is because SUMOylation is a covalent modification, while the KapB-MK2 interaction is a non-covalent interaction (McCormick and Ganem 2005); such an interaction would be abolished under denaturing conditions. Therefore, a RIPA

buffer-based native co-IP approach was used to determine what fraction of MK2 KapB may be binding; however, this approach posed several challenges. The most obvious problem encountered with any IP approach is access to high specificity and/or high affinity antibodies for the target, and this problem was encountered during initial attempts to precipitate KapB using the polyclonal KapB antibody. The first attempt using this rabbit polyclonal KapB antibody resulted in the detection of a ~50 kDa species in anti-KapB and anti-FLAG immunoblots of all co-immunoprecipitants when KapB and FLAG-MK2 were not expressed in the cell lysate (Fig. 3.4C). This species was likely caused by a large amount of antibody heavy chain present in the co-immunoprecipitants, which would have been transferred to the immunoblot. Another possibility is that the anti-KapB antibody was cross-reacting and precipitating other cellular proteins. This cross reactivity could be due to the highly repetitive nature of the KapB protein (Sadler et al., 1999), and algorithms predicted it to be intrinsically disordered (Corcoran, unpublished), meaning the KapB antibody could be binding similar motifs common to KapB and cellular proteins.

Since the KapB antibody could not be used for co-IP, I decided to use GFP-tagged KapB for transfection and immunoprecipiation with monoclonal mouse anti-GFP antibody. The GFP-KapB construct has been demonstrated to disassemble PBs and stabilize ARE-mRNAs (MacNeil and Corcoran, unpublished). While antibody cross reactivity was reduced in this experiment compared to the one using KapB antibody, different issues became apparent. While the GFP antibody appeared to precipitate GFP-KapB, immunoblotting for MK2 resulted in detection of protein species in lysates that should not have produced signal; namely, when MK2 was expressed with empty vector and with GFP (Fig. 3.5C). The most likely identity of this protein species is antibody

heavy chain, though it is also possible that off-target binding/interactions were occurring at some point during the co-IP. Since MK2 was detected in the cell lysates when expressed with GFP prior to co-IP, GFP may have bound to MK2, leading to the co-precipitation of the complex by GFP antibody. If this was occurring, the GFP-KapB construct would be automatically ruled out as a candidate for this assay, due to uncertainty about the contributions of each protein (KapB or GFP) to the MK2 precipitation.

Due to these issues, the identity of the ~50 kDa bands in the MK2 blots is uncertain. (Fig. 3.5C). Bands of approximately the same size were also detected on the mouse anti-IgG1control IP blot (Fig. 3.5D), suggesting that these bands may be non-specific background. However, the mouse IgG1 control antibody IP was not isotype matched to the mouse anti-GFP antibody, which was an IgG2a class mouse antibody; therefore, it cannot be said with certainty that the background bands present in the mouse anti-GFP IP blots are a result of non-specific mouse IgG2a antibody interactions with cellular proteins. Additionally, it is likely that an excessive amount of mouse IgG1 isotype control was added to the protein lysates prior to IP, and likely contributed to excessive background signal. While researching potential causes for the results of this co-IP (Fig. 3.5), it was discovered from the IgG1 product information sheet that the isotype control antibody should have been diluted to the same concentration as the test antibody prior to use. In that experiment (Fig. 3.5D), the isotype control was not diluted prior to use and was added to lysates at the same dilution as mouse anti-GFP, likely contributing to excessive background signal. Due to these issues, few conclusions can be drawn from the results of the control IgG1co-IP blots. From these pilot co-IP experiments, it could not be determined if KapB was binding to a specific subset of the

MK2 pool. Creating a KapB construct that is tagged with an epitope for which reliable IP antibodies have been created (such as HA or myc) would likely prove to be more successful than the current approach (Kimple et al., 2013). Alternatively, affinity tags (such as histidine) could be used to bypass the need for antibodies all together (Kimple et al., 2013).

In these experiments, many of the drawbacks of co-IP were put on display, namely the need for reliable IP antibodies and the high degree of optimization that is often required for these assays. An additional factor not addressed so far is the possibility that this approach could provide false-negatives for possible MK2 subsets KapB could be binding. Given the difficulty of preserving SUMO modification under native (i.e. RIPA) conditions, it is possible that these co-IPs could give inaccurate impressions about the MK2 subsets KapB may bind.

4.3 Hyper-SUMOylation of MK2-EE Suggests SUMOylation may be Enhanced by Phosphorylation

Many interesting results were observed while establishing the MK2 SUMOylation profile, one being that MK2 constructs containing phospho-mimicking glutamic acid substitutions were hyper-SUMOylated compared to their non-constitutively active counterparts (Fig. 3.2C). The implications of this observation will be expanded upon below. Another interesting observation was that abolishing MK2 SUMOylation at K353 did not affect the MK2 SUMOylation profile (Fig. 3.2C), suggesting that K353 is not the major SUMOylation site of MK2 and that multiple unvalidated SUMOylation sites are present within MK2. Analysis of the structure of MK2 provides insights into the possible implications this observation could have for the regulation of MK2 activity.

4.3.1 SUMOylation of MK2-KR Indicative of Multiple SUMO Sites

It is unlikely that K353 is the only SUMOylation site within MK2, as was demonstrated in the MK2 SUMOylation assay (Fig. 3.2C). This is because little change in SUMOylation was observed for MK2-K353R, despite the K353 mutation to prevent covalent addition of SUMO to this residue, indicating that other unvalidated SUMOylation sites are likely present within MK2. Analysis of the primary amino acid sequence of MK2 by algorithms that identify putative SUMOylation sites (such as Joined Advanced SUMOylation site & SIM Analayzer [JASSA]) identifies numerous lysines within MK2 with a low probability of being SUMOylated. These include K229, K307, K343, and K374, as well as two other lysine residues with high probability of being SUMOylated; namely, K64 (inverted consensus motif) and K188 (consensus motif) (Fig. 4.1). These two lysines are of interest due to their location within the MK2 structure; K64 is located at the N-terminal end of the kinase domain of MK2 (Fig. 1.3; Fig. 4.1). It has been suggested that the N-terminus of MK2 may be important for protein-protein interactions and was shown to be important for actin-related MK2 phenotypes (Gaestel, 2006; Kotlyarov et al., 2002). If K64 is SUMOylated, it may provide an additional interface to mediate protein-protein interactions through SIM domains present in other protein interaction partners. Due to its proximity to the beginning of the catalytic domain, SUMOylation at this site may also influence kinase activity. K188 is of interest due to its position within the catalytic domain, being next to the catalytic D186 residue of MK2 (Fig. 4.1) (Meng et al., 2002). SUMOylation at this site may obstruct the MK2 catalytic site, attenuating MK2 activity. However, for this site to be accessed by the SUMOylation machinery, T334 would likely need to be phosphorylated, so that the autoinhibitory helix would release from the catalytic domain. SUMOylation at this site may provide an added

layer of regulatory complexity. Additionally, MK2 may contain non-consensus SUMO sites that would not be identified by algorithms (Flotho and Melchior, 2013). Further studies need to be conducted to determine which additional lysines within MK2 are SUMOylated, and to characterize their impact on MK2 function.

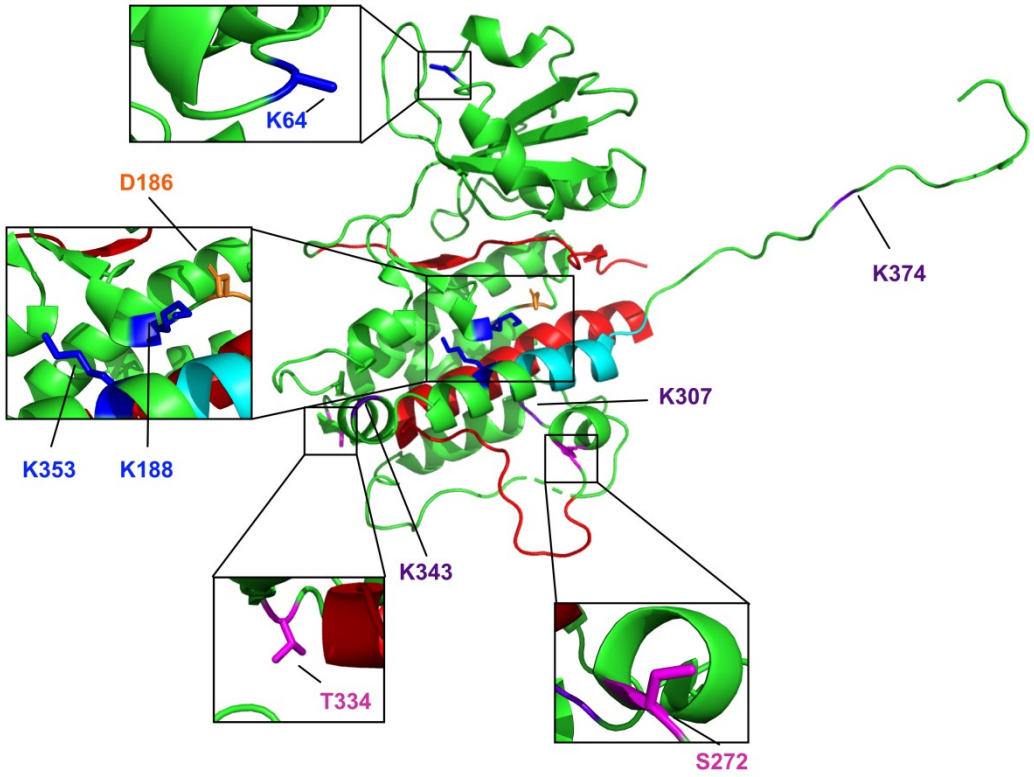

Figure 4.1 The structure of MK2. MK2 is activated by phosphorylation at T222 (not resolved), T334 and S272 (pink). The catalytic residue of MK2 is D186 (orange). MK2 is SUMOylated at K353 (blue) and has high probability SUMOylation sites at K64 and K188 (blue). Low-probability SUMOylation sites at K229 (not resolved), K307, K343 and K374 (purple). Red: putative KapB binding region. Cyan: nuclear export sequence. Structure generated in PyMOL 2.3.3 (Schrodinger) from PBD 1KWP (Meng et al., 2002).

4.3.2 Possible Mechanisms for SUMOylation as a Kinase "Off" Switch

When Chang et al. (2011) discovered that MK2 was SUMOylated, they suggested that this modification might act as a dampener for kinase activity based on the observation that when SUMOylation at K353 was prevented, kinase activity was increased (Chang et al., 2011). However, in this study the prevention of SUMOylation at K353 had little impact on both the SUMOylation profile of MK2 and its activity. Here, I have shown that constitutively-active MK2 is hyper-SUMOylated (Fig. 3.2C), suggesting that phosphorylation may be regulating the degree of MK2 SUMOylation. It has been demonstrated that phosphorylation and SUMOylation can have intertwined roles in regulating kinase activity, with phosphorylation being observed to regulate the SUMOylation of certain substrates (Flotho and Melchior, 2013). A subset of SUMOylation-targetting motifs has been attributed to the phenomenon (phosphorylation dependent SUMO motifs [PDSMs]), which consist of the core consensus SUMO motif, typically followed downstream by a phosphorylated serine residue (Flotho and Melchior, 2013; Vanhatupa et al., 2008; Yao et al., 2011). While K353 of MK2 is recognized as a PDSM by algorithms (such as JASSA) that identify putative SUMOylation sites, the serine downstream of K353 is not known to be phosphorylated, and has not been listed as a phosphorylation site by databases such as PhosphoSitePlus (Ben-Levy et al., 1995; Soni et al., 2019). Analysis of the structure of unphosphorylated MK2 reveals that K353 is positioned on an inward facing turn of the autoinhibitory helix, facing into the catalytic pocket of unphosphorylated MK2 (Fig. 4.1). This means that K353 may only be accessible to the SUMOylation machinery after activation of MK2, when the autoinhibitory helix releases from the catalytic domain. In this way, the SUMOylation of

MK2 at K353 may be dictated through conformational changes that occur because of MK2 phosphorylation.

If MK2 SUMOylation at K353 is preceded by phosphorylation of T334, SUMOylation at this site could affect kinase activity in several ways. As has been observed for other proteins, modification of MK2 by SUMO may result in conformational changes in the kinase, decreasing its affinity and/or specificity for substrates and attenuating the downstream signaling cascade initiated by its activation (Flotho and Melchior, 2013). Given the proximity of this SUMOylation site to the nuclear export sequence, SUMOylation may interfere with the nuclear export of MK2, preventing it from acting on its downstream substrates (Fig. 4.1). The protein modification database PhosphoSitePlus lists K353 as an ubiquitination site identified in a high-throughput study of protein ubiquitination sites by mass spectrometry (Udeshi et al., 2013); to date this event has not been confirmed in low-throughput, site-specific studies and the possible function of this ubiquitination event is not known. If this site is ubiquitinated, it is likely SUMOylation would compete for modification of the site, likely leading to different outcomes depending on the function of the ubiquitination event. If K63 ubiquitin chains form at this site, it may serve a non-degradative purpose, such as directing protein localization and interactions (Swatek and Komander, 2016). Alternatively, the formation of K48 ubiquitin chains at this site may flag MK2 for degradation; SUMOylation may compete with ubiquitination to prevent such an outcome (Swatek and Komander, 2016)

Another way SUMO may affect kinase activity is through the formation of SUMO2/3 chains. The presence of SUMO2/3 chains on MK2 may make it a target for SUMO-targeted ubiquitin ligases (STUbLs), potentially leading to a variety of outcomes

depending on the types of ubiquitin linkages attached to SUMO. STUbLs can add both K48 and K63 ubiquitin chains to SUMO, as well as mono-ubiquitinate SUMO chains (Sriramachandran and Dohmen, 2014). K48 linkages would be expected to flag MK2 for degradation, while mono-ubiquitination and K63 linkages would likely confer non-degradative functions such as altered sub-cellular localization (Sriramachandran and Dohmen, 2014). Additionally, it has been observed that composite SUMO-ubiquitin linkages may facilitate interaction with proteins containing both SUMO and ubiquitin binding motifs, such as RAP80, which coordinates DNA damage responses (DDRs) (Sriramachandran and Dohmen, 2014). Considering that KSHV triggers DDRs and has been shown to modulate them (Di Domenico et al., 2016; Leidal et al., 2012), it is tempting to speculate that KSHV may modulate the STUbL-mediated coordination of DDRs during infection. Considering the amount of evidence indicating that p38 MAPK and MK2 may coordinate DDRs, this could make an interesting line of investigation (Reinhardt and Yaffe, 2009; Soni et al., 2019). I observed the conjugation of multiple SUMO proteins to MK2 (Fig. 3.2) suggesting that SUMO2/3 chains may form on MK2; an alternative hypothesis is that MK2 is mono-SUMOylated at multiple sites. If MK2 is mono-SUMOylated at multiple sites and SUMO2/3 chains do not form, MK2 would not be expected to interact with STUbLs. If SUMO2/3 chains on MK2 are ubiquitinated by STUbLs, it can have diverse consequences for its activity.

4.4 Possible Mechanisms to Explain why KapB Expression did not Alter MK2 SUMOylation

Activation of MK2 triggers the induction of actin stress fibres, the dispersal of PBs and the stabilization of inflammatory ARE-mRNAs; KapB elicits these same phenotypes by binding to and activating MK2 by an unknown mechanism (Corcoran et

al., 2015; McCormick and Ganem, 2005). When MK2 SUMOylation was impaired by substitution of K353 with arginine, this led to prolonged HSP27 phosphorylation and exacerbated stress fibre formation after TNF treatment (Chang et al., 2011). Because these phenotypes were like those induced by KapB, I hypothesized that KapB might be activating MK2 by disrupting its SUMOylation. To test this, I performed immunoprecipitation assays to examine the covalent modification of MK2 with SUMO in the presence and absence of KapB. Contrary to my hypothesis, the presence of KapB did not alter MK2 SUMOylation in my assays compared to when KapB was absent (Fig. 3.3D). While the simplest explanation for this result is that KapB is not affecting MK2 SUMOylation, and instead may be activating MK2 by displacing the autoinhibitory helix or by shielding activated MK2 from phosphatases (McCormick and Ganem, 2005), I have considered several other possible explanations for this observation, which are expanded on below.

4.4.1 KapB may be Binding a Specific MK2 Subset That is Difficult to Detect through Immunoprecipitation

One explanation for the lack of change in the MK2 SUMOylation profile in the presence of KapB is that KapB may be binding a certain subset of the MK2 pool, and the denaturing IP assays utilized in this study are not sensitive enough to detect SUMOylation changes of this subset. Attempts to determine what subset of MK2 this might be were inconclusive for reasons described in section 4.2.2 (Figs. 3.4, 3.5); therefore, this remains an open question. While it could not be determined if KapB is binding a specific subset of MK2, another theory may explain why KapB did not appear to disrupt MK2 SUMOylation (Fig. 3.3D).

4.4.2 KapB-Mediated Disruption of MK2 SUMOylation may Trigger SUMOylation at Other Sites

As was seen during the MK2 SUMOylation assay (Fig. 3.2C), the loss of the K353 SUMOylation site had little effect on the MK2 SUMOylation profile. This is contrary to the observations made by Chang et al. (2011), who noted that arginine substitution at this site resulted in decreased MK2 SUMOylation; however, in that study they worked with murine MK2, which may behave differently from human MK2. It has been observed that mutation of one SUMO site sometimes leads to SUMO attachment at other sites (Enserink 2015). In order to test this hypothesis, the identity of other SUMOylation sites within MK2 would first have to be confirmed, either through site-directed mutagenesis of putative lysines to arginine, or through mass spectrometry. Historically, it has been difficult to identify SUMO conjugation sites using mass spectrometry. Unlike ubiquitin, which leaves a di-glycine signal on the modified residue after trypsin digestion, SUMO leaves a large signature (19 amino acids for SUMO1, 32 for SUMO2/3) that makes identification of modified proteins difficult (Impens et al., 2014). To circumvent this, Impens et al. (2014) developed mutant His-tagged SUMO1 & 2 constructs introducing one arginine residue immediately upstream of the SUMO di-glycine motif (T95R in SUMO1, T91R in SUMO2), mimicking the ubiquitin sequence, resulting in a di-glycine signature on SUMO-modified lysines following trypsin digestion. Importantly, these mutations had little impact on SUMO protein function, though they appeared to be conjugated less efficiently than their wild-type counterparts. This approach was combined with stable isotope labeling of amino acids in cell culture (SILAC), enrichment of SUMOylated proteins using nickel chromatography and immunoprecipitation, as well as mass spectrometry to identify SUMOylated lysines

within their samples, validating the approach by comparing their results to PhosphoSitePlus database entries (Impens et al., 2014). A similar approach could be taken to identify MK2 SUMOylation sites, and to characterize potential changes in MK2 SUMOylation patterns when KapB is expressed. However, the cost of SILAC is prohibitive to implementation of this approach (Corcoran, personal communication). An alternative could be to mutate every lysine in MK2 to arginine, then reintroduce them both alone and in combination to determine which sites are *bona fide* SUMO sites; however, this approach would likely be very time intensive, and it is uncertain what the functional outcomes of such drastic mutagenesis would be.

4.5 MK2-KR-EE Recapitulates Some Features of KapB Expression

While IPs showed that KapB did not change MK2 SUMOylation, a second approach was employed using K353R MK2 mutants to determine if loss of the K353 SUMO site could recapitulate the specific KapB phenotypes of ARE-mRNA stabilization, PB disassembly and actin stress fibre induction.

4.5.1 MK2-KR-EE Recapitulates KapB ARE-mRNA Stabilization

Luciferase assays for ARE-mRNA decay were utilized to study the ability of the various MK2 constructs to stabilize the ARE-containing firefly luciferase reporter construct (Corcoran et al., 2011). Compared to WT-MK2 the K353R mutation alone no little impact on MK2's ability to stabilize ARE-containing mRNAs (FLAG-MK2-KR, Fig. 3.6), though this result was not entirely shocking; often, mutation of a single SUMO-target site within a protein has no clear effect on protein function (Enserink, 2015). In this regard, it was interesting to observe that the addition of the two glutamic acid mutations (T222E, T334E) to the K353R MK2 mutant caused an increase in ARE-mRNA stability to levels that are comparable to what was observed during KapB

expression (Fig. 3.6). This result suggests that MK2-KR-EE recapitulates the ARE-mRNA stabilizing aspect of the KapB phenotypes, though more experiments would need to be conducted to determine how important the KR substitution is to this phenotype. Another MK2 construct that could have been added to this assay is a kinase-dead MK2 construct (MK2-K93R in human MK2) in which the conserved lysine residue of the ATP binding domain has been mutated to arginine (Winzen et al., 1999). The level of ARE-mRNA stabilization when MK2 cannot phosphorylate its downstream effectors would provide a reference for the levels of stability when the MK2 pathway is not engaged, and without this reference, it cannot be determined whether the WT-MK2 and MK2-KR constructs were phosphorylating downstream effectors and contributing to increased stability. This result is also supported by the observation that each of these MK2 constructs could disassemble PBs to a significant degree, which will be expanded on below.

4.5.2 MK2-KR-EE did not Disassemble PBs to the Same Extent as KapB

PBs are cytoplasmic granules comprised of translationally repressed mRNAs and machinery associated with translational repression and mRNA decay (Luo et al., 2018). Activation of the MK2-RhoA signaling axis results in the disassembly of PBs, which is associated with increases in ARE-mRNA stability and expression (Corcoran et al., 2015). Expression of constitutively-active MK2 induces this signaling cascade, due to its mimicry of phosphorylated and activated MK2. By binding to and activating MK2, KapB also initiates the MK2-RhoA signaling cascade, resulting in the same phenotypes (Corcoran et al., 2015). The ability of MK2-KR-EE to recapitulate the PB disassembly and stress fibre (SF) phenotypes was tested in HeLa cells overexpressing dox-inducible GFP-tagged Dcp1a, providing a visible green fluorescent marker of PB puncta in cells.

To validate this overexpression system as a surrogate for endogenous PBs, cells were stained for the endogenous PB resident protein Hedls, a decapping co-factor. Dcp1a co-localized with Hedls 96.9% of the time (Fig. 3.8 C, D), indicating that most of these puncta behaved like *bona fide* PBs. There was no significant difference between the MK2 constructs in terms of their ability to disassemble GFP-Dcp1a foci (Fig. 3.8 A, E). This could be caused by MK2 being activated in each condition, regardless of whether they contained the phospho-mimicking mutations, as inferred from the predominantly cytoplasmic localization of MK2 in each condition. This was expected for the constructs containing glutamic acid substitutions; activated MK2 is known to localize to the cytoplasm (Gaestel, 2006). In theory WT-MK2 and MK2-KR should only localize to the cytoplasm if a cellular stressor activated them. However, this may have more to do with MK2 not having time to localize to the nucleus from the cytoplasm after expression. In this respect, the MK2-K93R mutant would have been beneficial for elucidating the effects of kinase-dead MK2 on Dcp1a puncta disassembly. Regardless, none of the MK2 constructs dispersed PBs to the same extent as KapB, which caused a more than 7-fold reduction in GFP-Dcp1a foci compared to vector.

4.5.3 HeLa Cells are not a Robust System for the Study of Stress Fibres

Given that activation of MK2, whether through mutagenesis or KapB binding, is associated with the induction of stress fibres (SF) (Corcoran et al., 2015), I sought to characterize how each MK2 mutant impacted SF induction. While MK2-EE, MK2-KR-EE and KapB appeared to cause a more pronounced induction of stress fibres compared to vector, WT-MK2 and MK2-KR, the increased appearance of SF and the morphological change usually associated with ectopic expression of KapB in primary ECs was not as robust in the HeLa cell line used here (Corcoran et al., 2015; Kayyali et

al., 2002; Liu et al., 2009). Since KapB, as the positive control for the phenotype, did not robustly elicit SF, it was difficult to determine with certainty the ability of each construct to recapitulate this phenotype. These experiments would have to be repeated in primary endothelial cells to definitively answer this question.

4.6 Potential Mechanisms of KapB Activation of MK2

While MK2-KR-EE recapitulated the ability of KapB to stabilize ARE-mRNAs, it could not recapitulate the disassembly of PBs to the same degree. Several possibilities exist that may provide an explanation for this observation. One explanation is that the microscopy-based approach to study PB disassembly does not have the dynamic range required to accurately distinguish between more or less PB disassembly; these experiments would also benefit from being repeated in primary endothelial cells. The most obvious explanation is that KapB is not activating MK2 by altering its SUMOylation, which is in line with the observation that KapB expression did not alter the MK2 SUMOylation profile (Fig. 3.3D). However, these data can be interpreted in another way; if SUMOylation flags MK2 for SUMO-targeted ubiquitination by STUbLs, then KapB could maintain MK2 activity by shielding it from these STUbLs, preventing its degradation. Such a hypothesis could reconcile the observation that KapB does not alter the MK2 SUMOylation profile, as well as the observation that MK2-KR-EE does not recapitulate all KapB phenotypes. If KapB is not disrupting MK2 SUMOylation as suggested by this hypothesis, then it would not be expected that the MK2-KR mutant would recapitulate KapB phenotypes. To elucidate this, experiments would first have to be conducted to determine if STUbLs actually do target SUMOylated MK2, and if this targeting is for degradation, since STUbLs can mediate other functions besides degradation, which is suggested by their ability to attach K63-linked ubiquitin chains to

SUMOylated substrates (Sriramachandran and Dohmen, 2014; Yin et al., 2012). However, if STUbLs are targeting MK2 for degradation, and if KapB is preventing the STUbL-mediated degradation of MK2, it would be expected that less MK2 protein would be detected on anti-FLAG immunoblots when KapB is absent (Fig. 3.2C, 3.3D), which was not observed. This might be due to the overexpression of MK2, Ubc9 and SUMO3 masking the effects of any STUbL-mediated degradation that may have been occurring.

Another theory is that the wrong MK2 SUMOylation site was targeted in these studies, and because of this, the KapB phenotype was not faithfully recapitulated by the MK2-KR-EE mutant. As demonstrated in the MK2 SUMOylation assays (Fig. 3.2C), it is very likely that other SUMOylation sites exist within MK2, with the most probable sites being K64 near the N-terminus of MK2 and K188 next to the catalytic D186 residue of MK2 (Meng et al., 2002). One can speculate that if SUMOylation were to occur at K188, through steric interference it would likely prevent substrates from interacting with the catalytic residue of MK2, attenuating MK2 activity. KapB binds to MK2 somewhere between residues 200-270 of MK2 (McCormick and Ganem, 2005), which is significantly upstream of K353; based upon proximity, it is difficult to theorize how KapB could be disrupting SUMOylation at this site. K188 is much closer to the putative KapB binding region, and if SUMOylation at this site did in fact interfere with MK2 substrate interactions, KapB binding might either prevent SUMOylation at this site (through conformational change or steric interference) or promote the removal of SUMO through the recruitment of SENPs. A similar mutagenesis approach to the one utilized in this study could be employed at this site to first determine if it is in fact a *bona fide* SUMOylation site. If such studies revealed that K188 is a SUMOylation site,

experiments could be conducted to determine what the outcome of SUMOylation at this site is, and if a loss of SUMOylation at this site can recapitulate KapB phenotypes.

Outlined above are several possibilities outlining how SUMOylation may be regulating MK2 activity, how phosphorylation of MK2 may play a role in regulating SUMOylation, and how KapB may or may not interfere with this regulatory spider web (summarized in Fig. 4.2). Regardless of these possibilities, based upon the conformational changes that MK2 undergoes upon phosphorylation at T334 and subsequent activation, it is highly likely that T334 phosphorylation precedes any possible SUMOylation events at K188 and K353. It is possible that KapB binds phosphorylated and activated MK2, since in its inactive conformation the autoinhibitory helix of MK2 obstructs the putative KapB binding site. However, it has also been suggested that the binding of KapB to MK2 might displace the MK2 autoinhibitory helix, resulting in its activation (McCormick and Ganem, 2005).

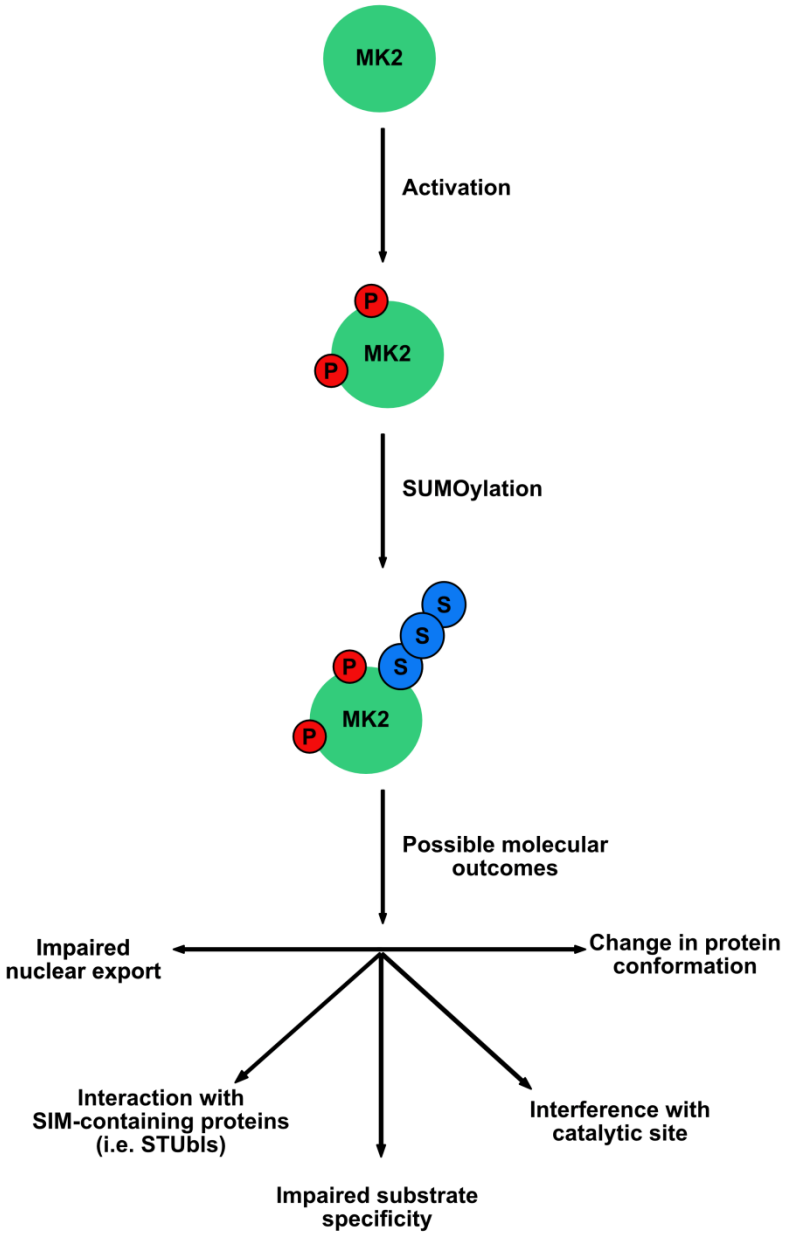

Figure 4.2 Possible molecular outcomes of MK2 SUMOylation. SUMOylation may cause changes in MK2 protein conformation and impair substrate specificity, leading to decreased activity. SUMO conjugation may facilitate interactions with MK2 and SIM-containing interaction partners, such as STUbLs, which may ubiquitinate SUMO chains and cause the degradation of MK2 by the proteasome, or mediate other interactions and functions. Due to the proximity of K353 to the nuclear export sequence, SUMOylation may impair nuclear export of MK2, interfering with its cellular localization. P: phosphate. S: SUMO.

The least complicated model to explain my data is that KapB does not impact MK2 SUMOylation in any way and may be activating MK2 by shielding it from phosphatases after activation, or by displacing the autoinhibitory helix upon binding to MK2 (McCormick and Ganem, 2005). However, as outlined above, there are a multitude of other explanations for the results reported herein. One possibility that explains both the failure of MK2-KR-EE to recapitulate all KapB phenotypes, as well as the unchanged SUMOylation profile of MK2 when KapB is expressed, is that KapB shields SUMOylated MK2 from degradation mediated by STUbLs (Fig. 4.3A); however, this hypothesis is contingent on SUMO targeting MK2 for ubiquitination and subsequent degradation by STUbLs. KapB may also be blocking (Fig. 4.3B) or promoting removal of SUMO conjugation (Fig. 4.3C), either through steric interference, changes in conformation that make MK2 a poor candidate for SUMOylation, or through the recruitment of SENPs. If this were occurring, it may not be detectable using the IP approach utilized in this study. Additionally, KapB may be preferentially binding and modulating the SUMOylation of a select subset of the MK2 pool, which also might not have been detectable with the IP protocols used in this study.

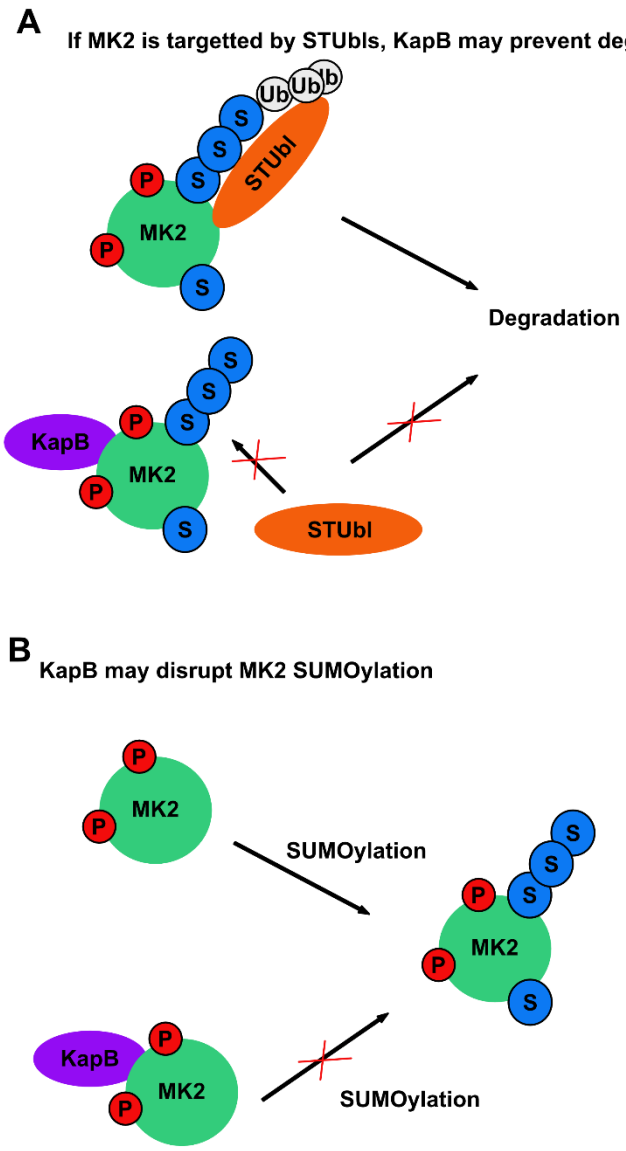
A
If MK2 is targetted by STUbls, KapB may prevent degradation
Ub
Ub
Ub
S
S
S
P
STUbl
MK2
P
S
Degradation
S
S
P
S
KapB
MK2
P
S
STUbl
B
KapB may disrupt MK2 SUMOylation
P
MK2
P
SUMOylation
S
S
P
S
MK2
P
S
P
KapB
MK2
P
SUMOylation

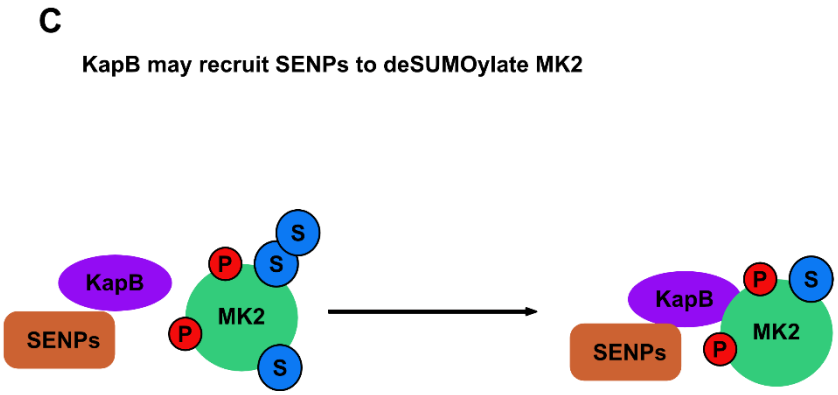

Figure 4.3 Potential models of KapB interaction with MK2 SUMOylation. A) If SUMOylated MK2 is ubiquitinated by STUbLs and degraded, KapB may bind to and protect MK2 from degradation. **B)** KapB binding to MK2 may cause conformational changes that prevent or reduce the amount of MK2 that is SUMOylated. **C)** KapB may recruit SUMO proteases (SENPs) to deSUMOylate MK2, leading to enhanced activity. P: phosphate. S: SUMO. Ub: ubiquitin.

4.7 Concluding Remarks

Kaposi's sarcoma is a complex cancer caused by KSHV (Ganem, 2006). Latently infected spindle cells are the major proliferative element of KS lesions, and the ectopic expression of the latently-expressed Kaposin B protein in endothelial cells recapitulates the inflammatory and angiogenic aspects of the KS lesion (Corcoran et al., 2015; McCormick and Ganem, 2005). The expression of KapB causes the stabilization of inflammatory ARE-mRNAs (which contributes to the inflammatory environment), the induction of actin stress fibres, and the dispersal of PBs, which is correlated with the stabilization of inflammatory mRNAs (Corcoran et al., 2015; McCormick and Ganem, 2005). KapB causes these phenotypes by binding to and activating MK2, initiating the MK2/RhoA signaling cascade (Corcoran et al., 2015); however, it is currently unknown how KapB activates MK2. This study hypothesized that KapB may be activating MK2 by disrupting its SUMOylation, based on the similarity of phenotypes caused by KapB expression and the prevention of MK2 SUMOylation as reported by Chang et al (2011). In this thesis, I tested the ability of KapB to disrupt MK2 SUMOylation but observed no noticeable changes in MK2 SUMOylation when KapB was present. Though it is possible that KapB binds only a small subset of the MK2 pool to prevent its SUMOylation, my attempts to determine the KapB-bound pool of MK2 pool were inconclusive. In parallel, I analyzed mutant versions of MK2 (MK2-KR, MK2-EE, MK2-KR-EE) to determine their ability to recapitulate KapB three phenotypes: the stabilization of ARE-mRNAs, PB disassembly and actin stress fibre induction. Constitutively-active MK2-KR stabilized ARE-mRNAs to a similar degree as KapB; however, this same MK2 construct did not disassemble PBs to the same extent as KapB. While my results do not conclusively demonstrate whether KapB is or is not disrupting MK2 SUMOylation, I have uncovered

a complex regulatory interplay between phosphorylation and SUMOylation in regulating MK2 activity, which may provide insights into the regulation of inflammatory responses during a variety of cellular stress events, including, but not limited to latent KSHV infection and tumourigenesis.

REFERENCES

Aizer, A., Brody, Y., Ler, L.W., Sonenberg, N., Singer, R.H., and Shav-Tal, Y. (2008). The Dynamics of Mammalian P Body Transport, Assembly, and Disassembly In Vivo. MBoC *19*, 4154–4166.

Aoki, Y., Jaffe, E.S., Chang, Y., Jones, K., Teruya-Feldstein, J., Moore, P.S., and Tosato, G. (1999). Angiogenesis and Hematopoiesis Induced by Kaposi's Sarcoma-Associated Herpesvirus-Encoded Interleukin-6. Blood *93*, 11.

Ayers, L.W., Barbachano-Guerrero, A., McAllister, S.C., Ritchie, J.A., Asiago-Reddy, E., Bartlett, L.C., Cesarman, E., Wang, D., Rochford, R., Martin, J.N., et al. (2018). Mast Cell Activation and KSHV Infection in Kaposi Sarcoma. Clin Cancer Res 1078-0432.CCR-18–0873.

Bayer, P., Arndt, A., Metzger, S., Mahajan, R., Melchior, F., Jaenicke, R., and Becker, J. (1998). Structure determination of the small ubiquitin-related modifier SUMO-1. Journal of Molecular Biology *280*, 275–286.

Ben-Levy, R., Leighton, I.A., Doza, Y.N., Attwood, P., Morrice, N., Marshall, C.J., and Cohen, P. (1995). Identification of novel phosphorylation sites required for activation of MAPKAP kinase-2. The EMBO Journal *14*, 5920–5930.

Ben-Levy, R., Hooper, S., Wilson, R., Paterson, H.F., and Marshall, C.J. (1998). Nuclear export of the stress-activated protein kinase p38 mediated by its substrate MAPKAP kinase-2. Current Biology *8*, 1049–1057.

Benndorf, R., Hayess, K., Ryazantsev, S., Wieske, M., Behlke, J., and Lutsch, G. (1994). Phosphorylation and Supramolecular Organization of Murine Small Heat Shock Protein HSP25 Abolish Its Actin Polymerization-inhibiting Activity. The Journal of Biological Chemistry *269*.

Bentz, G.L., Whitehurst, C.B., and Pagano, J.S. (2011). Epstein-Barr Virus Latent Membrane Protein 1 (LMP1) C-Terminal-Activating Region 3 Contributes to LMP1-Mediated Cellular Migration via Its Interaction with Ubc9. Journal of Virology *85*, 10144–10153.

Bentz, G.L., Moss, C.R., Whitehurst, C.B., Moody, C.A., and Pagano, J.S. (2015). LMP1-Induced Sumoylation Influences the Maintenance of Epstein-Barr Virus Latency through KAP1. J. Virol. *89*, 7465–7477.

Bischof, O., Schwamborn, K., Martin, N., Werner, A., Sustmann, C., Grosschedl, R., and Dejean, A. (2006). The E3 SUMO Ligase PIASy Is a Regulator of Cellular Senescence and Apoptosis. Molecular Cell *22*, 783–794.

Boggio, R., Colombo, R., Hay, R.T., Draetta, G.F., and Chiocca, S. (2004). A Mechanism for Inhibiting the SUMO Pathway. Molecular Cell *16*, 549–561.

Boggio, R., Passafaro, A., and Chiocca, S. (2007). Targeting SUMO E1 to Ubiquitin Ligases: A Viral Strategy to Counteract Sumoylation. J. Biol. Chem. *282*, 15376–15382.

Boudreau, B.Q. (2018). Designing an overexpression model to study the effects of Kaposin B on processing body dynamics. Honours thesis, Dalhousie University.

Brengues, M., Teixeira, D., and Parker, R. (2005). Movement of Eukaryotic mRNAs Between Polysomes and Cytoplasmic Processing Bodies. Science *310*, 486–489.

Cai, Q., Cai, S., Zhu, C., Verma, S.C., Choi, J.-Y., and Robertson, E.S. (2013). A Unique SUMO-2-Interacting Motif within LANA Is Essential for KSHV Latency. PLoS Pathog *9*, e1003750.

Campbell, M., and Izumiya, Y. (2012). Post-Translational Modifications of Kaposi's Sarcoma-Associated Herpesvirus Regulatory Proteins – SUMO and KSHV. Front. Microbio. *3*.

Cargnello, M., and Roux, P.P. (2011). Activation and Function of the MAPKs and Their Substrates, the MAPK-Activated Protein Kinases. Microbiology and Molecular Biology Reviews *75*, 50–83.

Castle, E.L. (2019). Kaposin B-Mediated Mechanoresponsive Signalling Controls Processing Body Disassembly. M.Sc. thesis, Dalhousie University.

Cesarman, E., Damania, B., Krown, S.E., Martin, J., Bower, M., and Whitby, D. (2019). Kaposi sarcoma. Nat Rev Dis Primers *5*, 9.

Chakraborty, S., Veettil, M.V., and Chandran, B. (2012). Kaposi's Sarcoma Associated Herpesvirus Entry into Target Cells. Front. Microbio. *3*.

Chang, P.-C., and Kung, H.-J. (2014). SUMO and KSHV Replication. Cancers *6*, 1905–1924.

Chang, E., Heo, K.-S., Woo, C.-H., Lee, H., Le, N.-T., Thomas, T.N., Fujiwara, K., and Abe, J. (2011). MK2 SUMOylation regulates actin filament remodeling and subsequent migration in endothelial cells by inhibiting MK2 kinase and HSP27 phosphorylation. Blood *117*, 2527–2537.

Chang, P.-C., Izumiya, Y., Wu, C.-Y., Fitzgerald, L.D., Campbell, M., Ellison, T.J., Lam, K.S., Luciw, P.A., and Kung, H.-J. (2010). Kaposi's Sarcoma-associated Herpesvirus (KSHV) Encodes a SUMO E3 ligase That Is SIM-dependent and SUMO-2/3-specific. J. Biol. Chem. *285*, 5266–5273.

Chang, Y., Cesarman, E., Pessin, M., Lee, F., Culpepper, J., Knowles, D., and Moore, P. (1994). Identification of herpesvirus-like DNA sequences in AIDS-associated Kaposi's sarcoma. Science *266*, 1865–1869.

Chatterjee, M., Osborne, J., Bestetti, G., Chang, Y., and Moore, P. (2002). Viral IL-6-induced cell proliferation and immune evasion of interferon activity. Science *298*.

Conn, K.L., Wasson, P., McFarlane, S., Tong, L., Brown, J.R., Grant, K.G., Domingues, P., and Boutell, C. (2016). Novel Role for Protein Inhibitor of Activated STAT 4 (PIAS4) in the Restriction of Herpes Simplex Virus 1 by the Cellular Intrinsic Antiviral Immune Response. J. Virol. *90*, 4807–4826.

Corcoran, J.A., Khaperskyy, D.A., and McCormick, C. (2011). Assays for monitoring viral manipulation of host ARE-mRNA turnover. Methods *55*, 172–181.

Corcoran, J.A., Johnston, B.P., and McCormick, C. (2015). Viral Activation of MK2-hsp27-p115RhoGEF-RhoA Signaling Axis Causes Cytoskeletal Rearrangements, P-body Disruption and ARE-mRNA Stabilization. PLoS Pathog *11*, e1004597.

Damania, B., and Cesarman, E. (2013). Kaposi's sarcoma-associated herpesvirus. In Fields Virology, (Philidelphia, PA: Wolters Kluwer), p.

Di Domenico, E., Toma, L., Bordignon, V., Trento, E., D'Agosto, G., Cordiali-Fei, P., and Ensoli, F. (2016). Activation of DNA Damage Response Induced by the Kaposi's Sarcoma-Associated Herpes Virus. IJMS *17*, 854.

Eifler, K., and Vertegaal, A.C.O. (2015). SUMOylation-Mediated Regulation of Cell Cycle Progression and Cancer. Trends in Biochemical Sciences *40*, 779–793.

Enserink, J.M. (2015). Sumo and the cellular stress response. Cell Div *10*, 4.

Ensoli, B., Sgadari, C., Barillari, G., Sirianni, M.C., Stürzl, M., and Monini, P. (2001). Biology of Kaposi's sarcoma. European Journal of Cancer *37*, 1251–1269.

Eulalio, A., Behm-Ansmant, I., Schweizer, D., and Izaurralde, E. (2007). P-Body Formation Is a Consequence, Not the Cause, of RNA-Mediated Gene Silencing. Molecular and Cellular Biology *27*, 3970–3981.

Evdokimov, E., Sharma, P., Lockett, S.J., Lualdi, M., and Kuehn, M.R. (2008). Loss of SUMO1 in mice affects RanGAP1 localization and formation of PML nuclear bodies, but is not lethal as it can be compensated by SUMO2 or SUMO3. Journal of Cell Science *121*, 4106–4113.

Flotho, A., and Melchior, F. (2013). Sumoylation: A Regulatory Protein Modification in Health and Disease. Annu. Rev. Biochem. *82*, 357–385.

Franks, T.M., and Lykke-Andersen, J. (2007). TTP and BRF proteins nucleate processing body formation to silence mRNAs with AU-rich elements. Genes & Development *21*, 719–735.

Gaestel, M. (2006). MAPKAP kinases — MKs — two's company, three's a crowd. Nat Rev Mol Cell Biol *7*, 120–130.

Ganem, D. (2006). KSHV infection and the pathogenesis of Kaposi's sarcoma. Annu. Rev. Pathol. Mech. Dis. *1*, 273–296.

Ganem, D. (2010). KSHV and the pathogenesis of Kaposi sarcoma: listening to human biology and medicine. J. Clin. Invest. *120*, 939–949.

Garcia, M.C., Ray, D.M., Lackford, B., Rubino, M., Olden, K., and Roberts, J.D. (2009). Arachidonic Acid Stimulates Cell Adhesion through a Novel p38 MAPK-RhoA Signaling Pathway That Involves Heat Shock Protein 27. J. Biol. Chem. *284*, 20936–20945.

Gossen, M., and Bujard, H. (1992). Tight control of gene expression in mammalian cells by tetracycline-responsive promoters. Proceedings of the National Academy of Sciences *89*, 5547–5551.

Gramolelli, S., and Schulz, T.F. (2015). The role of Kaposi sarcoma-associated herpesvirus in the pathogenesis of Kaposi sarcoma: Kaposi sarcoma pathogenesis. J. Pathol. *235*, 368–380.

Grinde, B. (2013). Herpesviruses: latency and reactivation – viral strategies and host response. Journal of Oral Microbiology *5*, 22766.

Guo, D., Li, M., Zhang, Y., Yang, P., Eckenrode, S., Hopkins, D., Zheng, W., Purohit, S., Podolsky, R.H., Muir, A., et al. (2004). A functional variant of SUMO4, a new IκBα modifier, is associated with type 1 diabetes. Nat Genet *36*, 837–841.

Hong, Y.-K., Foreman, K., Shin, J.W., Hirakawa, S., Curry, C.L., Sage, D.R., Libermann, T., Dezube, B.J., Fingeroth, J.D., and Detmar, M. (2004). Lymphatic reprogramming of blood vascular endothelium by Kaposi sarcoma–associated herpesvirus. Nat Genet *36*, 683–685.

Horita, H., Law, A., and Middleton, K. (2018). Utilizing a Comprehensive Immunoprecipitation Enrichment System to Identify an Endogenous Post-translational Modification Profile for Target Proteins. JoVE 56912.

Hu, J., Garber, A.C., and Renne, R. (2002). The Latency-Associated Nuclear Antigen of Kaposi's Sarcoma-Associated Herpesvirus Supports Latent DNA Replication in Dividing Cells. Journal of Virology *76*, 11677–11687.

Huang, C.-H., Su, M.-G., Kao, H.-J., Jhong, J.-H., Weng, S.-L., and Lee, T.-Y. (2016). UbiSite: incorporating two-layered machine learning method with substrate motifs to predict ubiquitin-conjugation site on lysines. BMC Syst Biol *10*, S6.

Hubstenberger, A., Courel, M., Bénard, M., Souquere, S., Ernoult-Lange, M., Chouaib, R., Yi, Z., Morlot, J.-B., Munier, A., Fradet, M., et al. (2017). P-Body Purification Reveals the Condensation of Repressed mRNA Regulons. Molecular Cell *68*, 144-157.e5.

Impens, F., Radoshevich, L., Cossart, P., and Ribet, D. (2014). Mapping of SUMO sites and analysis of SUMOylation changes induced by external stimuli. PNAS *111*, 6.

Izumiya, Y., Ellison, T.J., Yeh, E.T.H., Jung, J.U., Luciw, P.A., and Kung, H.-J. (2005). Kaposi's Sarcoma-Associated Herpesvirus K-bZIP Represses Gene Transcription via SUMO Modification. Journal of Virology *79*, 9912–9925.

Karhausen, J., Bernstock, J.D., Johnson, K.R., Sheng, H., Ma, Q., Shen, Y., Yang, W., Hallenbeck, J.M., and Paschen, W. (2018). Ubc9 overexpression and SUMO1 deficiency blunt inflammation after intestinal ischemia/reperfusion. Lab Invest *98*, 799–813.

Kayyali, U.S., Pennella, C.M., Trujillo, C., Villa, O., Gaestel, M., and Hassoun, P.M. (2002). Cytoskeletal Changes in Hypoxic Pulmonary Endothelial Cells Are Dependent on MAPK-activated Protein Kinase MK2. J. Biol. Chem. *277*, 42596–42602.

Kimple, M.E., Brill, A.L., and Pasker, R.L. (2013). Overview of Affinity Tags for Protein Purification: Affinity Tags for Protein Purification. In Current Protocols in Protein Science, J.E. Coligan, B.M. Dunn, D.W. Speicher, and P.T. Wingfield, eds. (Hoboken, NJ, USA: John Wiley & Sons, Inc.), pp. 9.9.1-9.9.23.

Knipscheer, P., Flotho, A., Klug, H., Olsen, J.V., van Dijk, W.J., Fish, A., Johnson, E.S., Mann, M., Sixma, T.K., and Pichler, A. (2008). Ubc9 Sumoylation Regulates SUMO Target Discrimination. Molecular Cell *31*, 371–382.

Kotlyarov, A., Neininger, A., Schubert, C., Eckert, R., Birchmeier, C., Volk, H.-D., and Gaestel, M. (1999). MAPKAP kinase 2 is essential for LPS-induced TNF-α biosynthesis. Nat Cell Biol *1*, 94–97.

Kotlyarov, A., Yannoni, Y., Fritz, S., Laass, K., Telliez, J.-B., Pitman, D., Lin, L.-L., and Gaestel, M. (2002). Distinct Cellular Functions of MK2. Molecular and Cellular Biology *22*, 4827–4835.

Krumova, P., Meulmeester, E., Garrido, M., Tirard, M., Hsiao, H.-H., Bossis, G., Urlaub, H., Zweckstetter, M., Kügler, S., Melchior, F., et al. (2011). Sumoylation inhibits α-synuclein aggregation and toxicity. J Cell Biol *194*, 49–60.

Leidal, A.M., Cyr, D.P., Hill, R.J., Lee, P.W.K., and McCormick, C. (2012). Subversion of Autophagy by Kaposi's Sarcoma-Associated Herpesvirus Impairs Oncogene-Induced Senescence. Cell Host & Microbe *11*, 167–180.

Leung, T., Chen, X.-Q., Manser, E., and Lim, L. (1996). The p160 RhoA-Binding Kinase ROK␣ Is a Member of a Kinase Family and Is Involved in the Reorganization of the Cytoskeleton. MOL. CELL. BIOL. *16*, 15.

Li, H., Komatsu, T., Dezube, B.J., and Kaye, K.M. (2002). The Kaposi's Sarcoma-Associated Herpesvirus K12 Transcript from a Primary Effusion Lymphoma Contains Complex Repeat Elements, Is Spliced, and Initiates from a Novel Promoter. Journal of Virology *76*, 11880–11888.

Liu, T., Guevara, O.E., Warburton, R.R., Hill, N.S., Gaestel, M., and Kayyali, U.S. (2009). Modulation of HSP27 alters hypoxia-induced endothelial permeability and related signaling pathways. J. Cell. Physiol. *220*, 600–610.

Lowrey, A.J., Cramblet, W., and Bentz, G.L. (2017). Viral manipulation of the cellular sumoylation machinery. Cell Commun Signal *15*, 27.

Luo, Y., Na, Z., and Slavoff, S.A. (2018). P-Bodies: Composition, Properties, and Functions. Biochemistry *57*, 2424–2431.

Matta, H., and Chaudhary, P.M. (2004). Activation of alternative NF- B pathway by human herpes virus 8-encoded Fas-associated death domain-like IL-1 -converting enzyme inhibitory protein (vFLIP). Proceedings of the National Academy of Sciences *101*, 9399–9404.

Matta, H., Surabhi, R.M., Zhao, J., Punj, V., Sun, Q., Schamus, S., Mazzacurati, L., and Chaudhary, P.M. (2007). Induction of spindle cell morphology in human vascular endothelial cells by human herpesvirus 8-encoded viral FLICE inhibitory protein K13. Oncogene *26*, 1656–1660.

McCormick, C., and Ganem, D. (2005). The Kaposin B Protein of KSHV Activates the p38/MK2 Pathway and Stabilizes Cytokine mRNAs. Science *307*, 4.

McCormick, C., and Ganem, D. (2006). Phosphorylation and Function of the Kaposin B Direct Repeats of Kaposi's Sarcoma-Associated Herpesvirus. Journal of Virology *80*, 6165–6170.

Meng, W., Swenson, L.L., Fitzgibbon, M.J., Hayakawa, K., ter Haar, E., Behrens, A.E., Fulghum, J.R., and Lippke, J.A. (2002). Structure of Mitogen-activated Protein Kinase-activated Protein (MAPKAP) Kinase 2 Suggests a Bifunctional Switch That Couples Kinase Activation with Nuclear Export. J. Biol. Chem. *277*, 37401–37405.

Montaner, S., Sodhi, A., Molinolo, A., Bugge, T.H., Sawai, E.T., He, Y., Li, Y., Ray, P.E., and Gutkind, J.S. (2003). Endothelial infection with KSHV genes in vivo reveals that vGPCR initiates Kaposi's sarcomagenesis and can promote the tumorigenic potential of viral latent genes. Cancer Cell *3*, 23–36.

Myoung, J., and Ganem, D. (2011). Infection of primary human tonsillar lymphoid cells by KSHV reveals frequent but abortive infection of T cells. Virology *413*, 1–11.

Nayak, A., and Müller, S. (2014). SUMO-specific proteases/isopeptidases: SENPs and beyond. Genome Biol *15*, 422.

Parker, R., and Sheth, U. (2007). P Bodies and the Control of mRNA Translation and Degradation. Molecular Cell *25*, 635–646.

Pellet, P., and Roizman, B. (2013). Herpesviridae. In Fields Virology, (Philidelphia, PA: Wolters Kluwer), p.

Pichler, A., Fatouros, C., Lee, H., and Eisenhardt, N. (2017). SUMO conjugation – a mechanistic view. Biomolecular Concepts *8*.

Piolot, T., Tramier, M., Coppey, M., Nicolas, J.-C., and Marechal, V. (2001). Close but Distinct Regions of Human Herpesvirus 8 Latency-Associated Nuclear Antigen 1 Are Responsible for Nuclear Targeting and Binding to Human Mitotic Chromosomes. Journal of Virology *75*, 3948–3959.

Raingeaud, J., Gupta, S., Rogers, J., Dickens, M., Han, J., Ulevitch, R., and Davis, R. (1995). Pro-inflammatory cytokines and environmental stress cause p38 mitogen-activated protein kinase activation by dual phosphorylation on tyrosine and threonine. The Journal of Biological Chemistry *270*, 7420–7426.

Rappocciolo, G., Jenkins, F.J., Hensler, H.R., Piazza, P., Jais, M., Borowski, L., Watkins, S.C., and Rinaldo, C.R. (2006). DC-SIGN Is a Receptor for Human Herpesvirus 8 on Dendritic Cells and Macrophages. J Immunol *176*, 1741–1749.

Reinhardt, H.C., and Yaffe, M.B. (2009). Kinases that control the cell cycle in response to DNA damage: Chk1, Chk2, and MK2. Current Opinion in Cell Biology *21*, 245–255.

Rogalla, T., Ehrnsperger, M., Preville, X., Kotlyarov, A., and Lutsch, G. (1999). Regulation of Hsp27 Oligomerization, Chaperone Function, and Protective Activity against Oxidative Stress/Tumor Necrosis Factor by Phosphorylation. The Journal of Biological Chemistry *274*, 11.

Russo, J.J., Bohenzky, R.A., Chien, M.-C., Chen, J., Yan, M., Maddalena, D., Parry, J.P., Peruzzi, D., Edelman, I.S., Chang, Y., et al. (1996). Nucleotide sequence of the Kaposi sarcoma-associated herpesvirus (HHV8). Proceedings of the National Academy of Sciences *93*, 14862–14867.

Sadler, R., Wu, L., Forghani, B., Renne, R., Zhong, W., Herndier, B., and Ganem, D. (1999). A Complex Translational Program Generates Multiple Novel Proteins from the Latently Expressed Kaposin (K12) Locus of Kaposi's Sarcoma-Associated Herpesvirus. J. VIROL. *73*, 9.

Saitoh, H., and Hinchey, J. (2000). Functional Heterogeneity of Small Ubiquitin-related Protein Modifiers SUMO-1 versus SUMO-2/3. J. Biol. Chem. *275*, 6252–6258.

Salsman, J., Zimmerman, N., Chen, T., Domagala, M., and Frappier, L. (2008). Genome-Wide Screen of Three Herpesviruses for Protein Subcellular Localization and Alteration of PML Nuclear Bodies. PLoS Pathog *4*, e1000100.

Saracco, S.A., Miller, M.J., Kurepa, J., and Vierstra, R.D. (2007). Genetic Analysis of SUMOylation in Arabidopsis: Conjugation of SUMO1 and SUMO2 to Nuclear Proteins Is Essential. Plant Physiol. *145*, 119–134.

Schulz, T.F. (2000). Kaposi's sarcoma-associated herpesvirus (human herpesvirus 8): epidemiology and pathogenesis. Journal of Antimicrobial Chemotherapy *45*, 15–27.

Shi, J., Wu, X., Surma, M., Vemula, S., Zhang, L., Yang, Y., Kapur, R., and Wei, L. (2013). Distinct roles for ROCK1 and ROCK2 in the regulation of cell detachment. Cell Death Dis *4*, e483–e483.

Soni, S., Anand, P., and Padwad, Y.S. (2019). MAPKAPK2: the master regulator of RNA-binding proteins modulates transcript stability and tumor progression. J Exp Clin Cancer Res *38*, 121.

Sriramachandran, A.M., and Dohmen, R.J. (2014). SUMO-targeted ubiquitin ligases. Biochimica et Biophysica Acta (BBA) - Molecular Cell Research *1843*, 75–85.

Su, Y.-F., Yang, T., Huang, H., Liu, L.F., and Hwang, J. (2012). Phosphorylation of Ubc9 by Cdk1 Enhances SUMOylation Activity. PLoS ONE *7*, e34250.

Subramaniam, S., Mealer, R.G., Sixt, K.M., Barrow, R.K., Usiello, A., and Snyder, S.H. (2010). Rhes, a Physiologic Regulator of Sumoylation, Enhances Cross-sumoylation between the Basic Sumoylation Enzymes E1 and Ubc9. J. Biol. Chem. *285*, 20428–20432.

Swatek, K.N., and Komander, D. (2016). Ubiquitin modifications. Cell Res *26*, 399–422.

Tomkowicz, B., Singh, S.P., Cartas, M., and Srinivasan, A. (2002). Human Herpesvirus-8 Encoded Kaposin: Subcellular Localization Using Immunofluorescence and Biochemical Approaches. DNA and Cell Biology *21*, 151–162.

Udeshi, N.D., Svinkina, T., Mertins, P., Kuhn, E., Mani, D.R., Qiao, J.W., and Carr, S.A. (2013). Refined Preparation and Use of Anti-diglycine Remnant (K-ε-GG) Antibody Enables Routine Quantification of 10,000s of Ubiquitination Sites in Single Proteomics Experiments. Mol Cell Proteomics *12*, 825–831.

Ullmann, R., Chien, C.D., Avantaggiati, M.L., and Muller, S. (2012). An Acetylation Switch Regulates SUMO-Dependent Protein Interaction Networks. Molecular Cell *46*, 759–770.

Vanhatupa, S., Ungureanu, D., Paakkunainen, M., and Silvennoinen, O. (2008). MAPK-induced Ser727 phosphorylation promotes SUMOylation of STAT1. Biochem. J. *409*, 179–185.

Wang, H.-W., Trotter, M.W.B., Lagos, D., Bourboulia, D., Henderson, S., Mäkinen, T., Elliman, S., Flanagan, A.M., Alitalo, K., and Boshoff, C. (2004). Kaposi sarcoma herpesvirus–induced cellular reprogramming contributes to the lymphatic endothelial gene expression in Kaposi sarcoma. Nat Genet *36*, 687–693.

Werner, A., Flotho, A., and Melchior, F. (2012). The RanBP2/RanGAP1∗SUMO1/Ubc9 Complex Is a Multisubunit SUMO E3 Ligase. Molecular Cell *46*, 287–298.

Whitley, R. (1996). Herpesviruses. In Medical Microbiology, (Galveston (TX): University of Texas Medical Branch at Galveston), p.

Winzen, R., Kracht, M., Ritter, B., Wilhelm, A., Chen, C.-Y., Shyu, A.-B., Muller, M., Gaestel, M., Resch, K., and Holtmann, H. (1999). The p38 MAP kinase pathway signals for cytokine-induced mRNA stabilization via MAP kinase-activated protein kinase 2 and an AU-rich region-targeted mechanism. The EMBO Journal *18*, 4969–4980.

Wood, N.H., and Feller, L. (2008). The malignant potential of HIV-associated Kaposi sarcoma. Cancer Cell Int *8*, 14.

Wu, Y.-C., Roark, A.A., Bian, X.-L., and Wilson, V.G. (2008). Modification of papillomavirus E2 proteins by the small ubiquitin-like modifier family members (SUMOs). Virology *378*, 329–338.

Xiao, Y., Pollack, D., Nieves, E., Winchell, A., Callaway, M., and Vigodner, M. (2015). Can your protein be sumoylated? A quick summary and important tips to study SUMO-modified proteins. Analytical Biochemistry *477*, 95–97.

Yao, Q., Li, H., Liu, B.-Q., Huang, X.-Y., and Guo, L. (2011). SUMOylation-regulated Protein Phosphorylation, Evidence from Quantitative Phosphoproteomics Analyses. J. Biol. Chem. *286*, 27342–27349.

Yin, Y., Seifert, A., Chua, J.S., Maure, J.-F., Golebiowski, F., and Hay, R.T. (2012). SUMO-targeted ubiquitin E3 ligase RNF4 is required for the response of human cells to DNA damage. Genes & Development *26*, 1196–1208.

Yuan, H., Zhou, J., Deng, M., Liu, X., Bras, M.L., The, H. de, Chen, S.J., Chen, Z., Liu, T.X., and Zhu, J. (2010). Small ubiquitin-related modifier paralogs are indispensable but functionally redundant during early development of zebrafish. Cell Res *20*, 185–196.

Zarubin, T., and Han, J. (2005). Activation and signaling of the p38 MAP kinase pathway. Cell Res *15*, 11–18.

Zhang, Y., Li, Y., Tang, B., and Zhang, C. (2017). The strategies for identification and quantification of SUMOylation. Chem. Commun. *53*, 6989–6998.

Zhao, J. (2007). Sumoylation regulates diverse biological processes. Cell. Mol. Life Sci. *64*, 3017–3033.

Zou, X., and Blank, M. (2017). Targeting p38 MAP kinase signaling in cancer through post-translational modifications. Cancer Letters *384*, 19–26.

Zu, Y.-L., Wu, F., Gilchrist, A., Ai, Y., Labadia, M., and Huang, C.-K. (1994). The primary structure of a human MAP kinase activated protein kinase 2. Biochemical and Biophysical Research Communications *200*, 1118–1124.

APPENDIX A: MK2 SEQUENCES

pcDNA3.1-FLAG-MK2

GACGGATCGGGAGATCTCCCGATCCCCTATGGTGCACTCTCAGTACAATCTG
CTCTGATGCCGCATAGTTAAGCCAGTATCTGCTCCCTGCTTGTGTGTTGGAGG
TCGCTGAGTAGTGCGCGAGCAAAATTTAAGCTACAACAAGGCAAGGCTTGAC
CGACAATTGCATGAAGAATCTGCTTAGGGTTAGGCGTTTTGCGCTGCTTCGC
GATGTACGGGCCAGATATACGCGTTGACATTGATTATTGACTAGTTATTAAT
AGTAATCAATTACGGGGTCATTAGTTCATAGCCCATATATGGAGTTCCGCGTT
ACATAACTTACGGTAAATGGCCCGCCTGGCTGACCGCCCAACGACCCCCGCC
CATTGACGTCAATAATGACGTATGTTCCCATAGTAACGCCAATAGGGACTTT
CCATTGACGTCAATGGGTGGAGTATTTACGGTAAACTGCCCACTTGGCAGTA
CATCAAGTGTATCATATGCCAAGTACGCCCCCTATTGACGTCAATGACGGTA
AATGGCCCGCCTGGCATTATGCCCAGTACATGACCTTATGGGACTTTCCTACT
TGGCAGTACATCTACGTATTAGTCATCGCTATTACCATGGTGATGCGGTTTTG
GCAGTACATCAATGGGCGTGGATAGCGGTTTGACTCACGGGGATTTCCAAGT
CTCCACCCCATTGACGTCAATGGGAGTTTGTTTTGGCACCAAAATCAACGGG
ACTTTCCAAAATGTCGTAACAACTCCGCCCCATTGACGCAAATGGGCGGTAG
GCGTGTACGGTGGGAGGTCTATATAAGCAGAGCTCTCTGGCTAACTAGAGAA
CCCACTGCTTACTGGCTTATCGAAATTAATACGACTCACTATAGGGAGACCC
AAGCTGGCTAGCGGAACCATGGACTACAAAGACGATGACGACAAGGGAGGC
GGTGGGGGAGGCCTGTCCAACTCCCAGGGCCAGAGCCCGCCGGTGCCGTTCC
CCGCCCCGGCCCCGCCGCCGCAGCCCCCCACCCCTGCCCTGCCGCACCCCCC
GGCGCAGCCGCCGCCGCCGCCCCCGCAGCAGTTCCCGCAGTTCCACGTCAAG
TCCGGCCTGCAGATCAAGAAGAACGCCATCATCGATGACTACAAGGTCACCA
GCCAGGTCCTGGGGCTGGGCATCAACGGCAAAGTTTTGCAGATCTTCAACAA
GAGGACCCAGGAGAAATTCGCCCTCAAAATGCTTCAGGACTGCCCCAAGGCC
CGCAGGGAGGTGGAGCTGCACTGGCGGGCCTCCCAGTGCCCGCACATCGTAC
GGATCGTGGATGTGTACGAGAATCTGTACGCAGGGAGGAAGTGCCTGCTGAT
TGTCATGGAATGTTTGGACGGTGGAGAACTCTTTAGCCGAATCCAGGATCGA
GGAGACCAGGCATTCACAGAAAGAGAAGCATCCGAAATCATGAAGAGCATC
GGTGAGGCCATCCAGTATCTGCATTCAATCAACATTGCCCATCGGGATGTCA

AGCCTGAGAATCTCTTATACACCTCCAAAAGGCCCAACGCCATCCTGAAACT
CACTGACTTTGGCTTTGCCAAGGAAACCACCAGCCACAACTCTTTGACCACT
CCTTGTTATACACCGTACTATGTGGCTCCAGAAGTGCTGGGTCCAGAGAAGT
ATGACAAGTCCTGTGACATGTGGTCCCTGGGTGTCATCATGTACATCCTGCTG
TGTGGGTATCCCCCCTTCTACTCCAACCACGGCCTTGCCATCTCTCCGGGCAT
GAAGACTCGCATCCGAATGGGCCAGTATGAATTTCCCAACCCAGAATGGTCA
GAAGTATCAGAGGAAGTGAAGATGCTCATTCGGAATCTGCTGAAAACAGAG
CCCACCCAGAGAATGACCATCACCGAGTTTATGAACCACCCTTGGATCATGC
AATCAACAAAGGTCCCTCAAACCCCACTGCACACCAGCCGGGTCCTGAAGGA
GGACAAGGAGCGGTGGGAGGATGTCAAGGAGGAGATGACCAGTGCCTTGGC
CACAATGCGCGTTGACTACGAGCAGATCAAGATAAAAAAGATTGAAGATGC
ATCCAACCCTCTGCTGCTGAAGAGGCGGAAGAAAGCTCGGGCCCTGGAGGCT
GCGGCTCTGGCCCACTGAGGCGGAGGAGGATCCACTAGTCCAGTGTGGTGGA
ATTCTGCAGATATCCAGCACAGTGGCGGCCGCTCGAGTCTAGAGGGCCCGTT
TAAACCCGCTGATCAGCCTCGACTGTGCCTTCTAGTTGCCAGCCATCTGTTGT
TTGCCCCTCCCCCGTGCCTTCCTTGACCCTGGAAGGTGCCACTCCCACTGTCC
TTTCCTAATAAAATGAGGAAATTGCATCGCATTGTCTGAGTAGGTGTCATTCT
ATTCTGGGGGGTGGGGTGGGGCAGGACAGCAAGGGGGAGGATTGGGAAGAC
AATAGCAGGCATGCTGGGGATGCGGTGGGCTCTATGGCTTCTGAGGCGGAAA
GAACCAGCTGGGGCTCTAGGGGGTATCCCCACGCGCCCTGTAGCGGCGCATT
AAGCGCGGCGGGTGTGGTGGTTACGCGCAGCGTGACCGCTACACTTGCCAGC
GCCCTAGCGCCCGCTCCTTTCGCTTTCTTCCCTTCCTTTCTCGCCACGTTCGCC
GGCTTTCCCCGTCAAGCTCTAAATCGGGGGCTCCCTTTAGGGTTCCGATTTAG
TGCTTTACGGCACCTCGACCCCAAAAAACTTGATTAGGGTGATGGTTCACGT
AGTGGGCCATCGCCCTGATAGACGGTTTTTCGCCCTTTGACGTTGGAGTCCAC
GTTCTTTAATAGTGGACTCTTGTTCCAAACTGGAACAACACTCAACCCTATCT
CGGTCTATTCTTTTGATTTATAAGGGATTTTGCCGATTTCGGCCTATTGGTTA
AAAAATGAGCTGATTTAACAAAAATTTAACGCGAATTAATTCTGTGGAATGT
GTGTCAGTTAGGGTGTGGAAAGTCCCCAGGCTCCCCAGCAGGCAGAAGTATG
CAAAGCATGCATCTCAATTAGTCAGCAACCAGGTGTGGAAAGTCCCCAGGCT
CCCCAGCAGGCAGAAGTATGCAAAGCATGCATCTCAATTAGTCAGCAACCAT

AGTCCCGCCCCTAACTCCGCCCATCCCGCCCCTAACTCCGCCCAGTTCCGCCC
ATTCTCCGCCCCATGGCTGACTAATTTTTTTTATTTATGCAGAGGCCGAGGCC
GCCTCTGCCTCTGAGCTATTCCAGAAGTAGTGAGGAGGCTTTTTTGGAGGCCT
AGGCTTTTGCAAAAAGCTCCCGGGAGCTTGTATATCCATTTTCGGATCTGATC
AAGAGACAGGATGAGGATCGTTTCGCATGATTGAACAAGATGGATTGCACG
CAGGTTCTCCGGCCGCTTGGGTGGAGAGGCTATTCGGCTATGACTGGGCACA
ACAGACAATCGGCTGCTCTGATGCCGCCGTGTTCCGGCTGTCAGCGCAGGGG
CGCCCGGTTCTTTTTGTCAAGACCGACCTGTCCGGTGCCCTGAATGAACTGCA
GGACGAGGCAGCGCGGCTATCGTGGCTGGCCACGACGGGCGTTCCTTGCGCA
GCTGTGCTCGACGTTGTCACTGAAGCGGGAAGGGACTGGCTGCTATTGGGCG
AAGTGCCGGGGCAGGATCTCCTGTCATCTCACCTTGCTCCTGCCGAGAAAGT
ATCCATCATGGCTGATGCAATGCGGCGGCTGCATACGCTTGATCCGGCTACC
TGCCCATTCGACCACCAAGCGAAACATCGCATCGAGCGAGCACGTACTCGGA
TGGAAGCCGGTCTTGTCGATCAGGATGATCTGGACGAAGAGCATCAGGGGCT
CGCGCCAGCCGAACTGTTCGCCAGGCTCAAGGCGCGCATGCCCGACGGCGA
GGATCTCGTCGTGACCCATGGCGATGCCTGCTTGCCGAATATCATGGTGGAA
AATGGCCGCTTTTCTGGATTCATCGACTGTGGCCGGCTGGGTGTGGCGGACC
GCTATCAGGACATAGCGTTGGCTACCCGTGATATTGCTGAAGAGCTTGGCGG
CGAATGGGCTGACCGCTTCCTCGTGCTTTACGGTATCGCCGCTCCCGATTCGC
AGCGCATCGCCTTCTATCGCCTTCTTGACGAGTTCTTCTGAGCGGGACTCTGG
GGTTCGAAATGACCGACCAAGCGACGCCCAACCTGCCATCACGAGATTTCGA
TTCCACCGCCGCCTTCTATGAAAGGTTGGGCTTCGGAATCGTTTTCCGGGACG
CCGGCTGGATGATCCTCCAGCGCGGGGATCTCATGCTGGAGTTCTTCGCCCA
CCCCAACTTGTTTATTGCAGCTTATAATGGTTACAAATAAAGCAATAGCATC
ACAAATTTCACAAATAAAGCATTTTTTTCACTGCATTCTAGTTGTGGTTTGTC
CAAACTCATCAATGTATCTTATCATGTCTGTATACCGTCGACCTCTAGCTAGA
GCTTGGCGTAATCATGGTCATAGCTGTTTCCTGTGTGAAATTGTTATCCGCTC
ACAATTCCACACAACATACGAGCCGGAAGCATAAAGTGTAAAGCCTGGGGT
GCCTAATGAGTGAGCTAACTCACATTAATTGCGTTGCGCTCACTGCCCGCTTT
CCAGTCGGGAAACCTGTCGTGCCAGCTGCATTAATGAATCGGCCAACGCGCG
GGGAGAGGCGGTTTGCGTATTGGGCGCTCTTCCGCTTCCTCGCTCACTGACTC

GCTGCGCTCGGTCGTTCGGCTGCGGCGAGCGGTATCAGCTCACTCAAAGGCG
GTAATACGGTTATCCACAGAATCAGGGGATAACGCAGGAAAGAACATGTGA
GCAAAAGGCCAGCAAAAGGCCAGGAACCGTAAAAAGGCCGCGTTGCTGGCG
TTTTTCCATAGGCTCCGCCCCCCTGACGAGCATCACAAAAATCGACGCTCAA
GTCAGAGGTGGCGAAACCCGACAGGACTATAAAGATACCAGGCGTTTCCCCC
TGGAAGCTCCCTCGTGCGCTCTCCTGTTCCGACCCTGCCGCTTACCGGATACC
TGTCCGCCTTTCTCCCTTCGGGAAGCGTGGCGCTTTCTCATAGCTCACGCTGT
AGGTATCTCAGTTCGGTGTAGGTCGTTCGCTCCAAGCTGGGCTGTGTGCACG
AACCCCCCGTTCAGCCCGACCGCTGCGCCTTATCCGGTAACTATCGTCTTGAG
TCCAACCCGGTAAGACACGACTTATCGCCACTGGCAGCAGCCACTGGTAACA
GGATTAGCAGAGCGAGGTATGTAGGCGGTGCTACAGAGTTCTTGAAGTGGTG
GCCTAACTACGGCTACACTAGAAGAACAGTATTTGGTATCTGCGCTCTGCTG
AAGCCAGTTACCTTCGGAAAAAGAGTTGGTAGCTCTTGATCCGGCAAACAAA
CCACCGCTGGTAGCGGTTTTTTTGTTTGCAAGCAGCAGATTACGCGCAGAAA
AAAAGGATCTCAAGAAGATCCTTTGATCTTTTCTACGGGGTCTGACGCTCAG
TGGAACGAAAACTCACGTTAAGGGATTTTGGTCATGAGATTATCAAAAAGGA
TCTTCACCTAGATCCTTTTAAATTAAAAATGAAGTTTTAAATCAATCTAAAGT
ATATATGAGTAAACTTGGTCTGACAGTTACCAATGCTTAATCAGTGAGGCAC
CTATCTCAGCGATCTGTCTATTTCGTTCATCCATAGTTGCCTGACTCCCCGTC
GTGTAGATAACTACGATACGGGAGGGCTTACCATCTGGCCCCAGTGCTGCAA
TGATACCGCGAGACCCACGCTCACCGGCTCCAGATTTATCAGCAATAAACCA
GCCAGCCGGAAGGGCCGAGCGCAGAAGTGGTCCTGCAACTTTATCCGCCTCC
ATCCAGTCTATTAATTGTTGCCGGGAAGCTAGAGTAAGTAGTTCGCCAGTTA
ATAGTTTGCGCAACGTTGTTGCCATTGCTACAGGCATCGTGGTGTCACGCTCG
TCGTTTGGTATGGCTTCATTCAGCTCCGGTTCCCAACGATCAAGGCGAGTTAC
ATGATCCCCCATGTTGTGCAAAAAAGCGGTTAGCTCCTTCGGTCCTCCGATCG
TTGTCAGAAGTAAGTTGGCCGCAGTGTTATCACTCATGGTTATGGCAGCACT
GCATAATTCTCTTACTGTCATGCCATCCGTAAGATGCTTTTCTGTGACTGGTG
AGTACTCAACCAAGTCATTCTGAGAATAGTGTATGCGGCGACCGAGTTGCTC
TTGCCCGGCGTCAATACGGGATAATACCGCGCCACATAGCAGAACTTTAAAA
GTGCTCATCATTGGAAAACGTTCTTCGGGGCGAAAACTCTCAAGGATCTTAC

CGCTGTTGAGATCCAGTTCGATGTAACCCACTCGTGCACCCAACTGATCTTCA
GCATCTTTTACTTTCACCAGCGTTTCTGGGTGAGCAAAAACAGGAAGGCAAA
ATGCCGCAAAAAAGGGAATAAGGGCGACACGGAAATGTTGAATACTCATAC
TCTTCCTTTTTCAATATTATTGAAGCATTTATCAGGGTTATTGTCTCATGAGCG
GATACATATTTGAATGTATTTAGAAAAATAAACAAATAGGGGTTCCGCGCAC
ATTTCCCCGAAAAGTGCCACCTGACGTC

FLAG-MK2-K353R (no plasmid sequence)

GCTAGCGGAACCATGGACTACAAAGACGATGACGACAAGGGAGGCGGTGGG
GGAGGCCTGTCCAACTCCCAGGGCCAGAGCCCGCCGGTGCCGTTCCCCGCCC
CGGCCCCGCCGCCGCAGCCCCCCACCCCTGCCCTGCCGCACCCCCCGGCGCA
GCCGCCGCCGCCGCCCCCGCAGCAGTTCCCGCAGTTCCACGTCAAGTCCGGC
CTGCAGATCAAGAAGAACGCCATCATCGATGACTACAAGGTCACCAGCCAG
GTCCTGGGGCTGGGCATCAACGGCAAAGTTTTGCAGATCTTCAACAAGAGGA
CCCAGGAGAAATTCGCCCTCAAAATGCTTCAGGACTGCCCCAAGGCCCGCAG
GGAGGTGGAGCTGCACTGGCGGGCCTCCCAGTGCCCGCACATCGTACGGATC
GTGGATGTGTACGAGAATCTGTACGCAGGGAGGAAGTGCCTGCTGATTGTCA
TGGAATGTTTGGACGGTGGAGAACTCTTTAGCCGAATCCAGGATCGAGGAGA
CCAGGCATTCACAGAAAGAGAAGCATCCGAAATCATGAAGAGCATCGGTGA
GGCCATCCAGTATCTGCATTCAATCAACATTGCCCATCGGGATGTCAAGCCT
GAGAATCTCTTATACACCTCCAAAAGGCCCAACGCCATCCTGAAACTCACTG
ACTTTGGCTTTGCCAAGGAAACCACCAGCCACAACTCTTTGACCACTCCTTGT
TATACACCGTACTATGTGGCTCCAGAAGTGCTGGGTCCAGAGAAGTATGACA
AGTCCTGTGACATGTGGTCCCTGGGTGTCATCATGTACATCCTGCTGTGTGGG
TATCCCCCCTTCTACTCCAACCACGGCCTTGCCATCTCTCCGGGCATGAAGAC
TCGCATCCGAATGGGCCAGTATGAATTTCCCAACCCAGAATGGTCAGAAGTA
TCAGAGGAAGTGAAGATGCTCATTCGGAATCTGCTGAAAACAGAGCCCACCC
AGAGAATGACCATCACCGAGTTTATGAACCACCCTTGGATCATGCAATCAAC
AAAGGTCCCTCAAACCCCACTGCACACCAGCCGGGTCCTGAAGGAGGACAA
GGAGCGGTGGGAGGATGTCCGTGAGGAGATGACCAGTGCCTTGGCCACAAT
GCGCGTTGACTACGAGCAGATCAAGATAAAAAAGATTGAAGATGCATCCAA

CCCTCTGCTGCTGAAGAGGCGGAAGAAAGCTCGGGCCCTGGAGGCTGCGGCT
CTGGCCCACTGAGGCGGAGGAGGATCC

pcDNA3.1-FLAG-MK2-T222E-T334E

GACGGATCGGGAGATCTCCCGATCCCCTATGGTGCACTCTCAGTACAATCTG
CTCTGATGCCGCATAGTTAAGCCAGTATCTGCTCCCTGCTTGTGTGTTGGAGG
TCGCTGAGTAGTGCGCGAGCAAAATTTAAGCTACAACAAGGCAAGGCTTGAC
CGACAATTGCATGAAGAATCTGCTTAGGGTTAGGCGTTTTGCGCTGCTTCGC
GATGTACGGGCCAGATATACGCGTTGACATTGATTATTGACTAGTTATTAAT
AGTAATCAATTACGGGGTCATTAGTTCATAGCCCATATATGGAGTTCCGCGTT
ACATAACTTACGGTAAATGGCCCGCCTGGCTGACCGCCCAACGACCCCCGCC
CATTGACGTCAATAATGACGTATGTTCCCATAGTAACGCCAATAGGGACTTT
CCATTGACGTCAATGGGTGGAGTATTTACGGTAAACTGCCCACTTGGCAGTA
CATCAAGTGTATCATATGCCAAGTACGCCCCCTATTGACGTCAATGACGGTA
AATGGCCCGCCTGGCATTATGCCCAGTACATGACCTTATGGGACTTTCCTACT
TGGCAGTACATCTACGTATTAGTCATCGCTATTACCATGGTGATGCGGTTTTG
GCAGTACATCAATGGGCGTGGATAGCGGTTTGACTCACGGGGATTTCCAAGT
CTCCACCCCATTGACGTCAATGGGAGTTTGTTTTGGCACCAAAATCAACGGG
ACTTTCCAAAATGTCGTAACAACTCCGCCCCATTGACGCAAATGGGCGGTAG
GCGTGTACGGTGGGAGGTCTATATAAGCAGAGCTCTCTGGCTAACTAGAGAA
CCCACTGCTTACTGGCTTATCGAAATTAATACGACTCACTATAGGGAGACCC
AAGCTGGCTAGCGGAACCATGGACTACAAAGACGATGACGACAAGGGAGGC
GGTGGGGGAGGCCTGTCCAACTCCCAGGGCCAGAGCCCGCCGGTGCCGTTCC
CCGCCCCGGCCCCGCCGCCGCAGCCCCCCACCCCTGCCCTGCCGCACCCCCC
GGCGCAGCCGCCGCCGCCGCCCCCGCAGCAGTTCCCGCAGTTCCACGTCAAG
TCCGGCCTGCAGATCAAGAAGAACGCCATCATCGATGACTACAAGGTCACCA
GCCAGGTCCTGGGGCTGGGCATCAACGGCAAAGTTTTGCAGATCTTCAACAA
GAGGACCCAGGAGAAATTCGCCCTCAAAATGCTTCAGGACTGCCCCAAGGCC
CGCAGGGAGGTGGAGCTGCACTGGCGGGCCTCCCAGTGCCCGCACATCGTAC
GGATCGTGGATGTGTACGAGAATCTGTACGCAGGGAGGAAGTGCCTGCTGAT
TGTCATGGAATGTTTGGACGGTGGAGAACTCTTTAGCCGAATCCAGGATCGA
GGAGACCAGGCATTCACAGAAAGAGAAGCATCCGAAATCATGAAGAGCATC

GGTGAGGCCATCCAGTATCTGCATTCAATCAACATTGCCCATCGGGATGTCA
AGCCTGAGAATCTCTTATACACCTCCAAAAGGCCCAACGCCATCCTGAAACT
CACTGACTTTGGCTTTGCCAAGGAAACCACCAGCCACAACTCTTTGACCGAG
CCTTGTTATACACCGTACTATGTGGCTCCAGAAGTGCTGGGTCCAGAGAAGT
ATGACAAGTCCTGTGACATGTGGTCCCTGGGTGTCATCATGTACATCCTGCTG
TGTGGGTATCCCCCCTTCTACTCCAACCACGGCCTTGCCATCTCTCCGGGCAT
GAAGACTCGCATCCGAATGGGCCAGTATGAATTTCCCAACCCAGAATGGTCA
GAAGTATCAGAGGAAGTGAAGATGCTCATTCGGAATCTGCTGAAAACAGAG
CCCACCCAGAGAATGACCATCACCGAGTTTATGAACCACCCTTGGATCATGC
AATCAACAAAGGTCCCTCAAGAGCCACTGCACACCAGCCGGGTCCTGAAGG
AGGACAAGGAGCGGTGGGAGGATGTCAAGGAGGAGATGACCAGTGCCTTGG
CCACAATGCGCGTTGACTACGAGCAGATCAAGATAAAAAAGATTGAAGATG
CATCCAACCCTCTGCTGCTGAAGAGGCGGAAGAAAGCTCGGGCCCTGGAGG
CTGCGGCTCTGGCCCACTGAGGCGGAGGAGGATCCACTAGTCCAGTGTGGTG
GAATTCTGCAGATATCCAGCACAGTGGCGGCCGCTCGAGTCTAGAGGGCCCG
TTTAAACCCGCTGATCAGCCTCGACTGTGCCTTCTAGTTGCCAGCCATCTGTT
GTTTGCCCCTCCCCCGTGCCTTCCTTGACCCTGGAAGGTGCCACTCCCACTGT
CCTTTCCTAATAAAATGAGGAAATTGCATCGCATTGTCTGAGTAGGTGTCATT
CTATTCTGGGGGGTGGGGTGGGGCAGGACAGCAAGGGGGAGGATTGGGAAG
ACAATAGCAGGCATGCTGGGGATGCGGTGGGCTCTATGGCTTCTGAGGCGGA
AAGAACCAGCTGGGGCTCTAGGGGGTATCCCCACGCGCCCTGTAGCGGCGCA
TTAAGCGCGGCGGGTGTGGTGGTTACGCGCAGCGTGACCGCTACACTTGCCA
GCGCCCTAGCGCCCGCTCCTTTCGCTTTCTTCCCTTCCTTTCTCGCCACGTTCG
CCGGCTTTCCCCGTCAAGCTCTAAATCGGGGGCTCCCTTTAGGGTTCCGATTT
AGTGCTTTACGGCACCTCGACCCCAAAAAACTTGATTAGGGTGATGGTTCAC
GTAGTGGGCCATCGCCCTGATAGACGGTTTTTCGCCCTTTGACGTTGGAGTCC
ACGTTCTTTAATAGTGGACTCTTGTTCCAAACTGGAACAACACTCAACCCTAT
CTCGGTCTATTCTTTTGATTTATAAGGGATTTTGCCGATTTCGGCCTATTGGTT
AAAAAATGAGCTGATTTAACAAAAATTTAACGCGAATTAATTCTGTGGAATG
TGTGTCAGTTAGGGTGTGGAAAGTCCCCAGGCTCCCCAGCAGGCAGAAGTAT
GCAAAGCATGCATCTCAATTAGTCAGCAACCAGGTGTGGAAAGTCCCCAGGC

TCCCCAGCAGGCAGAAGTATGCAAAGCATGCATCTCAATTAGTCAGCAACCA
TAGTCCCGCCCCTAACTCCGCCCATCCCGCCCCTAACTCCGCCCAGTTCCGCC
CATTCTCCGCCCCATGGCTGACTAATTTTTTTTATTTATGCAGAGGCCGAGGC
CGCCTCTGCCTCTGAGCTATTCCAGAAGTAGTGAGGAGGCTTTTTTGGAGGC
CTAGGCTTTTGCAAAAAGCTCCCGGGAGCTTGTATATCCATTTTCGGATCTGA
TCAAGAGACAGGATGAGGATCGTTTCGCATGATTGAACAAGATGGATTGCAC
GCAGGTTCTCCGGCCGCTTGGGTGGAGAGGCTATTCGGCTATGACTGGGCAC
AACAGACAATCGGCTGCTCTGATGCCGCCGTGTTCCGGCTGTCAGCGCAGGG
GCGCCCGGTTCTTTTTGTCAAGACCGACCTGTCCGGTGCCCTGAATGAACTGC
AGGACGAGGCAGCGCGGCTATCGTGGCTGGCCACGACGGGCGTTCCTTGCGC
AGCTGTGCTCGACGTTGTCACTGAAGCGGGAAGGGACTGGCTGCTATTGGGC
GAAGTGCCGGGGCAGGATCTCCTGTCATCTCACCTTGCTCCTGCCGAGAAAG
TATCCATCATGGCTGATGCAATGCGGCGGCTGCATACGCTTGATCCGGCTAC
CTGCCCATTCGACCACCAAGCGAAACATCGCATCGAGCGAGCACGTACTCGG
ATGGAAGCCGGTCTTGTCGATCAGGATGATCTGGACGAAGAGCATCAGGGG
CTCGCGCCAGCCGAACTGTTCGCCAGGCTCAAGGCGCGCATGCCCGACGGCG
AGGATCTCGTCGTGACCCATGGCGATGCCTGCTTGCCGAATATCATGGTGGA
AAATGGCCGCTTTTCTGGATTCATCGACTGTGGCCGGCTGGGTGTGGCGGAC
CGCTATCAGGACATAGCGTTGGCTACCCGTGATATTGCTGAAGAGCTTGGCG
GCGAATGGGCTGACCGCTTCCTCGTGCTTTACGGTATCGCCGCTCCCGATTCG
CAGCGCATCGCCTTCTATCGCCTTCTTGACGAGTTCTTCTGAGCGGGACTCTG
GGGTTCGAAATGACCGACCAAGCGACGCCCAACCTGCCATCACGAGATTTCG
ATTCCACCGCCGCCTTCTATGAAAGGTTGGGCTTCGGAATCGTTTTCCGGGAC
GCCGGCTGGATGATCCTCCAGCGCGGGGATCTCATGCTGGAGTTCTTCGCCC
ACCCCAACTTGTTTATTGCAGCTTATAATGGTTACAAATAAAGCAATAGCAT
CACAAATTTCACAAATAAAGCATTTTTTTCACTGCATTCTAGTTGTGGTTTGT
CCAAACTCATCAATGTATCTTATCATGTCTGTATACCGTCGACCTCTAGCTAG
AGCTTGGCGTAATCATGGTCATAGCTGTTTCCTGTGTGAAATTGTTATCCGCT
CACAATTCCACACAACATACGAGCCGGAAGCATAAAGTGTAAAGCCTGGGG
TGCCTAATGAGTGAGCTAACTCACATTAATTGCGTTGCGCTCACTGCCCGCTT
TCCAGTCGGGAAACCTGTCGTGCCAGCTGCATTAATGAATCGGCCAACGCGC

GGGGAGAGGCGGTTTGCGTATTGGGCGCTCTTCCGCTTCCTCGCTCACTGACT
CGCTGCGCTCGGTCGTTCGGCTGCGGCGAGCGGTATCAGCTCACTCAAAGGC
GGTAATACGGTTATCCACAGAATCAGGGGATAACGCAGGAAAGAACATGTG
AGCAAAAGGCCAGCAAAAGGCCAGGAACCGTAAAAAGGCCGCGTTGCTGGC
GTTTTTCCATAGGCTCCGCCCCCCTGACGAGCATCACAAAAATCGACGCTCA
AGTCAGAGGTGGCGAAACCCGACAGGACTATAAAGATACCAGGCGTTTCCC
CCTGGAAGCTCCCTCGTGCGCTCTCCTGTTCCGACCCTGCCGCTTACCGGATA
CCTGTCCGCCTTTCTCCCTTCGGGAAGCGTGGCGCTTTCTCATAGCTCACGCT
GTAGGTATCTCAGTTCGGTGTAGGTCGTTCGCTCCAAGCTGGGCTGTGTGCAC
GAACCCCCCGTTCAGCCCGACCGCTGCGCCTTATCCGGTAACTATCGTCTTGA
GTCCAACCCGGTAAGACACGACTTATCGCCACTGGCAGCAGCCACTGGTAAC
AGGATTAGCAGAGCGAGGTATGTAGGCGGTGCTACAGAGTTCTTGAAGTGGT
GGCCTAACTACGGCTACACTAGAAGAACAGTATTTGGTATCTGCGCTCTGCT
GAAGCCAGTTACCTTCGGAAAAAGAGTTGGTAGCTCTTGATCCGGCAAACAA
ACCACCGCTGGTAGCGGTTTTTTTGTTTGCAAGCAGCAGATTACGCGCAGAA
AAAAAGGATCTCAAGAAGATCCTTTGATCTTTTCTACGGGGTCTGACGCTCA
GTGGAACGAAAACTCACGTTAAGGGATTTTGGTCATGAGATTATCAAAAAGG
ATCTTCACCTAGATCCTTTTAAATTAAAAATGAAGTTTTAAATCAATCTAAAG
TATATATGAGTAAACTTGGTCTGACAGTTACCAATGCTTAATCAGTGAGGCA
CCTATCTCAGCGATCTGTCTATTTCGTTCATCCATAGTTGCCTGACTCCCCGTC
GTGTAGATAACTACGATACGGGAGGGCTTACCATCTGGCCCCAGTGCTGCAA
TGATACCGCGAGACCCACGCTCACCGGCTCCAGATTTATCAGCAATAAACCA
GCCAGCCGGAAGGGCCGAGCGCAGAAGTGGTCCTGCAACTTTATCCGCCTCC
ATCCAGTCTATTAATTGTTGCCGGGAAGCTAGAGTAAGTAGTTCGCCAGTTA
ATAGTTTGCGCAACGTTGTTGCCATTGCTACAGGCATCGTGGTGTCACGCTCG
TCGTTTGGTATGGCTTCATTCAGCTCCGGTTCCCAACGATCAAGGCGAGTTAC
ATGATCCCCCATGTTGTGCAAAAAAGCGGTTAGCTCCTTCGGTCCTCCGATCG
TTGTCAGAAGTAAGTTGGCCGCAGTGTTATCACTCATGGTTATGGCAGCACT
GCATAATTCTCTTACTGTCATGCCATCCGTAAGATGCTTTTCTGTGACTGGTG
AGTACTCAACCAAGTCATTCTGAGAATAGTGTATGCGGCGACCGAGTTGCTC
TTGCCCGGCGTCAATACGGGATAATACCGCGCCACATAGCAGAACTTTAAAA

GTGCTCATCATTGGAAAACGTTCTTCGGGGCGAAAACTCTCAAGGATCTTAC
CGCTGTTGAGATCCAGTTCGATGTAACCCACTCGTGCACCCAACTGATCTTCA
GCATCTTTTACTTTCACCAGCGTTTCTGGGTGAGCAAAAACAGGAAGGCAAA
ATGCCGCAAAAAAGGGAATAAGGGCGACACGGAAATGTTGAATACTCATAC
TCTTCCTTTTTCAATATTATTGAAGCATTTATCAGGGTTATTGTCTCATGAGCG
GATACATATTTGAATGTATTTAGAAAAATAAACAAATAGGGGTTCCGCGCAC
ATTTCCCCGAAAAGTGCCACCTGACGTC

pcDNA3.1-FLAG-MK2-K353R-T222E-T334E

GACGGATCGGGAGATCTCCCGATCCCCTATGGTGCACTCTCAGTACAATCTG
CTCTGATGCCGCATAGTTAAGCCAGTATCTGCTCCCTGCTTGTGTGTTGGAGG
TCGCTGAGTAGTGCGCGAGCAAAATTTAAGCTACAACAAGGCAAGGCTTGAC
CGACAATTGCATGAAGAATCTGCTTAGGGTTAGGCGTTTTGCGCTGCTTCGC
GATGTACGGGCCAGATATACGCGTTGACATTGATTATTGACTAGTTATTAAT
AGTAATCAATTACGGGGTCATTAGTTCATAGCCCATATATGGAGTTCCGCGTT
ACATAACTTACGGTAAATGGCCCGCCTGGCTGACCGCCCAACGACCCCCGCC
CATTGACGTCAATAATGACGTATGTTCCCATAGTAACGCCAATAGGGACTTT
CCATTGACGTCAATGGGTGGAGTATTTACGGTAAACTGCCCACTTGGCAGTA
CATCAAGTGTATCATATGCCAAGTACGCCCCCTATTGACGTCAATGACGGTA
AATGGCCCGCCTGGCATTATGCCCAGTACATGACCTTATGGGACTTTCCTACT
TGGCAGTACATCTACGTATTAGTCATCGCTATTACCATGGTGATGCGGTTTTG
GCAGTACATCAATGGGCGTGGATAGCGGTTTGACTCACGGGGATTTCCAAGT
CTCCACCCCATTGACGTCAATGGGAGTTTGTTTTGGCACCAAAATCAACGGG
ACTTTCCAAAATGTCGTAACAACTCCGCCCCATTGACGCAAATGGGCGGTAG
GCGTGTACGGTGGGAGGTCTATATAAGCAGAGCTCTCTGGCTAACTAGAGAA
CCCACTGCTTACTGGCTTATCGAAATTAATACGACTCACTATAGGGAGACCC
AAGCTGGCTAGCGGAACCATGGACTACAAAGACGATGACGACAAGGGAGGC
GGTGGGGGAGGCCTGTCCAACTCCCAGGGCCAGAGCCCGCCGGTGCCGTTCC
CCGCCCCGGCCCCGCCGCCGCAGCCCCCCACCCCTGCCCTGCCGCACCCCCC
GGCGCAGCCGCCGCCGCCGCCCCCGCAGCAGTTCCCGCAGTTCCACGTCAAG
TCCGGCCTGCAGATCAAGAAGAACGCCATCATCGATGACTACAAGGTCACCA
GCCAGGTCCTGGGGCTGGGCATCAACGGCAAAGTTTTGCAGATCTTCAACAA

GAGGACCCAGGAGAAATTCGCCCTCAAAATGCTTCAGGACTGCCCCAAGGCC
CGCAGGGAGGTGGAGCTGCACTGGCGGGCCTCCCAGTGCCCGCACATCGTAC
GGATCGTGGATGTGTACGAGAATCTGTACGCAGGGAGGAAGTGCCTGCTGAT
TGTCATGGAATGTTTGGACGGTGGAGAACTCTTTAGCCGAATCCAGGATCGA
GGAGACCAGGCATTCACAGAAAGAGAAGCATCCGAAATCATGAAGAGCATC
GGTGAGGCCATCCAGTATCTGCATTCAATCAACATTGCCCATCGGGATGTCA
AGCCTGAGAATCTCTTATACACCTCCAAAAGGCCCAACGCCATCCTGAAACT
CACTGACTTTGGCTTTGCCAAGGAAACCACCAGCCACAACTCTTTGACCGAG
CCTTGTTATACACCGTACTATGTGGCTCCAGAAGTGCTGGGTCCAGAGAAGT
ATGACAAGTCCTGTGACATGTGGTCCCTGGGTGTCATCATGTACATCCTGCTG
TGTGGGTATCCCCCCTTCTACTCCAACCACGGCCTTGCCATCTCTCCGGGCAT
GAAGACTCGCATCCGAATGGGCCAGTATGAATTTCCCAACCCAGAATGGTCA
GAAGTATCAGAGGAAGTGAAGATGCTCATTCGGAATCTGCTGAAAACAGAG
CCCACCCAGAGAATGACCATCACCGAGTTTATGAACCACCCTTGGATCATGC
AATCAACAAAGGTCCCTCAAGAGCCACTGCACACCAGCCGGGTCCTGAAGG
AGGACAAGGAGCGGTGGGAGGATGTCAGGGAGGAGATGACCAGTGCCTTGG
CCACAATGCGCGTTGACTACGAGCAGATCAAGATAAAAAAGATTGAAGATG
CATCCAACCCTCTGCTGCTGAAGAGGCGGAAGAAAGCTCGGGCCCTGGAGG
CTGCGGCTCTGGCCCACTGAGGCGGAGGAGGATCCACTAGTCCAGTGTGGTG
GAATTCTGCAGATATCCAGCACAGTGGCGGCCGCTCGAGTCTAGAGGGCCCG
TTTAAACCCGCTGATCAGCCTCGACTGTGCCTTCTAGTTGCCAGCCATCTGTT
GTTTGCCCCTCCCCCGTGCCTTCCTTGACCCTGGAAGGTGCCACTCCCACTGT
CCTTTCCTAATAAAATGAGGAAATTGCATCGCATTGTCTGAGTAGGTGTCATT
CTATTCTGGGGGGTGGGGTGGGGCAGGACAGCAAGGGGGAGGATTGGGAAG
ACAATAGCAGGCATGCTGGGGATGCGGTGGGCTCTATGGCTTCTGAGGCGGA
AAGAACCAGCTGGGGCTCTAGGGGGTATCCCCACGCGCCCTGTAGCGGCGCA
TTAAGCGCGGCGGGTGTGGTGGTTACGCGCAGCGTGACCGCTACACTTGCCA
GCGCCCTAGCGCCCGCTCCTTTCGCTTTCTTCCCTTCCTTTCTCGCCACGTTCG
CCGGCTTTCCCCGTCAAGCTCTAAATCGGGGGCTCCCTTTAGGGTTCCGATTT
AGTGCTTTACGGCACCTCGACCCCAAAAAACTTGATTAGGGTGATGGTTCAC
GTAGTGGGCCATCGCCCTGATAGACGGTTTTTCGCCCTTTGACGTTGGAGTCC

ACGTTCTTTAATAGTGGACTCTTGTTCCAAACTGGAACAACACTCAACCCTAT
CTCGGTCTATTCTTTTGATTTATAAGGGATTTTGCCGATTTCGGCCTATTGGTT
AAAAAATGAGCTGATTTAACAAAAATTTAACGCGAATTAATTCTGTGGAATG
TGTGTCAGTTAGGGTGTGGAAAGTCCCCAGGCTCCCCAGCAGGCAGAAGTAT
GCAAAGCATGCATCTCAATTAGTCAGCAACCAGGTGTGGAAAGTCCCCAGGC
TCCCCAGCAGGCAGAAGTATGCAAAGCATGCATCTCAATTAGTCAGCAACCA
TAGTCCCGCCCCTAACTCCGCCCATCCCGCCCCTAACTCCGCCCAGTTCCGCC
CATTCTCCGCCCCATGGCTGACTAATTTTTTTTATTTATGCAGAGGCCGAGGC
CGCCTCTGCCTCTGAGCTATTCCAGAAGTAGTGAGGAGGCTTTTTTGGAGGC
CTAGGCTTTTGCAAAAAGCTCCCGGGAGCTTGTATATCCATTTTCGGATCTGA
TCAAGAGACAGGATGAGGATCGTTTCGCATGATTGAACAAGATGGATTGCAC
GCAGGTTCTCCGGCCGCTTGGGTGGAGAGGCTATTCGGCTATGACTGGGCAC
AACAGACAATCGGCTGCTCTGATGCCGCCGTGTTCCGGCTGTCAGCGCAGGG
GCGCCCGGTTCTTTTTGTCAAGACCGACCTGTCCGGTGCCCTGAATGAACTGC
AGGACGAGGCAGCGCGGCTATCGTGGCTGGCCACGACGGGCGTTCCTTGCGC
AGCTGTGCTCGACGTTGTCACTGAAGCGGGAAGGGACTGGCTGCTATTGGGC
GAAGTGCCGGGGCAGGATCTCCTGTCATCTCACCTTGCTCCTGCCGAGAAAG
TATCCATCATGGCTGATGCAATGCGGCGGCTGCATACGCTTGATCCGGCTAC
CTGCCCATTCGACCACCAAGCGAAACATCGCATCGAGCGAGCACGTACTCGG
ATGGAAGCCGGTCTTGTCGATCAGGATGATCTGGACGAAGAGCATCAGGGG
CTCGCGCCAGCCGAACTGTTCGCCAGGCTCAAGGCGCGCATGCCCGACGGCG
AGGATCTCGTCGTGACCCATGGCGATGCCTGCTTGCCGAATATCATGGTGGA
AAATGGCCGCTTTTCTGGATTCATCGACTGTGGCCGGCTGGGTGTGGCGGAC
CGCTATCAGGACATAGCGTTGGCTACCCGTGATATTGCTGAAGAGCTTGGCG
GCGAATGGGCTGACCGCTTCCTCGTGCTTTACGGTATCGCCGCTCCCGATTCG
CAGCGCATCGCCTTCTATCGCCTTCTTGACGAGTTCTTCTGAGCGGGACTCTG
GGGTTCGAAATGACCGACCAAGCGACGCCCAACCTGCCATCACGAGATTTCG
ATTCCACCGCCGCCTTCTATGAAAGGTTGGGCTTCGGAATCGTTTTCCGGGAC
GCCGGCTGGATGATCCTCCAGCGCGGGGATCTCATGCTGGAGTTCTTCGCCC
ACCCCAACTTGTTTATTGCAGCTTATAATGGTTACAAATAAAGCAATAGCAT
CACAAATTTCACAAATAAAGCATTTTTTTCACTGCATTCTAGTTGTGGTTTGT

CCAAACTCATCAATGTATCTTATCATGTCTGTATACCGTCGACCTCTAGCTAG
AGCTTGGCGTAATCATGGTCATAGCTGTTTCCTGTGTGAAATTGTTATCCGCT
CACAATTCCACACAACATACGAGCCGGAAGCATAAAGTGTAAAGCCTGGGG
TGCCTAATGAGTGAGCTAACTCACATTAATTGCGTTGCGCTCACTGCCCGCTT
TCCAGTCGGGAAACCTGTCGTGCCAGCTGCATTAATGAATCGGCCAACGCGC
GGGGAGAGGCGGTTTGCGTATTGGGCGCTCTTCCGCTTCCTCGCTCACTGACT
CGCTGCGCTCGGTCGTTCGGCTGCGGCGAGCGGTATCAGCTCACTCAAAGGC
GGTAATACGGTTATCCACAGAATCAGGGGATAACGCAGGAAAGAACATGTG
AGCAAAAGGCCAGCAAAAGGCCAGGAACCGTAAAAAGGCCGCGTTGCTGGC
GTTTTTCCATAGGCTCCGCCCCCCTGACGAGCATCACAAAAATCGACGCTCA
AGTCAGAGGTGGCGAAACCCGACAGGACTATAAAGATACCAGGCGTTTCCC
CCTGGAAGCTCCCTCGTGCGCTCTCCTGTTCCGACCCTGCCGCTTACCGGATA
CCTGTCCGCCTTTCTCCCTTCGGGAAGCGTGGCGCTTTCTCATAGCTCACGCT
GTAGGTATCTCAGTTCGGTGTAGGTCGTTCGCTCCAAGCTGGGCTGTGTGCAC
GAACCCCCCGTTCAGCCCGACCGCTGCGCCTTATCCGGTAACTATCGTCTTGA
GTCCAACCCGGTAAGACACGACTTATCGCCACTGGCAGCAGCCACTGGTAAC
AGGATTAGCAGAGCGAGGTATGTAGGCGGTGCTACAGAGTTCTTGAAGTGGT
GGCCTAACTACGGCTACACTAGAAGAACAGTATTTGGTATCTGCGCTCTGCT
GAAGCCAGTTACCTTCGGAAAAAGAGTTGGTAGCTCTTGATCCGGCAAACAA
ACCACCGCTGGTAGCGGTTTTTTTGTTTGCAAGCAGCAGATTACGCGCAGAA
AAAAAGGATCTCAAGAAGATCCTTTGATCTTTTCTACGGGGTCTGACGCTCA
GTGGAACGAAAACTCACGTTAAGGGATTTTGGTCATGAGATTATCAAAAAGG
ATCTTCACCTAGATCCTTTTAAATTAAAAATGAAGTTTTAAATCAATCTAAAG
TATATATGAGTAAACTTGGTCTGACAGTTACCAATGCTTAATCAGTGAGGCA
CCTATCTCAGCGATCTGTCTATTTCGTTCATCCATAGTTGCCTGACTCCCCGTC
GTGTAGATAACTACGATACGGGAGGGCTTACCATCTGGCCCCAGTGCTGCAA
TGATACCGCGAGACCCACGCTCACCGGCTCCAGATTTATCAGCAATAAACCA
GCCAGCCGGAAGGGCCGAGCGCAGAAGTGGTCCTGCAACTTTATCCGCCTCC
ATCCAGTCTATTAATTGTTGCCGGGAAGCTAGAGTAAGTAGTTCGCCAGTTA
ATAGTTTGCGCAACGTTGTTGCCATTGCTACAGGCATCGTGGTGTCACGCTCG
TCGTTTGGTATGGCTTCATTCAGCTCCGGTTCCCAACGATCAAGGCGAGTTAC

ATGATCCCCCATGTTGTGCAAAAAAGCGGTTAGCTCCTTCGGTCCTCCGATCG
TTGTCAGAAGTAAGTTGGCCGCAGTGTTATCACTCATGGTTATGGCAGCACT
GCATAATTCTCTTACTGTCATGCCATCCGTAAGATGCTTTTCTGTGACTGGTG
AGTACTCAACCAAGTCATTCTGAGAATAGTGTATGCGGCGACCGAGTTGCTC
TTGCCCGGCGTCAATACGGGATAATACCGCGCCACATAGCAGAACTTTAAAA
GTGCTCATCATTGGAAAACGTTCTTCGGGGCGAAAACTCTCAAGGATCTTAC
CGCTGTTGAGATCCAGTTCGATGTAACCCACTCGTGCACCCAACTGATCTTCA
GCATCTTTTACTTTCACCAGCGTTTCTGGGTGAGCAAAAACAGGAAGGCAAA
ATGCCGCAAAAAAGGGAATAAGGGCGACACGGAAATGTTGAATACTCATAC
TCTTCCTTTTTCAATATTATTGAAGCATTTATCAGGGTTATTGTCTCATGAGCG
GATACATATTTGAATGTATTTAGAAAAATAAACAAATAGGGGTTCCGCGCAC
ATTTCCCCGAAAAGTGCCACCTGACGTC